Exploring Next Generation Packaging Systems in a Refrigerated Container Using CFD Modelling

by
Nurayn Adewale Tiamiyu

Thesis presented in partial fulfilment of the requirements for the degree of Master of Engineering (Mechanical) in the Faculty of Engineering at Stellenbosch University

Supervisor: Prof. Corné Coetzee
Co-supervisors: Dr. Tarl Berry, Prof. Umezuruike Linus Opara,
Dr. Alemayehu Ambaw

December 2020

DECLARATION

By submitting this dissertation electronically, I declare that the entirety of the work contained therein is my own, original work, that I am the sole author thereof (save to the extent explicitly otherwise stated), that reproduction and publication thereof by Stellenbosch University will not infringe any third party rights and that I have not previously in its entirety or in part submitted it for obtaining any qualification.

Date: November 2020

ABSTRACT

The ineffective utilisation of refrigerated container's (RC) space is a pressing problem for the South African fruit industry. Current packaging systems do not optimally make use of the refrigeration unit for airflow distribution and cooling efficiency of fruit. This results in heterogeneous airflow circulation and ineffective cooling of fruit. The aim of this research was to develop a validated computational fluid dynamics (CFD) model. The model was then used to explore novel packaging system for improved RC space utilisation and cooling performance. Both cooling and space utilisation aspects of the container need to be improved simultaneously, as market trends are increasingly demanding higher-quality fresh produce at lower costs.

Firstly, a 3D CFD model of a fully packed RC was developed and validated experimentally. Pallets were considered as a porous media, and their directional loss properties were experimentally determined. A functional refrigeration unit was incorporated in the model to account for the dynamic cooling modes of the container. The resulting model predicted acceptable results with respect to airflow and temperature. Modelling prediction error was 17% for airflow distribution and 11% for the temperature prediction.

Subsequently, the developed CFD model was used to evaluate conceptual packaging systems for space utilisation and cooling efficiency. Numerical simulations were performed to characterise the airflow distribution and cooling performance of the packaging system in a fully loaded refrigerated container. A multi-parameter approach was used to evaluate the performance of five loading scenarios, namely: Standard A, Standard B, Standard C, Hex and Tes in a fully loaded refrigerated container. The average convective heat transfer coefficient (CHTC) relative standard deviation (RSD) of the Standard packaging system is 47% higher than the Hex design and 51% higher than the Tes design. Overall, Tes design shows significant improved performance for space utilisation and quality preservation of packaged fruit. The results thus highlighted the substantial improvements that are possible concerning shipping costs and quality preservation if alternative packaging system designs are considered in the future.

Lastly, the pallet stack ventilation requirements of the Standard packaging system in a refrigerated container was characterised. The influence of packaging system directional loss properties (i.e. the pallets ventilation) on airflow patterns within the pallet stacks was demonstrated. This has significant implications on the cooling uniformity and quality preservation of packaged fruit. The study further provides, for the first time, a benchmark for the design of ventilation in fresh produce packaging towards improved usage of refrigerated containers.

OPSOMMING

Die ondoeltreffende benutting van koelhouers (KH) se ruimte is 'n dringende probleem vir die Suid-Afrikaanse vrugtebedryf. Huidige verpakkingstelsels maak nie optimaal gebruik van die koelhouer vir die verspreiding van lugvloei en die verkoeling van vrugte nie. Dit lei tot heterogene lugvloei sirkulasie en oneffektiewe verkoeling van vrugte. Die doel van hierdie navorsing was om 'n gevalideerde BVM-model te ontwikkel. Die model is toe gebruik om ’n nuwe verpakkingstelsel te ondersoek vir verbeterde KH-ruimtebenutting en verkoeling. Die afkoeling- en ruimtebenuttingsaspekte van die houer moet gelyktydig verbeter word, aangesien markneigings al hoe meer vars produkte van hoër gehalte teen laer koste vereis.

Eerstens is 'n 3D berekeningsvloeidinamika (BVM) model van 'n volgelaaide KH ontwikkel en eksperimenteel bekragtig. Palette word as 'n poreuse medium beskou en die rigtinggewende verlies-eienskappe daarvan is eksperimenteel bepaal. 'n Funksionele verkoelingseenheid is in die model ingesluit om voorsiening te maak vir die dinamiese verkoeling van die houer. Die gevolglike model het aanvaarbare resultate met betrekking tot lugvloei en temperatuur voorspel, met ’n fout van 17% in die verspreiding van lugvloei en 11% vir die voorspelling van die temperatuur.

Vervolgens is die ontwikkelde BVM-model gebruik om konseptuele verpakkingstelsels vir ruimtebenutting en verkoelingsdoeltreffendheid te evalueer. Numeriese simulasies is uitgevoer om die verspreiding van lugvloei en verkoeling van die verpakkingstelsel in 'n volgelaaide koelhouer te karakteriseer. 'n Multi-parameter benadering is gebruik om die prestasie van vyf laai-scenario's te evalueer, naamlik: Standaard A, Standaard B, Standaard C, Hex en Tes. Die gemiddelde konveksie warmteoordragkoëffisiënt se relatiewe standaardafwyking (RSD) van die standaard verpakkingstelsel is 47% hoër as dié van die Hex-ontwerp en 51% hoër as dié van die Tes-ontwerp. In die algemeen toon die Tes-ontwerp aansienlike verbeterde prestasies vir die gebruik van die ruimte en die behoud van gehalte van verpakte vrugte. Die resultate beklemtoon dus die aansienlike verbeterings wat moontlik is ten opsigte van die versendingskoste en die behoud van gehalte indien alternatiewe verpakkingstelselontwerpe in die toekoms oorweeg word.

Laastens word die ventilasievereistes van die paletstapel van die standaard verpakkingstelsel in 'n koelhouer gekarakteriseer. Die invloed van verpakkingstelsel se rigtingverlies-eienskappe (d.w.s. die paletsventilasie) op lugvloeipatrone binne die paletstapels is aangetoon. Dit het beduidende gevolge vir die verkoeling van die verpakking en die gehalte van verpakte vrugte. Verder verskaf hierdie studie, vir die eerste keer, 'n maatstaf vir die ontwerp van ventilasie in varsprodukteverpakkings en vir 'n beter gebruik van koelhouers.

ACKNOWLEDGEMENTS

I would like to express my appreciation to the South African National Research Foundation (NRF) for the award of postgraduate scholarship through the DST/NRF South African Research Chair in Postharvest Technology at Stellenbosch University.

I would like to thank my supervisors, Dr Alemayehu Ambaw, Prof. Corne Coetzee and Prof. Umezuruike Linus Opara for the academic mentorship and constant valuable inputs. A special gratitude to Dr Tarl Berry, I really appreciate all your commitments towards my academic development. Thanks for always providing necessary supports required to actualise this research, I am very grateful.

To my Parents (Alhaji Amidu Adetona and Alhaja Simiat Tiamiyu), thanks for always being there for me at all time. Because of you, I always have a reason to look forward to an uncertain future with joy. No matter how much I write, it will still be an underestimation of how grateful I am. To my siblings (Muftaudeen, Saheed, Abdul Mujeeb, Muhammad, Sabiat), thanks for the constant support and for always making me feel loved at all time. To my baby, Aisha Toye, thanks for always motivating me and making me feel loved.

I will like to thank the following organization and people for sharing their assistance and help in my research. To Adam Isgaaq and Henk Griessel, and staffs of Two-A-Day Group Ltd, thanks for always providing with necessary resources and assistance during my experiments. To Nazneen, thanks for the efficient administration and for always making things go smoothly. To Dr Tobi Fadiji, thanks for always being awesome and my support system. To Mikail Adekunle and Umar Abdul Rasaq, Thanks for everything.

This work was based upon research supported by the South African Research Chairs Initiative of the Department of Science and Technology and National Research Foundation. I would also like to thank Hortgro for their funding and support of this project.

To everyone going through a rough period in their life. Keep your head up, the sun that sets will rise again.

To God for his unending love and everlasting blessings

Table of Contents

List of Figures

List of Tables

Chapter 1. General Introduction

1.1 Background

The rapidly growing human population and global food crises has emphasised the need to mitigate the postharvest loss of food and horticultural produce. Postharvest losses is a worldwide phenomenon that affects both developed and developing nations (Opara, 2010). The high incidence of postharvest losses is a major hindrance in addressing food sustainability and security concerns. To curb the advent of postharvest losses caused by inefficient storage of horticultural produce, adequate cold chain management is necessary.

Refrigerated transportation is an integral element in cold chain system which also consist of cooled storage, refrigerated display and refrigerated retail outlets (Berry, 2017). Refrigerated container relies on the flow of cooled air around stacked fruit to remove field heat during transportation to a distant export or domestic market (Smale, 2004). The control of air temperature and circulation inside a refrigerated container depends on the following factors: (i) container thermal insulation (Laguerre et al., 2008), (ii) flooring design of the container (Smale, 2004), (iii) pallet stacking patterns and (iv) packaging designs (vent-hole configurations) (Berry, 2015; Defraeye et al., 2013; Fadiji, 2015; Getahun et al., 2018; Tanner and Amos, 2003).

Over the years, various modelling approaches have been used in cold chain applications (cold storage, refrigerated transport and refrigerated display) to investigate and predict airflow distribution and temperature evolution of fresh produce. The most widely used predictive tool for cold chain applications in recent studies is computational fluid dynamics (CFD), as it can generate relatively accurate predictions of airflow and temperature evolution using comparatively low computational resources (Ambaw et al., 2013a;Norton & Sun, 2006; Smale et al., 2006; Verboven et al., 2006). CFD solves the conservation equations that describes the mass, momentum and transfer of energy in cold chain facilities. The turbulence modelling type and boundary layer modelling approach influence to a great deal the accuracy of the simulation ((Ambaw et al., 2013a). CFD modelling of refrigerated containers loaded with fresh produce is incredibly valuable to the South African industry, which is a critical exporter of fruit. In contrast to experimental studies, which are often limited by how much equipment that can practically be installed into a container, modelling provides high-resolution insights into the cooling processes in the container. Furthermore, CFD modelling also allows the user to rapidly simulate and explore loading scenarios of interest.

1.2 Aim and objectives

The aim of this project is to develop a validated refrigerated container CFD model and explore improved fruit packaging systems in terms of space utilisation and cooling performance within a refrigerated freight container.

The specific objectives were to:

a) Develop and validate CFD model of airflow, heat and mass transfer in a refrigerated container.

b) Explore novel refrigerated container loading strategies for enhanced fruit packing densities and improved ecooling efficiency.

c) Identify optimal pallet air permeability needed to operated containers and cool fruit more effectively

1.3 Outline of research presented

Chapter 2 presents an overview of different CFD modelling approaches used in characterising airflow and temperature evolution of refrigerated containers. This detailed review serves as the knowledge background for this study.

Chapter 3 presents the development and validation of a 3D computational fluid dynamics model of a fully packed refrigerated container with a functional refrigeration unit.

Chapter 4 presents the evaluation of packaging systems for container space utilisation and cooling efficiency of packaged fruit.

Chapter 5 presents an explorative study of the packagings' directional loss properties on the pattern and quantity of flow in a fully packed refrigeration.

Chapter 2. Packaging and Refrigerated Freight Container System Performance – A Review of Modelling and Experimental Approaches

2.1 Introduction

Fresh produce export is an important component of the South African economy as evidenced by the significant contribution to the gross domestic product (GDP) and employment through agriculture, including horticulture. Fresh produce are primarily exported in refrigerated freight containers, as they are compatible with different intermodal transportation systems (road, rail, ship) across the world and enable storage at a wide range of temperature settings (Goedhals-Gerber et al., 2017), which extend quality preservation. South Africa (SA) and other agricultural focused countries are thus highly dependent on this freight method, as it facilitates cost-effective shipping. For instance, Agriculture contributes more than 2.5% to the South African GDP and fruit industry exports approximately 2.7 million tons of fresh produce annually to 87 countries (valued at about 2 billion US$) (Department of Agriculture, Forestry and Fisheries, 2017) The ability to export this quantity of fresh product thus allows agricultural industries in SA to employ more than 460 000 people who in turn support approximately two million dependants (Goedhals-Gerber et al., 2017).

2.1.1 Overview and contribution of the pome and stone fruit industry globally and in South Africa

One of the most significant contributors to the total agricultural export of South Africa are the pome and stone fruit industries which contribute an estimated export value of R11.59 billion in 2018. As of 2018, there were over 1500 producers, making use of about 54 000 ha of land, with 45% of the industry total production being exported to the global market (Hortgro, 2018).

Table 2.1 shows the 2018 total production and export of pome and stone fruit in tonnage. According to the South Africa fruit industry statistics (2015), fresh fruit account for 50% of all agricultural exports from South Africa and pome/stone fruit account for 37% of the export fruit annually. Pome fruit are members of the plant family *Rosaceae;* this fruit type has a core of several seeds, surrounded by a tough edible membrane, and the two primary examples include apples and pears. Stone fruit are indehiscent fruit, whereby an outer fleshy part surrounds a single shell of hardened endocarp with a seed inside, examples include peaches, nectarines and plums. Both pome and stone fruit are climacteric, and their ripening process, therefore, continues after harvest and must be regulated using refrigeration. According to HortGro deciduous fruit statistics (Hortgro, 2018),

93% of the pome fruit industry income were generated by fresh sales with an annual turnover of R8.94 billion. Stone fruit have an annual turnover of R2.64 billion and 81% of the revenue generated are by fresh sales. Africa is the largest import market for South Africa apples (114 070 ton) (Figure 2.1) and Europe is largest import market for South Africa plums (25 828 ton) (Figure 2.2) (Hortgro, 2018). There has been an increase in the number of refrigerated containers used in South Africa. In 2014/2015 export year, 14 368 refrigerated containers of pome fruits and 3 516 refrigerated containers of stone fruit were exported to international markets (Myburgh, 2016).

2.1.2 Role of packaging and refrigerated freight container in the stone and pome fruit cold chain

On a global scale, Europe imports 61% of South Africa fruit export (Ngcobo et al., 2012). South Africa is geographically distant from most of its export markets and the storage condition of fruit need to be carefully controlled to preserve acceptable quality. To maintain high quality and safety for food products, the cooling process and storage conditions must be properly carried out (Laguerre et al., 2014). Refrigerated shipping containers are used to transport fresh fruit from cold stores to international (global), as well as to different parts of the country for domestic use (Ngcobo et al., 2012). The duration of transport of fruit between South African and Europe cold stores ranges from 15 to 30 days (Fawole and Opara, 2013). Controlling the temperature of the fruit is important to the postharvest and shelf life as it influences to a large extent the physiological and biological changes that take place after harvest (Ravindra and Goswami, 2008). The respiration process causes a reduction in the quality of fruit after harvest (Caleb et al., 2013). To minimise the postharvest deterioration, horticultural produce are generally precooled after packaging to maintain the fruit at an optimal temperature during storage and shipment (Pathare et al., 2012).

Refrigerated freight containers rely on the flow of cold air around horticultural produce to prevent senescence and remove respiratory heat during transport (Smale, 2004). However, achieving uniform cooling and flow of cold air within the refrigerated container remains a challenge (Getahun, 2016). Non-uniform cooling that occurs during cold chain systems (cold storage, refrigerated transportation) is caused by non-homogenous airflow distribution within palletised stacks (Alvarez and Flick, 1999; Delele et al., 2013; Getahun et al., 2017b; Zou et al., 2006). Bouwer and Dodd (2016) identified the ineffective utilisation of 40ft (12.2 m) refrigerated containers as a critical problem in the South African fruit industry. Additionally, a refrigerated freight container volume is not fully utilised due to incompatible geometric characteristics of the packaged fruit and the container. Transport and freight costs make up 54% of the total costs

related to fruit exports (Fruit SA, 2015). Hence, there is need to optimise the refrigerated container volume by increasing the number of fruit to be exported. The positive trend of increasing supply and demand for apples, pears and stone fruit support the need to optimise space utilisation of a refrigerated container.

An important factor influencing refrigerated container usage is packaging, which Robertson (2016) defined as "the enclosure of products, items or packages in a wrapped pouch, bag, box, or other container to perform the following functions: containment; protection; and/or preservation; and utility or performance". Over the years, there has been a considerable growth in the development and application of packaging technologies for foods processed due to the increasing postharvest losses of climacteric fruit. The primary function of packaging materials is maintaining the quality of fruit during postharvest handling and storage by providing mechanical protection against injuries, minimizing produce moisture loss and retarding microbial growth (Opara, 2011). Also, horticultural products are stored in cooled enclosure to preserve the quality of the horticultural product by impeding the ripening process (Verboven et al., 2004). In postharvest storage of horticultural products, how the product is packaged and stacked is of considerable importance. Products can either be stored in bulk padded in bins or packages (Ambaw et al., 2013a). A wide variety of packages of different designs, sizes and materials are being used to store fruit.

In the fresh produce industry, many researches have investigated package design towards improved cooling performance (Berry et al., 2015; Defraeye et al., 2015a; Fadiji et al., 2016; Fadiji et al., 2018). The performance and rate of the precooling process for fresh produce depends critically on the packaging design (vent area, shape, number, position etc.), the fruit stacking pattern within the package and air-produce temperature difference (Pathare et al., 2012). These design factors directly influence the airflow distribution, cooling of produce and energy consumption within the container (Zhao et al., 2016). The cooling efficiency of the package depends on the arrangement of these units in the room/container and by the flow resistance (vertical or horizontal) induced by them and the contained product. Non-homogeneous flow of the cooling air inside the stack may cause uneven cooling and product quality; certainly, in the case of respiring and transpiring horticultural products. Hence, packages should be designed to optimise air penetration (Alvarez and Flick, 1999; Ambaw et al., 2013a; Verboven et al., 2006). This study aims to develop improved fruit packaging systems and to optimise packing density inside the refrigerated containers and facilitate efficient cooling performance.

2.2 Essentials of a packaging system

The pallet is a common packaging component used for material handling and transportation; it is a rigid base/platform for storing, stacking and transporting goods. Palletised loadings make it easier for companies to transport and store goods as a single unit. The pallet is a critical asset in optimizing costs of companies. Presently, there are many researchers focusing on addressing major issues of pallets, namely: product design problem, pallet loadings and pallet logistic design problem. The pallet product design problem focuses on how the materials and technologies for producing pallets can improve their performance and the pallet packing problem aims to identify an optimal configuration of pallets to reduce the transportation costs (Elia and Gnoni, 2015). The transport and freight costs make up a significant portion of fruit export, so there is a need to maximise the profits of the commodity without deteriorating the quality of the fruit. There are numerous designs and types of pallets used to bear different types of loadings. An important goal in any pallet design is to ensure ease in retrieving and delivering of goods/products (Khoo et al., 2008).

The various types of stone and pome fruit varieties and different markets require different types/sizes of cartons (Figure 2.3). There are different carton designs used in the transportation of pome/stone fruit and they can be broadly classified into “Display” and “Telescopic” cartons (Figure 2.4). Display cartons are usually placed on the shelf at the point of sale for the consumers while telescopic cartons are used to package fruit in layers or bulks at the point of retail (Berry et al., 2015).

2.2.1 Pallet base types

Pallets are usually made of several materials such as woods, metals and plastic (Elia and Gnoni, 2015) and wooden material are most commonly used in industrial applications (Buehlmann et al., 2009). Nearly 400 million wooden pallets are produced annually, which accounts for 86% of all the pallets sold worldwide (McCoy, 2003). Although wooden pallets are generally cheaper when compared to non-wooden pallets (plastics and metal), they have some disadvantages which limit their usage in some parts of the world. The international standard organization has no single pallet size standard for international trade. However,

Table 2.2 shows several common pallet sizes and dimensions currently in use for South African fruit exports. The payload calculation of a container is affected by the pallet dimensions as the pallets are restricted by weight and height. Also, the capacity of a pallet depends on factors such as packaging dimensions, types of

cartons and internal packaging used and export market requirements (Myburgh, 2016).

2.2.2 Pallet–stack arrangements

ISO 2 pallet and hi-cube standard pallet is the most widely used in South Africa export of stone and pome fruit (Myburgh, 2016). Most pallet stack patterns used in refrigerated containers are expected to cause heterogeneous airflow distribution. When pallets are loaded in the containers, the stacks at the front of the container (nearer to the evaporator fan) receive a higher volumetric flow of refrigerated air when compared to those at the far end of the container (farthest from the evaporator fan). These differences in airflow rate result in the developments of warm fruit regions (Verboven et al., 2004). Also, pallet layout (compactness and pattern) cause varying airflow resistance (vertical and lateral) and heterogeneous airflow distribution within the refrigerated container (Smale, 2004).

Stacking configuration patterns are mostly selected to maximise the container volume, balancing of the fruit and not to hinder the air-distribution within the produce. The increasing fuel costs and environmental concerns in the last decade pressured the fruit industry to optimise the refrigerated container volume. This would lead to a reduction in the number of refrigerated containers used in the fruit industry. Also, it would yield a considerable decrease in shipping costs and a reduction in the carbon footprint (Berry, 2017).

Berry et al. (2015) carried out a survey which identified four configurations of fruit stacks (pome/stone fruit) on a pallet (Figure 2.5) . Export ISO standard pallets (1.2 m ×1 m) (Figure 2.6) and pallets used for local markets (1.2 m × 0.9 m) were used in this configuration (Figure 2.5). Berry (2017) investigated different pallet stack loading strategies to determine the one that better utilises refrigerant freight container space and the effect on cooling effectiveness. The author investigated the floor area usage of different novel packaging systems (Hex, Tes, Eco and Qad, STD A, STD B, STD C) (Figure 2.7). In this study, the floor usage of the proposed Hex and Tes packaging systems was improved from 89.9% to 97.4% and 98.9% respectively.

2.3 Refrigerated freight container

Climacteric fruit such as pome and stone fruit are exported from South Africa to different destinations around the world. Refrigerated containers are used to transport the fruit, under cold conditions to minimise respiration and reduce quality loss over the shipping duration. Refrigeration generally refers to the

process of removing heat in an enclosed space to lower the temperature. The introduction of chilled transport systems has opened enormous opportunities in the world as it has increased the availability and ease at which countries can export fruit whilst preserving the quality of the fruit. This controlled system has made the refrigerated freight container a widely used tool to transport fruit in the world (Sinclair, 1989).

2.3.1 Refrigerated freight container in horticultural export

Refrigerated freight containers are one of the four main segments of the cold chain system: These include refrigerated storage, refrigerated transport, distribution centre/depots and refrigerated display in retail outlets. Refrigerated transport is a critical component in the horticultural chain (Berry, 2017). There has been a significant increase in the usage of a refrigerated freight container, and market trends indicate usage to increase further (Berry et al., 2018; Eyring et al., 2005; Opara, 2009). In 2011, approximately 2 million 20-foot equivalent units (TEUs) were used globally (Notteboom and Rodrigue, 2007). Refrigerated freight containers are similar in construction with their differences lying in size, types of insulation, air delivery systems and structure for conditioned cooling (Getahun et al., 2018). Refrigerated containers refer to all freight containers equipped with a refrigerating system (and heating systems) to condition the air within the enclosed space. Two basic types of a refrigerated freight container are used in international trade, namely port-hole containers and a plug-in type or integral refrigerated container. A plug-in type or integral container incorporates its own refrigeration unit. It can maintain temperatures between -18ºC and 20ºC, while a port-hole container is an insulated box which doesn't have its own refrigerated unit unless connected to a central-plant cold air circulation system (Getahun, 2016; Wild, 2009). The port-hole container possesses larger internal volume but their use has mostly been depreciated and are rarely used anymore. The sharp decline in the use of porthole containers for the distant transportation of fresh produce is due to its lack of integrated refrigeration unit. The enormous growth of Integral containers and the need to have monitored cooling for quality preservation of fresh produce also contributed to the reduced usage in porthole container technology (Wild, 2009). Integral refrigerated containers have built-in refrigeration unit and are widely used in transporting perishable fruit to the export market (Getahun, 2016; Wild, 2009). Refrigerated containers are also categorised by their sizes, floor type and air-delivery system. The length of refrigerated containers are usually 20 ft (6 m) or 40 ft (12.2 m) (ASHRAE, 2010), with polyurethane insulation at 7.62 cm in the walls and floor and 10.16 cm in the ceiling (Getahun, 2016). There have been many experimental and numerical studies performed on refrigerated

containers (Defraeye et al., 2016; Defraeye et al., 2015a; Delele et al., 2013; Getahun, 2016; Getahun et al., 2018; Zou et al., 2006).

2.3.2 Working principle of a refrigerated freight container

In postharvest handling systems such as a refrigerated freight container, controlling the conditions of fruit depends on the factors including thermal insulation of the container (Laguerre et al., 2008), floor design and stacking pattern of the packaging boxes (Berry, 2015; Berry et al., 2016; Defraeye et al., 2014; Fadiji, 2015; Getahun, 2016; Getahun et al., 2018; Tanner and Amos, 2003). Also, the required refrigerated capacity of a container can be affected by environmental impacts, insulation quality of the container, rate of air exchange, leakage and the initial temperature of cargo (Keller, 2006). Refrigerated containers typically do experience an increase in heat leakage of 3% to 5% yearly due to the extreme environmental conditions they are exposed to (Thermo King, 2007). The Insulation quality of refrigerated freight container also decreases with age of the container (IIR, 1995).

Many refrigerated container have an integrated refrigeration unit which is powered by a 3-phase electric supply. The 3-phase electrical power supply is connected to a power generator during transport by a ship or truck. During transport through ships, refrigerated containers are connected to on-board power supply systems. The refrigeration systems in a container uses four main components, namely a compressor, condenser, evaporator and an expansion valve. Considering the compactness of the refrigeration unit, the components are designed to be as small as possible. The refrigerant (R134a or R404a) that flows through the system absorb heat inside the system and then releases it to the ambience. Figure 2.8 shows the main components in a mechanically refrigerated container. The compressor causes the refrigerant to move through the system to carry heat within the system. High pressure on one system is created, and low pressure is on the other side. The differential pressures on both sides of the system control the boiling point of the refrigerant, causing it to boil in the evaporator and condense in the condenser, respectively. The condenser compartment causes the releases of heat to the outside air and the condensing of the refrigerant vapour. The expansion valve effects the flow of high-pressure liquid refrigerant to the evaporator from the condenser. The evaporator is located inside the refrigerated compartment and absorbs heat from it (IIR, 1995). To control the temperature in a refrigeration unit, air temperature measurement are recorded at two locations; at the entry to the evaporator coil (return air) and at the exit of the evaporator coil (supply air) (Smale, 2004). The operating status of a refrigerated container influences its power consumption. Also, the internal temperature of the container plays a critical role in determining the cooling capacity as it helps determine the

refrigerant evaporation temperature (Wild, 2009). Table 2.3 shows the cooling capacities and power consumption of Thermo king refrigeration unit at different container internal temperature.

2.3.3 Factors influencing the performance of a refrigerated container

During the transportation of fruit, several factors influence the performance of the refrigerated freight container. Factors include airflow, temperature control, humidity levels, artificial atmosphere, flooring system and stacking arrangements in the refrigerated freight container (Getahun et al., 2018; Sinclair, 1989). Airflow inside a refrigerated container is influenced by the type of packaging and stacking arrangement of the fruit (Getahun et al., 2018). Figure 2.9 shows the theoretical or intended airflow distribution in a packed refrigerated container.

2.3.3.1 Air distribution

A large percentage of integral container use the bottom air-delivery configuration. The load line is the airspace between the top of the container and the top of the pallet stack. The return air in this region is drawn by the evaporator fans and passed through the evaporator coil. Depending on the controller set-point requirements, the air can either be cooled or heated. The controlled air is passed through the delivery air ducts to the air plenum chamber. The delivery air plenum chamber is where the air is forced through the T-bar floor to reach all the lower stowed produce (Sinclair, 1989). The static air pressure differential between delivery air and return air cause the flow of air in the cargo (Sinclair, 1989). Other air distribution methods include top air delivery systems and side air delivery systems. Certain stowage arrangements of the palletised fruit in a refrigerated container can result in poor air distribution and thus ineffective cooling. To ensure good temperature distribution, it is essential to have air uniformly distributed throughout the load and to all fruit (Sinclair, 1989).

2.3.3.2 Flooring system

The floor design of a refrigerated container greatly influences the air exchange within containers, which can, in turn influence cooling time and temperature distributions (Smale, 2004; Vigneault et al., 2009). There has been many comparative studies on the effect of different flooring system on airflow distribution within a refrigerated container (Getahun et al., 2018; Smale, 2004). Getahun et al. (2018) investigated the effect of T-bar and flat floor design on the impact of airflow in different types of refrigerated containers using computational

fluid dynamics approach. There was less vertical airflow of air inside the refrigerated container with flat floor when compared with the T-bar floor structure. Smale (2004) applied flow resistance to a thermal network when comparing the effect of flat flooring system and perforated flooring systems of a refrigerated container. During the transport of fruits using a refrigerated container, the floor types and designs widely used includes T-bar, flat floor, castellated and perforated floors. All the flooring types have unique advantages and limitation in how they distribute airflow in the refrigerated container. Figure 2.10 shows the refrigerated container flooring types discussed below

2.3.3.2.1 Flat floor

Containers using flat floor systems rely on the open regions within the pallet bases to facilitate airflow within the container (Figure 2.10) (Smale, 2004). The pallet bases thus act as the air duct. An important benefit of the flat floor approach is the ease which they can be cleaned.

2.3.3.2.2 Castellated floor

Castellated floors make use of rectangular grooving running from inlet side to the door side (Figure 2.10). The tiny holes on the floor allows airflow to be distributed vertically into the container. There is an obstruction to airflow due to a reduction in free area. Castellated floor structure makes it easy to clean and are generally stronger than other flooring types (Smale, 2004).

2.3.3.2.3 Perforated floor

In this type of floor, there is better air-distribution and less obstruction to airflow with respect to the castellated floor type (Figure 2.10). To clean the perforated floor requires relatively more time and effort and usually needs to be removed if being cleaned properly (Smale, 2004).

2.3.3.2.4 T-bar floor

T-bar floor systems takes its name from the T-shaped aluminium extrusions of the floor (Figure 2.10). This type of floor design is beneficial to airflow distribution in the container, as it enables cold air to flow along the containers' bottom region, from the refrigeration unit (bottom air delivery system) (Figure 2.11) (Getahun et al., 2018). The pallets create an airflow channel due to the space between the container floor and cargo (Smale, 2004). T-bar floors are difficult to clean and can be damaged by forklifts during loading of the refrigerated container. Figure 2.12 shows a partially packed refrigerated container with a T-bar flooring system.

2.4 Computational fluid dynamics

Computational fluid dynamics is a numerical tool that allows for the simulation of fluid processes and has in recent years been used to evaluate agricultural systems (ventilation, drying, sterilisation, refrigeration, cold storage, mixing) (Ambaw et al., 2013a). CFD can thus provide unique insights into relatively complex food processes, which would not normally be possible experimentally. This has allowed commercial industries to better preserve food quality (Norton and Sun, 2006) and to increase the shelf life of fruit (Wang and Sun, 2003). (Versteeg and Malalasekera (2007) defined CFD as the analysis of the governing equation of a transport phenomenon (continuity equation, Naiver-Stokes equation). CFD has enabled the food industry to respond to expanding markets by enhancing and developing processing strategies, whilst maintaining high levels of product quality (Norton and Sun, 2006). In recent years, there has been major expansions in CFD application in the cold chain management of the food industry and in postharvest activities (Ambaw et al., 2013a; Xia and Sun, 2002).

CFD has become a widely used technique in postharvest applications (Ambaw et al., 2013a; Berry et al., 2018; Berry et al., 2016; Defraeye et al., 2015b; Delele et al., 2013; Getahun et al., 2018; Gruyters, 2019; Hoang et al., 2015; Laguerre et al., 2008; Zou et al., 2006). CFD can be used to predict steady and transient air distribution at high resolutions and high accuracy, so long as the correct meshing/grid method, discretization scheme, numerical methods, boundary conditions and turbulence models are applied (Versteeg and Malalasekera, 2007; Zhai et al., 2007). In CFD modelling, the real geometry of the system is being discretised and Navier-Stokes equation for mass, momentum and energy are solved using the finite volume numerical method (Versteeg and Malalasekera, 2007). The ability to predict the temperature of produce and the velocity of air inside the refrigerating equipment of the cold chain is the reason CFD models are being adopted by researchers (Defraeye et al., 2016; Delele et al., 2008; Getahun, 2016; Gruyters et al., 2018; Hoang et al., 2015; Hoang et al., 2000; Laguerre et al., 2013; Nahor et al., 2005). One of the significant advantages of the CFD approach is that it grants the food industry the ability to predict conditions in packaging and storage facilities (Laguerre et al., 2014). However, there is still a need to experimentally validate the spatio-temporal airflow and temperature distributions obtained with a CFD model. CFD is thus a cost-effective method to investigate and predict the cooling processes within the cold chain, both at small and large scales (Ambaw et al., 2013a).

Several methods can be used to simulate complex transport and cooling phenomena during cold chain processes, they include resistance network models and CFD. Resistance network models are mainly used in applications where the

majority of the flow path can be predetermined, which is rarely the case in postharvest applications. In this model, the region of interest are usually divided into interconnected and predetermined flow paths (Smale et al., 2006). A flow resistance is attributed to each flow path. The accuracy of this modelling approach depends on the flow resistance attributed to the channels (Smale et al., 2006).

For the Lattice Boltzmann method, fluid and solid materials are considered as quasiparticles on a regular lattice. The quasiparticles satisfy the conservation law via collisions of the quasiparticles moving across the lattice. This method has many limitations in postharvest application with the most prominent being that it requires uniform mesh spacing during discretization. Computational fluid dynamics using the Navier stokes governing equation alleviates the issues found in other methods (Gruyters, 2019). In CFD modelling, where transport phenomena inside a refrigerated container are considered, the bulk packed fruit can be treated as a porous media (Getahun, 2016). The porous media assumption, which relates the effects of particle size and shape, alignment with airflow and void fraction has been applied successfully in various applications within food research (Datta, 2007; Defraeye et al., 2012; Getahun, 2016; Gruyters, 2019; Hoang et al., 2015; Hoang et al., 2000).

Errors and uncertainty are an important aspect of evaluating CFD modelling results. To improve the level of confidence on CFD modelling results, rigorous methods have been developed to quantify this (Versteeg and Malalasekera, 2007). The two methods which are widely accepted include: The verification and validation approach (AIAA, 1998; Oberkampf and Trucano, 2002). To verify a model is to determine whether an implemented model aptly represent the conceptual description and solution of the model. This is done by quantifying the numerical errors associated with the model implementation. Such errors include; round off errors, discretisation error, and iterative convergence errors (Versteeg and Malalasekera, 2007). Roache (1998) describes this simply with the phrase “solving the right equations”. To validate a model is to determine the degree at which the model gives an accurate representation of the real physical situation. This can be achieved by conducting sensitivity analysis and experiments to compare the numerical results and the experimental results (Versteeg and Malalasekera, 2007).

The CFD setup process has been extensively described in various literature. However, a short summary is outlined below (Anderson and Wendt, 1995; Sun, 2007; Versteeg and Malalasekera, 2007). To run a simulation, the geometry of the system must be developed, and the computational domain will be discretised into a grid. Next, the simulation set-up of the systems must be specified (boundary conditions, turbulence model etc.). The governing partial differential equation will

be solved on the mesh or grids using finite volume discretization schemes. CFD simulations are more accurate when the mesh grid size is very fine, but it requires higher computational load (computational time and computational cost). The CFD engineer has the responsibility of applying mesh sensitivity analysis to determine the trade-off between optimal mesh size and computational (accuracy and computational time) (Gruyters, 2019).

2.4.1 Modelling approaches for packaging design and refrigerated container

The last decades have seen the development of many commercial codes which enable access to sophisticated modelling approaches for food engineering. The food industry requires processes that can predict surface heat, mass transfer coefficients, thermal properties of produce, flow characteristics of packaging system under various scenarios (Delgado and Sun, 2001; Wang and Sun, 2003). Transport phenomena involving airflow, heat and mass transfer are key processes in refrigerated storage (Verboven et al., 2006). However, CFD application to study large and complex postharvest systems like a refrigerated freight container remains a challenge due to high computational demand (James et al., 2006). There are generally two methods in modelling airflow, heat transfer in fresh produce; the porous medium approach and direct/explicit CFD modelling (Zhao et al., 2016). Other modelling approaches include multiscale modelling approaches and realistic filling pattern generation. Multiscale modelling often incorporates combinations of explicit modelling and porous medium approaches. Examples of these techniques can be seen by Delele et al. (2009) and Ambaw et al. (2014) for postharvest applications.

2.4.1.1 Explicit modelling

The direct CFD simulation approach explicitly models all geometrical complexities within the medium. The model must therefore consider the geometry of the fruit, packaging systems and refrigerated container. The benefit here is that this approach provides better insight into complex fluid flow in a refrigerated container. However, the successful simulation of these explicit geometries requires high computational resources (time, cost). Grid generation is thus more complex and much larger to accommodate the explicit geometries being considered and the numerical difficulties encountered during the simulation (Zhao et al., 2016). The limitations of direct CFD simulation in term of the computational resources thus make the porous medium approach a far more practical approach for food processes industry. Although the accuracy of the model depends on the accuracy of the model parameters, boundary conditions, discretization schemes and meshing types (Zhao et al., 2016).

To illustrate these differences, Ambaw et al. (2013b) performed a comparison between the explicit modelling and porous medium approach. The porous media approach yields 2.5×10^5 mesh elements, while explicit modelling approaches gives 5.37×10^6 mesh elements for the same simulation. Explicit modelling technique have been used in different postharvest applications (Ambaw et al., 2017; Berry, 2017; Berry et al., 2016; Defraeye et al., 2015a; Defraeye et al., 2013; Gruyters, 2019; Wu and Defraeye, 2018). Figure 2.13 shows an example of an explicit modelling technique where the package materials were explicitly modelled, and fruit filling pattern was also considered.

2.4.1.2 Porous media approaches

A porous medium is composed of a solid and fluid matrix (gas or liquid). Porous media has played a critical role in understanding the transport phenomena in different engineering applications (food, energy industry, metallurgical, chemical, and biophysics). In the food industry, a large range of processes with different scales can involve the transport of fluid, heat, and mass through porous media. Some of the examples include mixing, drying, cooking, sterilization as well as cooling of stacks bulk produce such as apples and pome fruit (Datta, 2007; Dehghannya et al., 2010). Transport phenomena in fruit storage systems are complex and mathematical models aid the understanding and design of refrigerated freight container (Verboven et al., 2006). Fruit inside reefers are packed loose in boxes and then stacked on pallets forming a complex geometry. For a typical reefer packed with 20 pallets, model discretization is very expensive due to the high size ratio of geometries that make up the domain (Zhao et al., 2016).

Due to the limitations in the computational resources and complex packaging configuration, the porous media approach is applied to model transport phenomena within packages (ventilated or unventilated) and refrigerated freight container. This approach allows the mathematical models to be simplified, which in turn reduces computing time and simulation costs (Zhao et al., 2016). Porous media approach makes use of a space-averaging technique whereby the fluid flow is characterised by an average superficial velocity (velocity based on volumetric flow rate). It is the major means of modelling transport phenomena in a packed bed (Verboven et al., 2006). In the treatment of transport phenomena in porous media, many unknowns are introduced in the space-averaging methods, which requires verification experimentally. This is due to the complexity of the flow paths and inter-pore and pore-pore fluid dynamic interactions. The space-averaging involves the integration of conservation equations over the representative elementary volume (Kaviany, 2012). A fundamental theory of

airflow in porous media and heat/mass transfer in porous media is discussed below.

2.4.1.2.1 Airflow in porous media

The porous media assumption relates the effects of particle size and shape as well as alignment with airflow and void fraction on pressure drop over the modelled products has been used in many recent studies (Ambaw al., 2013b; Getahun, 2016; Gruyters, 2019; Hoang et al., 2015; Hoang et al., 2000; Verboven et al., 2004). For small airflows (particle Reynolds number $Re_p < 1$) in porous media, the airflow rate is proportional to the pressure drop which is basically Darcy's law which relates the velocity drop through the pores to the pressure drop over the material.

Darcy's law establishes a linear relationship between the pressure gradient ∇p (Pa/m), and the volume-averaged velocity u (m/s) in porous media. This law is valid for small airflow (darcy's velocity u is between 0.02 m/s and 0.06 m/s)

$$\nabla p = -\frac{\mu}{\kappa} u \tag{2.1}$$

Where μ (kg $m^{-1}s^{-1}$) is the air dynamic viscosity of the fluid, and κ (m^2) is the Darcy permeability of the porous medium that depends on various factors including pore size, produce diameter and pore distribution. The vector u (m/s) is the superficial velocity which is the velocity averaged over the entire medium (pore space as well as solid matrix). The intrinsic air velocity (physical air velocity) is the true velocity through porous media pores. It can be calculated by $v = u/\varepsilon$ where ε is the porosity.

$$Re_p = \frac{\rho u\, d_{eff}}{\mu} \tag{2.2}$$

Re_p is the particle Reynolds number, and ρ (kg/m^3) is the fluid density and d_{eff} (m) is the effective diameter of the product. For spherical products, the effective diameter can be expressed as Eqn. (2.3);

$$d_{eff} = \frac{6V}{A} \tag{2.3}$$

where V is the volume (m^3) and A is the area (m^2).

Darcy's law only expresses the linear relationship between pressure drop and superficial velocity for small velocities. When the velocities are higher, Darcy-Forchheimer equation (Eqn. (2.4)) is applied to express the relationship between the pressure drop and the superficial velocity (Verboven et al., 2006).

$$\nabla p = -\frac{\mu}{\kappa} u - \rho \left(\frac{C_f}{\kappa^{\frac{1}{2}}}\right)(u)u \tag{2.4}$$

where C_f is the dimensionless Forchheimer coefficient that is mainly dependent on the geometry of the pore space. For a transient airflow, a time derivative term should be added to the equation. This corresponds to the most practical situations for food cooling applications, such as precooling and cold storage.

Darcy-Forchheimer equation is valid for unbounded porous media without walls only (Verboven et al., 2006). Packaging of fruit confines the fruit within a finite volume during the forced convection cooling of fresh produce. This confinement effect is accounted for by adding an additional viscous term called Brinkman term

$$\nabla p = -\frac{\mu}{\kappa}u - \rho\left(\frac{C_f}{\kappa^{\frac{1}{2}}}\right)(u)u + \mu_{eff}\nabla^2 u \tag{2.5}$$

Where μ_{eff} is the effective dynamic viscosity in the boundary layer at the solid-porous media interface. This property depends on the porosity and tortuosity of the porous medium.The effect of the Brinkman term is that it will give rise to a boundary layer, where the velocity reduces to zero exactly at the solid wall.

2.4.1.2.2 Heat and mass transfer in porous media

In the modelling of heat transfer in a packaging system or refrigerated freight container, there are many complexities. The transfer of heat within porous media is largely dependent on the physical and thermal properties of the two phases (solid and fluid). Porous matrix structure and thermal conductivity of the solid and fluid phase are critical in determining the conduction heat transfer in porous media (Dehghannya et al., 2010). Heat transfer models in porous media often consider local thermal equilibrium between the fluid and solid phases. For a transient two-phase application, which are often applied in food systems, the mathematical models of airflow, heat and mass transfer inside ventilated packages have been developed (Dehghannya et al., 2010). Two models namely local thermal equilibrium (LTE) and local thermal non-thermal equilibrium (LNTE) are used to model heat transfer in porous media. Local thermal equilibrium models are mostly used in porous mediums where the temperature differences between the solid and liquid phases are negligible. In most heat transfer cases within the porous medium, thermal equilibrium is assumed (Getahun, 2016).

In LTE, A single energy equation is used to describe the heat transfer in porous media assuming thermal equilibrium between the solid phase and moving fluid (Quintard et al., 1997)

The general equation (2.6) is based on this assumption (Hoang et al., 2015):

$$\left[\varepsilon_p\rho_f Cp_f + (1-\varepsilon_p)\rho_s Cp_s\right]\frac{\delta\bar{T}}{\delta t} + \rho_f Cp_f \bar{u_\iota}\left(\frac{\delta\bar{T}}{\delta x_i} + \frac{1}{\rho_f Cp_f}\frac{\delta\bar{p}}{\delta x_i}\right) = \frac{\delta}{\delta x_i}\left[\left(\varepsilon_p\lambda_{eff} + (1-\varepsilon_p)\lambda_s\frac{\delta\bar{T}}{\delta x_i}\right)\right] \tag{2.6}$$

The effective thermal conductivity λ_{eff} ($W\ m^{-1}k^{-1}$) is given by

$$\lambda_{eff} = \lambda_f + \frac{Cp_f\,\mu_t}{Pr_t} \tag{2.7}$$

Pr_t is the turbulent prandtl number (taken as 0.85) and ε_p is the porosity.

LTE assumption is valid in cases of fluid-saturated porous media (Nakayama and Kuwahara, 2005) and has been used recently by several researchers (Chourasia and Goswami, 2007; Getahun, 2016; Hoang et al., 2015; Laguerre et al., 2008).

For transient flows where there is heat generation of solids, LNTE model is used to predict this flow accurately. In this approach, the energy conservation equation for the fluid zone and solid zone are solved separately.

Energy conservation for the fluid zone

$$\left[\varepsilon_p \frac{\delta \bar{T}_i}{\delta x_i} + \bar{u}_\iota \left(\frac{\delta \bar{T}_f}{\delta x_i} + \frac{1}{\rho_f Cp_f}\frac{\delta \bar{p}}{\delta x_i}\right)\right] = \varepsilon_p \frac{\delta}{\delta x_i}\left(\frac{\lambda_{eff}}{\rho_f Cp_f}\frac{\delta \bar{T}_f}{\delta x_i}\right) + \frac{A_{sf} h_{sf}}{\rho_{f Cp_f}}(\bar{T}_s - \bar{T}_f) \tag{2.8}$$

Energy equation for the solid zone

$$\left[(1-\varepsilon_p)\frac{\delta \bar{T}_s}{\delta t}\right] = (1-\varepsilon_p)\frac{\delta}{\delta x_i}\left(\frac{\lambda_s}{\rho_s Cp_s}\frac{\delta \bar{T}_s}{\delta x_i}\right) + \frac{A_{sf} h_{sf}}{\rho_{f Cp_f}}(\bar{T}_f - \bar{T}_s) \tag{2.9}$$

Where A_{sf} is the interfacial area density (specific area) which is the ratio of the fluid-solid interface area to the volume of the porous zone. In a package box of apples, the carry bag offers heat transfer resistance between the cooling air and a single apple. This internal resistance is not neglected in LNTE model and can be expressed as $R/4\lambda$ (Hoang et al., 2015).

The fluid-solid convective heat transfer coefficient can be expressed by Eqn (2.10).

$$h_{sf} = \frac{1}{\left(\frac{1}{h_{conv}} + \frac{R}{4\lambda}\right)} \tag{2.10}$$

Wakao and Kagei (1982) proposed a Nusselt number correlation to determine the convective heat transfer coefficient (h_{conv}) for a disordered pack of spheres

$$Nu = \frac{h_{conv} D}{k_f} = 2 + 1.1 Re^{0.6} Pr^{1/3} \tag{2.11}$$

Where D is the diameter of fruit ($\approx$ 0.08m) and k_f is the thermal conductivity of the cooling air ($W\ m^{-1}k^{-1}$) , Pr is the air prandtl number which is 0.72, Re is the Reynolds number based on the diameter of fruit and the flow rate.

For a porous bed of spherical particles, Nield and Bejan (2013) also proposed a correlation for determining the fluid-solid convective heat transfer coefficient and

was used by Gruyters (2019) to determine the heat transfer within stacked fruit bins in a cold room.

$$h_{sf} = \frac{D}{Nuk_f} + \frac{D}{\beta k_s} \tag{2.12}$$

The solid-fluid convective heat transfer expression proposed by Hoang et al. (2015) and Nield and Bejan (2017) was correlated graphically with the Nusselt expression proposed by Wakao and Kagei (1982). Figure 2.14 shows the plot of solid-fluid convective heat transfer coefficient against the Nusselt number.

2.4.2 Turbulence modelling

There is a transition from orderly laminar flow to a chaotic turbulent flow when airflow is disturbed by stacks of packaged fruit in the refrigerated container. A turbulent flow is characterised by turbulent eddies. Turbulence modelling is integral in determining the accuracy of CFD simulation (Defraeye et al., 2013).

Turbulent flow regime can be characterised by the following properties (Schobeiri, 2010);

- Turbulent flow properties continuously undergo spatial and temporal changes because of the irregularity of the turbulent flow
- Turbulent flows are unsteady, three-dimensional flows
- Turbulent flow occurs at high Reynolds numbers
- Turbulent flows are characterised by rotational motions which produces different sized eddies in different direction.

Turbulent flows can be predicted with CFD using the following major approaches; Direct Numerical simulation (DNS), large-eddy simulation (LES), and Reynolds-averaged Navier stokes (RANS) simulation with turbulent models (Zhai et al., 2007). In the DNS which is the most accurate, the turbulent flow equation is solved without approximation, and the whole range of scales (spatial scale, temporal scale, Kolmogorov scale, integral scale) are explicitly resolved (Gruyters, 2019; Zhai et al., 2007). A very fine mesh grid resolution is used in this approach to capture all the turbulent fluctuations in turbulent flow (Gruyters, 2019; Zhai et al., 2007). The mesh grid resolution in DNS is smaller than the Kolmogorov microscale (η (m)) and the simulation is run at a very small-time steps (Kolmogorov time scale, τ (s^{-1})) to capture all the turbulent flow motions. The equations for the parameter are presented;

$$\eta = \left(\frac{\nu^3}{\varepsilon}\right)^{\frac{1}{4}} \tag{2.13}$$

$$\tau = \left(\frac{\nu}{\varepsilon}\right)^{\frac{1}{2}} \quad (2.14)$$

where ν is kinematic viscosity (m^2s^{-1}) and ε is turbulent dissipation rate (m^2s^{-3}) (Gruyters, 2019)

Large eddy simulation was developed with the hypothesis that the large eddies and small eddies in the turbulent motion are separated (Zhai et al., 2007). In this approach, the small eddies are implicitly accounted for using sub-grid scale model while the large eddies are explicitly resolved. LES approach provides an explicit insight in turbulence with a relatively more efficient computational cost and time (Gruyters, 2019). The RANS approach uses time-averaged Navier Stokes to describe the effects of turbulence on mean flow properties (Zhai et al., 2007). In this approach, the Reynolds-averaged flow parameters for steady-state and dynamic flows are calculated, and different turbulence models are used to simulate the fluctuating turbulence effect (Zhai et al., 2007). Limited Computational resources are required in this approach when compared to DNS and LES. Also, it is the mostly used in modelling enclosed environments (Zhai et al., 2007). Different turbulence modelling has been developed for different specific flows in engineering application.

2.4.2.1 Governing equations

The dynamic behaviour of fluid is represented by solving the conservation equations (mass, momentum and energy) represented below (Versteeg and Malalasekera, 2007);

Continuity equations

$$\frac{\partial \rho}{\partial t} + div(\rho \boldsymbol{u}) = 0 \quad (2.15)$$

Momentum equations

X-momentum

$$\frac{\partial(\rho u)}{\partial t} + div(\rho u \boldsymbol{u}) = -\frac{\partial \rho}{\partial x} + div(\mu\ grad\ u) + S_{Mx} \quad (2.16)$$

Y-momentum

$$\frac{\partial(\rho v)}{\partial t} + div(\rho v \boldsymbol{u}) = -\frac{\partial \rho}{\partial y} + div(\mu\ grad\ v) + S_{My} \quad (2.17)$$

Z-momentum

$$\frac{\partial(\rho w)}{\partial t} + div(\rho w \boldsymbol{u}) = -\frac{\partial \rho}{\partial z} + div(\mu\ grad\ w) + S_{Mz} \quad (2.18)$$

Energy Equation

$$\frac{\partial(\rho i)}{\partial t} + div(\rho i \boldsymbol{u}) = -p\ div\ \boldsymbol{u} + div(k\ grad\ T) + \Phi + S_i \quad (2.19)$$

where

p =p (ρ, T) and i = i (ρ, T)

Perfect gas $p=\rho RT$ and $i = C_v T$

2.4.2.2 Turbulence modelling in postharvest application

Choosing the appropriate turbulence models is an important consideration in CFD simulation because of the wide range of variability in their performance (Defraeye et al., 2010). Steady Reynolds-averaged Navier-Stokes (RANS) is mostly used in food engineering applications compared to unsteady approaches (Large eddy simulation) (Kondjoyan, 2006).

To compute the turbulent flows with the RANS equation, turbulence models are used to predict the Reynolds stress, the scalar transport system and close the equation (Versteeg and Malalasekera, 2007). All turbulence models rely on the turbulent kinetic energy (κ), turbulent dissipation rate (ε) and turbulent length scale. These properties incorporate the effect of turbulence in different turbulence models. Most RANS models are classified by the number of additional transport equations needed to be solved with the RANS flow equations (Versteeg and Malalasekera, 2007). Table 2.4 shows the classification of turbulence modelling based on the number of transport equations.

Standard two-equation turbulence model (κ-ε, κ-ω) have been used in different food engineering applications (Norton and Sun, 2006; Smale et al., 2006; Verboven et al., 2006; Xia and Sun, 2002; Zhao et al., 2016). Standard κ-ε utilised the additional transport equations to solve for κ and ε, assuming that the turbulent viscosity is isotropic (Launder and Spalding, 1974; Schobeiri, 2010). This model performs accurately at low Reynolds number, recirculating flows and where no or minor separation occurs. In application where there is adverse pressure gradient or where there is major separation, its performance is poor (Hu and Sun, 2001; Schobeiri, 2010). Menter (1992) noted the numerical stiffness of this model transport equation when the viscous sublayer is integrated. Standard κ-ω turbulence model performs better than the Standard κ-ε turbulence model under adverse pressure gradient conditions (Schobeiri, 2010). This model uses the turbulent specific dissipation rate (ω) transport equation as the second variable. Also, this model accurately captures the near-wall region (viscous sub layer) with Dirichlet boundary condition (Schobeiri, 2010; Versteeg and Malalasekera, 2007).

The model has more numerical stability than the standard (κ-ε) turbulence model. The dependency on the free stream values of the κ and ω is a major limitation in this model (Menter, 1993).

Menter (1992) suggested a hybrid model which transforms the κ-ε model to a κ-ω model at the near-wall region and uses the κ-ε model at the fully turbulent region far from the wall. This hybrid model is the shear stress transport (SST) κ-ω turbulence model, and it introduces a blending function that enhances the smooth transformation of the turbulence model at the near-wall region and fully turbulent region. Defraeye et al. (2013) evaluated the performance of several steady Reynolds averaged Navier-Stokes turbulence model for fluid flow across a representative model for spherical food products. Different flow parameters (drag coefficient, nusselt number, and separation angle) was compared with empirical data for a Reynold number range of 10 to 3.2×10^4. At high Reynolds number, all the standard κ-ε model version shows a huge difference from the empirical data. Standard κ-ω models show a better performance than all the versions of the κ-ε model. Shear stress transport (SST) κ-ω turbulence model performed best within the Reynolds range (airspeed) for postharvest application and food processing (Defraeye et al., 2013). Also, SST κ-ω produce the least error among other turbulence models in predicting the airflow distribution in a cold room (Delele et al., 2009). This model has been extensively used in CFD model development in postharvest applications (Ambaw et al., 2013b; Ambaw et al., 2014; Berry, 2017; Berry et al., 2016; Defraeye et al., 2014; Getahun, 2016; Getahun et al., 2018; Gruyters, 2019; Han et al., 2017; Han et al., 2015). Table 2.5 shows the percentage difference between the numerically obtained results of flow parameters and empirical data.

2.4.3 Performance evaluations techniques for cold chain systems

A detailed understanding of the influence of different design parameters and operating conditions of a refrigerated container is important to improve the performance of a cold chain system (O'Sullivan et al., 2014). These design parameters allow researchers to compare the performance of existing designs or condition to new ones (Zhao et al., 2016). Example of performance parameters being measured and evaluated in a cold chain system are cooling time, cooling rate, cooling uniformity (Ambaw et al., 2017; Berry, 2017; Delele et al., 2013; Getahun, 2016; Hoang et al., 2015; Hoang et al., 2000; Zhao et al., 2016), mechanical strength (Berry, 2017; Fadiji et al., 2018; Fadiji et al., 2016; Pathare et al., 2012), energy consumption (Getahun, 2016; Mukama et al., 2017) and heat transfer coefficient (CHTC) (Berry, 2017; Hoang et al., 2015). CFD provides essential information on the performance of postharvest activities. For cold

storage application like a refrigerated container, it is compulsory to validate your CFD models with experimental data experimentally.

Temperature, velocity and pressure measurement is highly recommended to validate postharvest CFD models. For quantitative local velocity measurements, there are several techniques available such as Lasser Doppler Anemometry (LDA), particle image velocimetry (PIV), thermal anemometry and data loggers with candle stick sensors. CFD practitioner will have to determine the prediction error using validation studies. CFD prediction error can be calculated as the ratio of the absolute difference of the numerical results and experimental results to the results obtained experimentally (Hoang et al., 2000).

$$Error = \frac{\sum_{i=1}^{n}(U_{cfd}^{i} - U_{exp}^{i})}{\sum_{i=1}^{n} U_{exp}^{i}} \quad (2.20)$$

2.4.3.1 Airflow measurement and evaluation technique

It is necessary to characterise the behaviour of airflow in cooling and drying applications because the understanding will lead to the development of a better design process (O'Sullivan et al., 2014). There are two major types of airflow measurement technique namely: Direct airflow techniques and non-invasive qualitative methods. Direct flow measurement employs the use of different devices to measure the air-flow velocities at different point values in a system. These techniques include thermal anemometry, vane anemometry and pressure anemometry. Thermal anemometry involves the use of a thermal anemometers to measure the air-velocity which is calculated/inferred from the power required to maintain the temperature of the sensor (*P=IV*, Power required to maintain temperature = current of the sensor × air velocity of the point of the system) (O'Sullivan et al., 2014). Several researchers have used thermal anemometry to measure airflow in different cold chain applications (Alvarez & Flick, 1999; Delele et al., 2008; Ngcobo, 2013; Verboven et al., 2005).

Vane anemometers are used to measure the average velocity of airflow of a region within the system. It is simple to use and mainly used where a portable measurement device is required (O'Sullivan et al., 2014). The accuracy of the measured velocities depends heavily on the vane angle, which must be precisely known before measurements can be taken (Mirade and Daudin, 1998). Several researches have used vane anemometry in measuring airflow velocities in food operations (Hossain and Bala, 2007; Lawrence and Maier, 2011; Nagle et al., 2010). Differential flow meters determine the flow velocity by calculating the pressure components, the devices used to record pressure differences are classified into manometers and pressure transducers (O'Sullivan et al., 2014).

Several researches in food operations have used differential flow meters in air-flow measurements (Dehghannya et al., 2008; Khatchatourian et al., 2009; Ngcobo et al., 2012). Non-invasive qualitative methods are visualisation techniques which gives accurate assessment of airflow behaviour in a system (O'Sullivan et al., 2014). Examples of this techniques include: smoke and helium bubbles (Ruegg et al., 1994), the smoke-wire technique (Lohan et al., 2002), tracer gas methods (Smale, 2004), laser doppler anemometry (Alvarez et al., 2003), as well as particle image velocimetry (Laguerre et al., 2009). Wind tunnels are used to experimentally investigate the aerodynamic characteristics for different models (Ristić et al., 2004). The flow velocity can be measured in a wind tunnel tests indirectly by measuring the stagnation and static pressures of the flow (Ristić et al., 2004) and can be measured directly using candle stick sensors at the wind tunnel outlet (Getahun, 2016). The relation between the mean velocity of flow, stagnation pressures and static pressures is as follow:

$$V = (2(P_t - P_{st})/\rho)^{0.5} \tag{2.21}$$

where P_{st} is the stagnation pressure and P_t is the static pressure. Pressures can also be measured in a wind tunnel with a combination of probes and elastic transducer (Ristić et al., 2004) and with a differential pressure meter (Getahun, 2016). Getahun (2016) uses a wind tunnel experiment set-up to determine the pressure drop characteristics of a stacked pallet. The author used plastic balls filled with water to represent the fruit in the pallet, and the pallet was halved into two equal parts along the y-axis. This set-up allows the characterisation of airflow with the pressure drop vs airflow data corresponding to flow of air in the horizontal, vertical and transverse directions. Superficial velocity can be measured at the outlet of the wind tunnel using a data logger with candlestick sensors. A differential pressure meter with a data controller was used to measure and record the pressure drop across the pallet stack. This gives the pressure drop characteristics of the stacked pallet (bottom and top half) (Getahun, 2016). The plot of the pressure drop vs airflow characteristics is used to investigate airflow resistance of the stacked pallet in all the direction, and it has a direct relationship with vent-hole area of packaging boxes (Delele et al., 2013). The fitting of the pressure drop and airflow data points into Darcy-Forchheimer equation (Eqn. (2.4)) gives the viscous ($C_f/\kappa^{0.5}$) and inertial coefficient (κ) when using the porous medium approach of CFD modelling (Getahun, 2016). Air velocity measurement in a loaded refrigerated container are measured using candlestick air sensors at different regions within the container. The sampling points of the measurement were at the free region between the pallet rows, the region between the stack and the container ceiling, and the region between the container door and stack (Getahun, 2016).

2.4.3.2 Cooling measurement and evaluation technique

The cooling rate and cooling uniformity of the packaged fruit indicates the efficiency of the cooling process (Vigneault et al., 2004). A dimensionless temperature can be used to analyse the cooling kinetics of the produce (Ambaw et al., 2017; Defraeye et al., 2013). The dimensionless temperature (*Y*) is expressed as (Zhao et al., 2016):

$$Y = \frac{T_p - T_a}{T_{pin} - T_a} \tag{2.22}$$

where T_p is the temperature of the fruit at different sampling points when loaded in a refrigerated container, T_a is the cooling air temperature of the refrigerated container and T_{pin} is the initial temperature of the fruit (Berry, 2017; Zhao et al., 2016).

The dimensionless cooling curve (dimensionless number against time) evaluates the cooling time of horticultural produce by determining the half cooling time (HCT) and the seven-eighths cooling time (SECT). They are analytically derived from the fruit temperature cooling curve (Eqn. (2.23). HCT is a robust parameter used in comparing cooling time of pallet.

$$t_{1/2} = \frac{\ln(2\,j)}{C}; \quad t_{7/8} = \frac{\ln(8\,j)}{C} \tag{2.23}$$

where *C* is the coefficient of cooling and *j* is the lag factor

Half cooling time (HCT) and seven-eighths cooling time (SECT) correspond to when *Y*= 0.5 and when *Y*= 0.125, respectively (Defraeye et al., 2016; Zhao et al., 2016). HCT and SECT are robust parameterused to evaluate the cooling rate and cooling uniformity of palletised fruit within a refrigerated container. It is useful to measure the cooling time of fruit as it enables direct comparison of cooling rates of fruit in different starting or finishing conditions (Defraeye et al., 2016). The temperature of fruit can be measured by inserting thermocouples to the core of the fruit at different sampling points in different regions (Ambaw et al., 2017; Defraeye et al., 2016; Getahun, 2016) within a refrigerated container.

Cooling uniformity can also be quantified using the heterogeneity index for temperature (Zhao et al., 2016) and convective heat transfer coefficient (CHTC) (Berry et al., 2016; Defraeye et al., 2015a). The CHTC is used to assess cooling heterogeneity by determining the relative standard deviation of the heat transfer coefficients across fruit surfaces. Low percentage of relative standard deviation indicates uniformity in cooling, while a high percentage indicates non-homogenous cooling (Berry, 2017).

2.4.3.3 Energy performance evaluation technique

A Refrigerated container energy consumption is determined by different operational and design parameters. The operational design parameters include the geometric design of the container, thermal insulation, operation of the container axial fan, packaging design type, pallet stacking types and the defrost load. The most dominant factor that affects the energy consumption of a refrigerated container is the heating load that is removed from the produce during long term transportation. The age of the refrigerated container and the respiration of loaded fruits also influence the energy consumed during the refrigerated container operation (Thompson et al., 2010). The highest heat load source from the refrigerated container is from the evaporator fan and can be expressed mathematically as (Evans et al., 2014);

$$Q_{fan} = \frac{N_m P_m}{\eta_{mot}} \tag{2.24}$$

where N_m is number of motor, η_{mot} is the efficiency of motors and P_m is the power of the motor.

Thompson et al. (2010) identified different opportunities by which energy consumed by the refrigerated container can be reduced without hindering the performance. They include improving the fan operation by using variable speed fans and using well-ventilated packaging boxes. During transportation, a standard energy meter can be used to measure the energy consumed (KWh) by the refrigerated container. This records the energy required to keep the compressor working, evaporator fans (Defraeye et al., 2016).

2.5 Conclusion

This review examined in detail the working principles of refrigerated containers and the importance of computational fluid dynamics as a tool in postharvest cold chain evaluations. Different modelling approaches have been used to investigate the airflow distribution and temperature evolution of fruits in cold chain applications. Explicit modelling approaches require higher computational load (time, cost) than the porous media approach. Both techniques have been widely used in different application in the food industry.

Porous media uses local thermal equilibrium (LTE) and local thermal non-equilibrium (LNTE) models to model heat transfer. The local thermal equilibrium method assumes negligible temperature difference between the solid and liquid phase and uses a single energy equation to describe the thermal equilibrium of the heat transfer. For applications that shows a significant temperature difference between the solid and fluid phase and heat generation of the solid, local non-

thermal equilibrium is used to predict the flow accurately. Energy equation of the solid and fluid phase are solved separately and coupled by the fluid-solid convective heat transfer coefficient.

The accurate modelling of turbulent flows is important in determining the accuracy of CFD simulations. The performance of different turbulence models (standard κ-ε, standard κ-ω, SST κ-ω) have been assessed for different postharvest and food application. From different studies, the hybrid model (SST κ-ω) yields the least error of different turbulence model. This hybrid model uses a blending function to combine the performance of the standard κ-ε and κ-ω turbulence models and it gives a the least error in predicting the flow parameters.

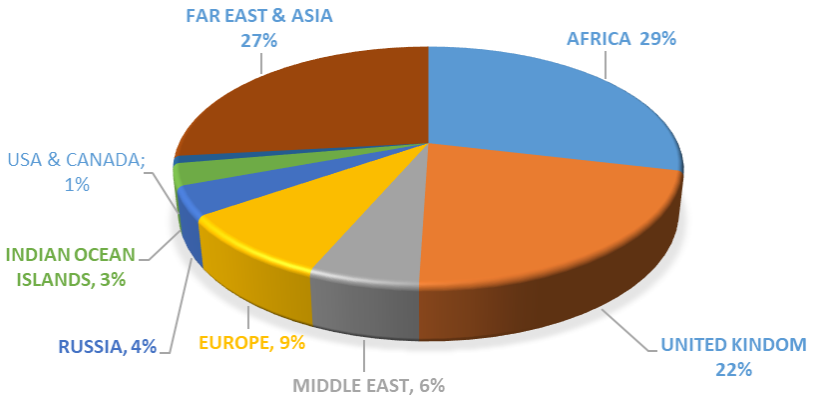

Figure 2.1: Pie-chart showing distribution of apple fruit exports from South Africa to the global regions (Hortgro, 2018).

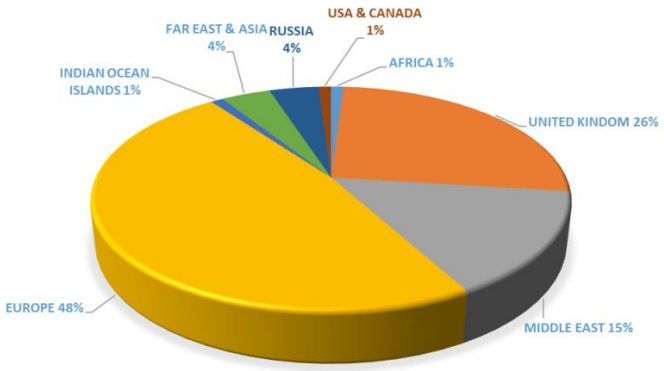

Figure 2.2:Pie-chart showing distribution of plum fruit export from South Africa to the global regions (Hortgro, 2018).

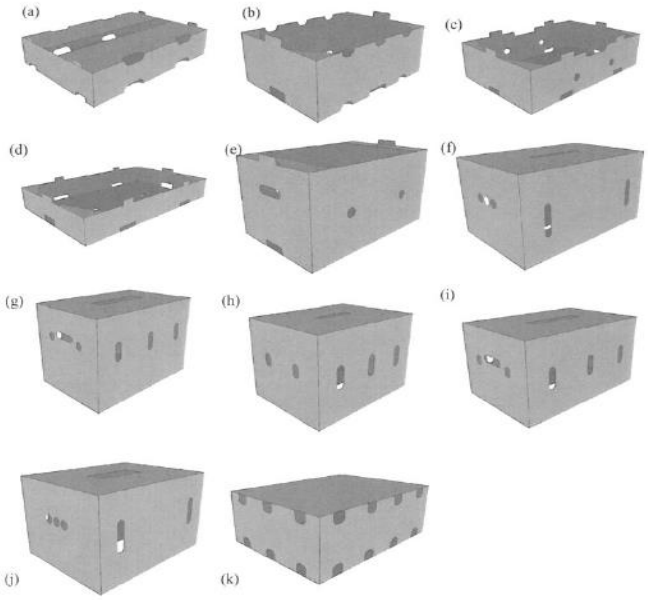

Figure 2.3: An outline of the IFCC classification of carton types a) micro D b) mini-mark 9 c) mark 9 d) mark 7 e) Econo D f) Econo T g) Bushel h) mark 6 i) mark 4 j) jumble and k) mini T (Berry et al., 2015).

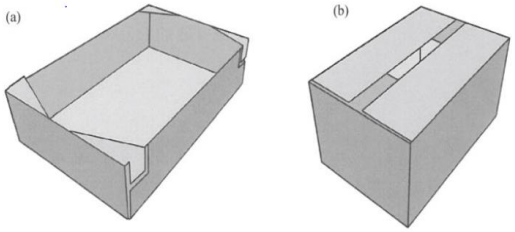

Figure 2.4: An outline of a) Display carton b) Telescopic carton design (Berry et al., 2015).

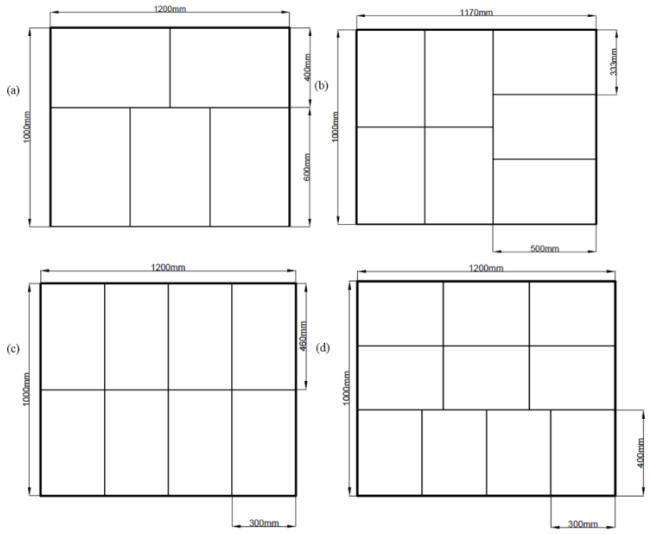

Figure 2.5: Pallet stacking configurations showing a) 5 b) 7 c) 8 d) 10 cartons per layer (Berry et al., 2015).

Figure 2.6: A general model of an Export ISO standard pallet design.

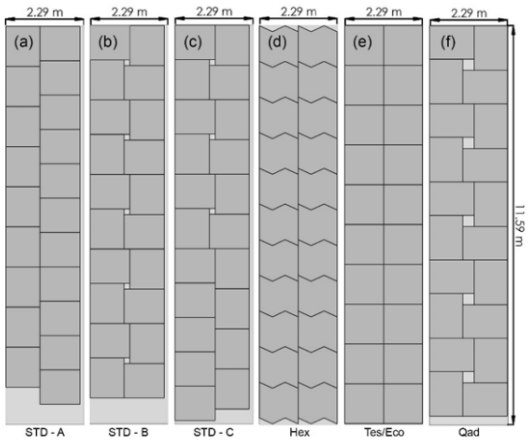

Figure 2.7: Pallet stack loading strategies investigated by Berry et al. (2018).

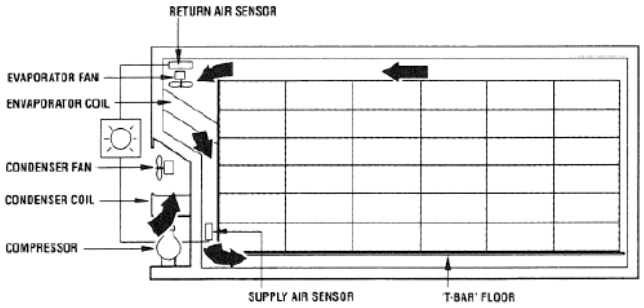

Figure 2.8: The main components in a mechanically refrigerated container (IIR, 1995).

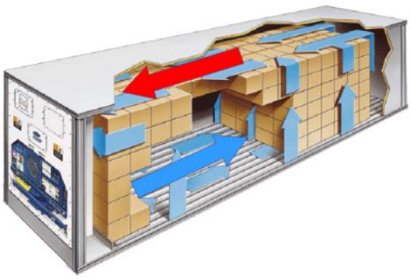

Figure 2.9: Airflow distribution in a refrigerated container (Wild, 2009).

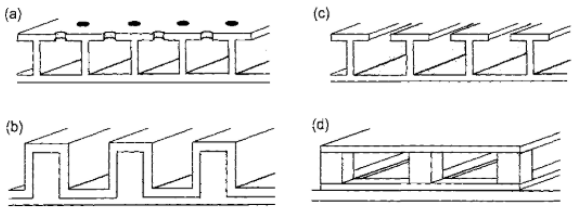

Figure 2.10: Different flooring types and design in refrigerated container (a) Perforated floor (b) Castellated floor (c) T-bar floor (d) Flat floor (Smale , 2004).

Figure 2.11: T-bar flooring system in a refrigerated container.

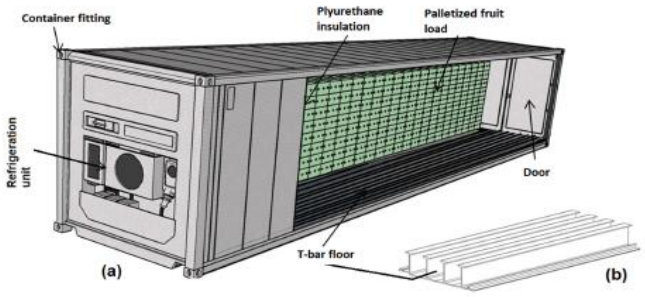

Figure 2.12: A partially packed refrigerated container with a T-bar floor (Getahun, 2016).

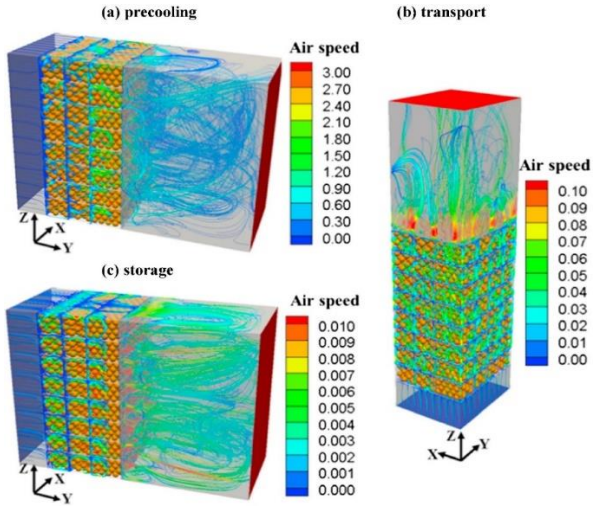

Figure 2.13: Explicit modelling approach example where the package materials were explicitly modelling and the fruit filling pattern was also explicitly considered (Wu & Defraeye, 2018).

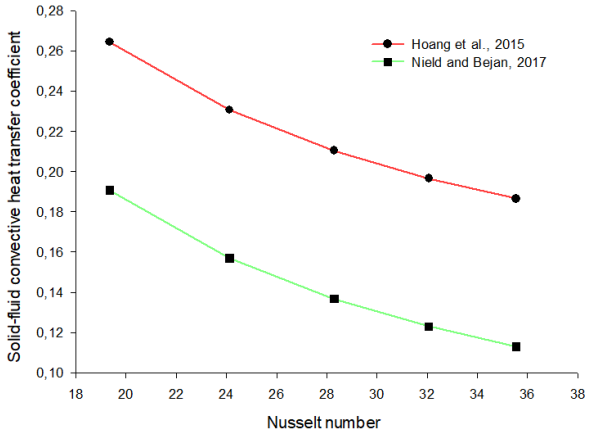

Figure 2.14: Plot of solid-fluid convective heat transfer coefficient against the Nusselt number (Hoang et al., 2015; Nield & Bejan, 2017).

Table 2.1: 2018 total pome/stone fruit total productions and exported(Hortgro, 2018).

Fruit types	Total production(tons)	Export (tons)
Pome fruit		
Apples	835 873	393 344
Pears	402 738	212 149
Stone fruit		
Plums	75 184	53 808
Apricots	39 849	3 435
Peaches	163 170	15 940
Cherries	611	277

Table 2.2: Pallet dimensions according to ISO standard (*Myburgh, 2016*).

Pallets according to the ISO standard	Countries mostly used in	Dimension (mm)		
		Length	Width	Height
ISO 1 pallet (Euro pallet)	Europe	1200	800	160
ISO 2 pallet (Standard pallet)	South Africa	1200	1000	162
ISO 3 pallet	American regions	1219	1016	142
ISO 4 pallet	North America, Europe and Asia	1067	1067	140
1SO 5 pallet	Asia Pacific region	1100	1100	160
ISO 6 pallet	Europe	1140	1140	138

Table 2.3: Power consumption and cooling capacity of Thermo king refrigeration unit at different container temperature (Wild, 2009)

Container temperature (℃)	Cooling capacity (W)	Power consumption (KW)
21	13 507	12
2	11 456	10.5
-18	5 604	6
-29	3 023	4.5

Table 2.4: Classification of turbulence modelling based on the number of transport equation (Versteeg & Malalasekera, 2007).

Number of extra transport equation	Turbulence models
Zero	Mixing length model
One	Spalart-Allmaras model
Two	Algebraic stress model
	Standard κ-ε model
	RNG κ-ε model
	Realizable κ-ε model
	Standard κ-ω model
	SST κ-ω model
Seven	Reynolds stress model

Table 2.5: Percentage difference between the numerically obtained results of different flow parameters and empirical data (Defraeye et al., 2013).

		Standard κ - ε model	RNG κ-ε model	Standard κ-ω model	SST κ-ω model
Re = 1 375	Drag Coeff.	24.88	24.07	-12.21	1.7
	Nu	4.01	5.67	-4.36	-3.36
	Angle	8.02	7.66	-1.29	0.84
Re = 4 500	Drag Coeff.	13.35	11.83	-11.52	1.95
	Nu	9.58	11.49	-3	-3.57
	Angle	9.87	9.27	-2.82	-0.57
Re = 20 000	Drag Coeff.	-99.05	-117.78	-28.6	-12.82
	Nu	22.07	24.28	-1.83	2.63
	Angle	21.4	21.44	-4.62	-1.47

Chapter 3. Modelling a Fully Loaded Refrigerated Container with a Functional Refrigeration Unit in CFD

3.1 Introduction

Refrigerated transport is an important component of the horticultural cold chain system which also includes pre-cooling of fruit, cold storage, distribution centre and refrigerated display in retail outlets (Berry et al. 2017). Fresh produce temperature is an essential factor that affects the fruit senescence rates, quality preservation and shelf life (Robertson, 2013; Thompson et al., 2010). Fresh produce deterioration rates are reduced by lowering the temperature during shipping using a refrigeration-controlled system in combination with ventilated packaging systems to allow cold air to reach the individual fruit (Ladanyia, 2010; Opara and Zou, 2006).

The objective of this study to develop and validate a CFD model that characterises the airflow and heat transfer inside a refrigerated container. The modelling approach of the components of this model is different from present work that has been developed. The cooling fan was implicitly represented by conducting an axial performance experiment on the refrigerated container. A swirling or mixing effect was considered to reduce the discrepancies between the simulation results and experiment results. The developed model further incorporates a realistic refrigeration unit with an accurate thermal sink. Local thermal non-equilibrium model was used to model heat transfer within the pallet stack (porous medium) as there is a substantial difference between the experimentally determined air and pulp temperature. The validated model results in realistic airflow distribution and cooling pattern of palletised fruit within the refrigerated container.

3.2 Numerical model development

3.2.1 Computational domain

The computational domain for the refrigerated container internal dimension is 11.59 m long, 2.29 m wide and 2.55 m high (internal volume: 67.6 m^3). The computational domain (Figure 3.1) contains twenty pallets which are arranged in two rows inside the container. The dimensions of the pallet stack in each row are specified in Table 3.1.

The pallet stacks are assumed as a porous media, and its directional loss properties are specified in Table 3.2. Local thermal non-equilibrium model was used to model the heat transfer in pallet porous media. The cooling fan, which includes a rotational/mixing or “swirling” effect, was implicitly represented in the model by

conducting an axial fan performance experiment. The physical properties of the apple fruit are listed in Table 3.3.

3.2.2 Governing equations

3.2.2.1 Air domain

Please refer to section 2.4.2.1 for a description of the air domain governing equations.

3.2.2.2 Pallet modelling

The modelling approach for the pallet is an important factor in the airflow characterisation and heat transfer in a refrigerated container. Two major strategies to model pallet stacks in the cold chain include the solid block approach and porous media approach. Hoang et al., (2015) examined these approaches (Solid block approach and porous media approach) and its influence in airflow and heat transfer predictions in a cold room. It was found that the solid block approach requires five times the computational time (cost) compared to the porous media approach.

The porous media approach was thus applied in this study. To achieve this, the airflow in the pallet stack is first characterised by Darcy- Forchheimer equation (Eqn. (3.1)). This equation expresses the pressure drop in relation to the Darcy velocity (Superficial velocity). Flow resistance is generated by adding a source term in the momentum equation.

$$\begin{aligned} S_{PM_x} &= -\frac{\mu}{K_{perm}}u - \rho\left(\frac{C_f}{K_{perm}^{\frac{1}{2}}}\right)|\boldsymbol{u}|u \\ S_{PM_y} &= -\frac{\mu}{K_{perm}}v - \rho\left(\frac{C_f}{K_{perm}^{\frac{1}{2}}}\right)|\boldsymbol{u}|v \\ S_{PM_z} &= -\frac{\mu}{K_{perm}}w - \rho\left(\frac{C_f}{K_{perm}^{\frac{1}{2}}}\right)|\boldsymbol{u}|w \end{aligned} \tag{3.1}$$

where the momentum loss (S_{PM_i}) in the pallet porous domain can be represented using the permeability (K_{perm}) and Forchheimer (C_f) coefficients (Zhao et al., 2016b).

The linear component of the momentum loss equation represents the viscous resistance coefficient D_l (kg m^{-3}s^{-1}) while the quadratic component of the equation represents the inertial resistance coefficients D_q (kg m^{-4}). The momentum loss equation can be re-written as

$$S_{PM_i} = -D_l u - D_q|\boldsymbol{u}|u \tag{3.2}$$

where *i* refers to Cartesian coordinates direction (*x*, *y* or *z*)

Getahun et al., (2017a) derived the values summarised in Table 2.2 experimentally using a wind tunnel that determines the pressure drop as a function of the superficial air velocity.

In transient problems where the apple is generating heat, a local thermal non-equilibrium model was used to simulate the transfer between apple and air. The energy conservation equation of the fluid (air) phase and solid (apple) phases are solved individually (Eqn. (3.3) and (3.4))

Conservation of Energy equation for the solid phase (apple) (Nield & Bejan, 2017)

$$\left[(1-\varphi)(\rho c)_s \frac{\delta T_s}{\delta t}\right] = \left[(1-\varphi)\nabla.(k_s \nabla T_s) + (1-\varphi)q_s''' + h(T_f - T_s)\right] \quad (3.3)$$

Conservation of Energy equation for the fluid phase (air) (Nield & Bejan, 2017)

$$\left[\varphi(\rho c_p)_f \frac{\delta T_f}{\delta t} + (\rho c_p)\mathbf{v}.\nabla T_f\right] = \left[\varphi\nabla.(k_f \nabla T_f) + \varphi q_f''' + h(T_s - T_f)\right] \quad (3.4)$$

where h is the heat transfer coefficient, φ is the volumetric porosity of the pallet stack, c_p is the specific heat capacity of air (1004.4 $Jkg^{-1}°C^{-1}$), c is the specific heat capacity of apple (3780 $Jkg^{-1}°C^{-1}$), s and f refers to subscripts for solid phase (apple) and fluid phase (air), k_s is the thermal conductivity of the apple (0.580 $Wm^{-1}°C^{-1}$), k_f is the thermal conductivity of the air (0.024 $Wm^{-1}°C^{-1}$), density of apple (898 kgm^{-3}) and density of air (1.28 kgm^{-3}), q_f''' and q_s''' represents heat generated per unit volume by solid phase (apple/packaging) and fluid phase (air) (Gruyters et al., 2018; Lisowa et al., 2001; Nield & Bejan, 2017). The energy equations for the solid (apple/packaging) and fluid (air) phase are coupled by the overall heat transfer coefficient (h) and interfacial specific area (A_{sf}) (Nield & Bejan, 2017).

The interfacial specific area (total surface area of apples per unit volume) (Eqn. (3.5)) is given by;

$$A_{sf} = 6(1-\varphi)/d \quad (3.5)$$

The overall heat transfer coefficient (Eqn. (3.6)) between the apple and air is determined using the Nusselt number expression (Eqn. (3.7)) (Nield & Bejan, 2017)

$$h = \frac{d}{Nuk_f} + \frac{d}{\beta k_s} \quad (3.6)$$

$$Nu = \frac{h_{conv} d}{k_f} = 2 + 1.1Re^{0.6}Pr^{1/3} \quad (3.7)$$

β equals to 10 for a porous bed of spherical particles, *Pr* is the Prandtl number for air (0.72) and d is the diameter of apple.

3.2.3 Refrigeration unit

To realistically replicate the mixing action of the axial fan blades on airflow, swirling flows with turbulence was incorporated in the refrigeration unit (RU) model. This feature was incorporated to ensure air exiting the simulated refrigerated unit was of uniform temperature. To achieve this, air entering the RU, which often has a temperature gradient perpendicular to the airflow must be mixed. The solution chosen in this study was to incorporate a swirling or rotational momentum source term and to design an appropriate geometric design that would induce the necessary air swirling and turbulent mixing of the cooling air. Various RU designs were tested in isolation. This iterative modelling approach aimed to determine the appropriate geometry of the refrigeration unit and duct design that would ensure turbulent mixing of cooling air and deliver cooling air at a constant temperature across the air supply region. At the air supply region of the container, the temperature of the cooling air was taken to determine the temperature gradient of air across the region. Figure 2.2 shows the different geometric designs of the refrigeration unit and the resulting temperature of air across the air supply region. There were large temperature gradients across the air supply region (Figure 3.2 (a), Figure 3.2 (b) Figure 3.2 (c), Figure 3.2 (d), Figure 3.2 (e)). These designs resulted in a supply of airflow with a heterogeneous temperature gradient. Turbulent mixing of air in the refrigeration unit achieved in the final design (Figure 3.2 (f)) to maintain a constant temperature of the supplied airflow.

3.2.4 Simulation set-up and assumptions

All numerical simulations were run using ANSYS CFX 19.1 CFD code, using high-resolution Advection scheme and high-resolution turbulence numeric for steady-state simulation. Steady-state simulation was first carried out to obtain the airflow characterisation in the refrigerated container and were then used as the initial conditions for the transient simulation.

The axial fans were implicitly represented in the model by performing an axial fan performance experiment. An expression using the geometry of the fan (fan length, fan radius), flow rate of the fan and fan system curve was coupled as a momentum source using CFX Expression language. The swirling effect of the fan was incorporated in the model as it allows the discharged airflow to better approximate experimental conditions (Hoang et al., 2015). For the transient cooling process of the fruit, the cooling capacity of the refrigerated container and the temperature cooling mode was implicitly represented in the model.

A SST k–ω turbulence model was used to determine the airflow characterisation and temperature distribution in the refrigerated container. Various assumptions were used in developing the numerical model of a refrigerated container.

- Volume porosity of the pallet stack was assumed to be uniform spatially and temporarily. The volume porosity of the pallet stack is the ratio between the volume of solid (apple and packaging materials) and the total volume of the porous domain (=0.567).
- A local thermal non-equilibrium model was used in modelling the transfer of heat from the packaged apples.
- The pallet stack was modelled as a two-phase porous model, and the appropriate interfacial area density and heat transfer were specified.
- The T-bar floor was modelled as a no-slip boundary wall.
- Second-Order Backward Euler transient scheme was used for transient simulations.

3.2.5 Mesh sensitivity and error calculation

Mesh Sensitivity analysis were performed to determine the best combination of mesh sizes that accurately predict the flow with the minimum computational load requirement. A steady-state simulation was carried out to show the velocity profile magnitude at the air supply region (Figure 3.4) and the middle section of the T-bar floor region (Figure 3.5). Fine meshes were made at the region of high computational interest (T-bar floor and refrigeration unit). Figure 3.3a and Figure 3.3b shows the computational domain geometry and computational mesh generated along XY section. Table 3.4 shows the number of cells of different meshing type for sensitivity analysis.

The mesh combination for the fine mesh gives approximately the same velocity magnitude profile with less computational load requirements compared to the finer mesh combinations.

A modelling prediction error was used to evaluate the accuracy and performance of the model when compared with the experimental data. The average modelling prediction for the airflow characterisation of the refrigerated container and temperature evolution of apples is obtained respectively using equations (3.8) and (3.9).

$$E_{velo} = \frac{1}{n}\sum_{i}^{n} \frac{||v|^{cfd} - |v|^{exp}|}{|v|^{exp}} \times 100 \quad (3.8)$$

$$E_{temp} = \frac{1}{n}\sum_{i}^{n} \frac{||T|^{cfd} - |T|^{exp}|}{|T|^{exp}} \times 100 \quad (3.9)$$

where E_{velo} and E_{temp} are the prediction errors percentages (%) for temperature (T; ℃) and air velocity (v; m s^{-1}), respectively, n is the number of samples and the subscript *exp* and *cfd* are for experimental and simulation values, respectively.

3.3 Experimental measurements

3.3.1 Axial fan performance experiment

The axial fans was implicitly represented in the model by conducting axial fan performance experiments. Characterisation of the fan was achieved by iteratively modifying the flow rates from the refrigeration unit, and measuring the reciprocal pressure drop across the unit fan using a pressure differential meter (Air Flow Meter Type A2G-50, WIKA, Alexander Wiegand SE & Co. KG, Klingenberg, Germany). Air velocities were measured at the air return region using a RS PRO RS-90 anemometer. The air outlet region was physically obstructed incrementally to capture the performance curve of the axial fan. The resulting axial performance curve and the corresponding function are shown in Figure 3.6.

3.3.2 Temperature gradient

The temperature at the inlet and outlet region of the cooling unit were measured using a Logtag HAXO-8 (South Africa) temperature logger, with a measurement range of -40˚C to +85˚C. Loggers were placed even distances across the inlet and outlet region of the cooling unit throughout the experimental duration. Figure 3.7(a) shows the positioning of the loggers across the inlet and outlet region of the cooling unit and Figure 3.7(b) shows the temperature gradient across the cooling unit.

3.4 Validation of model

3.4.1 Refrigerated container

Validation experiments on a refrigerated container were performed at Two-A-Day Group Ltd (Elgin, South Africa, March 2019). The container was a 40-foot Maersk model, with a Carrier Transicold thin line refrigeration unit (dimensions listed in Table 3.1). The refrigerated container has a T-bar flooring system, as shown in Figure 3.8. There are 35 T-bar extruded surfaces which run along the floor from the refrigeration unit up to the door. Twenty pallet stacks of apple fruit were loaded inside the refrigerated container. The container makes use of a bottom air delivery system to circulate cold air through the T-bar floors to the palletised fruit. Figure 3.9 shows the air circulation inside a refrigerated container equipped with a bottom air delivery system.

3.4.2 Fruit and packaging boxes

Apple fruit (cv. Golden Delicious) were packed into “thrift” carry plastic bags, which are in turn packed into the Econo-D carton and stacked on pallets, as shown in Figure 3.10. The physical properties of the apple are listed in Table 3.3. Sixty-four cartons are packed on each pallet base, which amounts to 768 kg of fruit. Each pallet stack was secured using pallet straps and cornering pieces. See Getahun et al. (2017a), for further detailed specifications of the packaging and its properties.

3.4.3 Air-velocity measurement

Candlestick sensors (Advanced Thermal Solutions Inc, Norwood, USA) were used in conjunction with a TVS 1100 Datalogger to measure air-velocities and air temperature at different regions in the refrigerated container. This instruments were calibrated using a reference calibrator (hot-wire anemometer). Measurements were taken at multiple regions in the container, with an emphasis at regions between the pallet stacks and container ceiling, and between the pallet stack and the container door (Figure 3.11).

3.4.4 Temperature measurement

Fruit and air temperatures in the container were measured using T-type thermocouple (RS PRO, 2core, -10˚C to 105˚C). This instruments were calibrated using ice water experiment. Data were recorded using a data logger (34970A data acquisition unit ±0.1˚C; Agilent Technologies, Santa Clara CA 95051, USA) at 10 min interval throughout the first experiment (16 hours) and the second experiment (42 hours). The probes were positioned in the core of fruit at three vertical layers in the stacks (top = second carton layer, middle = fourth carton layer, bottom = seventh carton layer) as indicated in Figure 3.12. Figure 3.12 further illustrates which pallet stacks were monitored for temperature during the two validation experiments.

3.5 Results and discussion

3.5.1 Airflow characterisation

The average airflow modelling prediction error for the two experimental scenarios (Void plug and No Void plug) was 17% (Figure 3.13). This shows that the model accurately predicts the velocity profile in the refrigerated container and previous studies have shown that the acceptable prediction error falls between 3 - 30%. Getahun et al. (2017a) reported an average prediction error of 26% ± 2% for airflow analysis inside fully packed refrigerated shipping container. In this study, the prediction error across the top, middle and bottom region of the container are 25%, 26% and 30% respectively. For airflow analysis in a loaded cold store,

Hoang et al. (2000) reported prediction error of 26% and 28.5% using RNG and standard κ-ε turbulence model respectively. Moureh et al. (2009) reported a maximum prediction error of 30% for airflow characterization in slot ventilation enclosure. The air velocity prediction error in this study is an improved from previous research studies

Air gaps between the pallet stack rows cause short-circuiting and large bypass of air in the refrigerated container. Air gaps are usually present between the pallets in a fully packed refrigerated container due to: (i) improper stacking of boxes on standard pallet (ii) unutilised floor area and container volume (Defraeye et al., 2015b). In current industry loading practise whereby 10% of the container floor area is left unused (Berry, 2017), there will always be huge bypass of air unless the gaps are closed when at all possible (Berry, 2017; Defraeye et al., 2015b). Defraeye et al. (2015b) evaluated the impact of air gaps between pallet on the cooling rate of fruit. The author discovered that the cooling time of fruit increases as the gap between pallet increase. The demonstrated impact of the air gap on the cooling rate of fruit has motivated researchers to eliminate air gap to reduce the short circuiting of airflow (Defraeye et al., 2015b). This air gap plays a dominant part in the heterogeneity of airflow within the pallet stack. This air gap plays a dominant part in the heterogeneity of airflow within the pallet stack.

Figure 3.14 shows the contour and graph of velocity magnitude of airflow in the free region between the pallet stacks. The simulation model was used to evaluate the airflow vertically across (bottom (T-bar), middle, pallet top) the freestream region between the pallet stack (Figure 3.15).The significant influence of air gaps in the heterogeneity of airflow within pallet stack demonstrated in Figure is consistent with valuable findings in previous studies (Defraeye et al., 2015b; Moureh et al., 2002; Wu and Defraeye, 2018). Figure 3.16 shows the velocity magnitude contour plot through the midline of the pallet stacks. For both pallet stack rows, high level of air penetration was observed in pallet stacks closer to the cooling unit. In contrast, a low level of air penetration was observed within pallet stacks closer to the container door.

3.5.2 Airflow distribution

Airflow in the container decreases across the length of the container as the distance to the cooling unit increases. Pallet stacks near the cooling unit are exposed to relatively high airflow rates and hence cool faster, while pallet stacks near the door of the container receive lower airflow rates (Figure 3.16). There was a sharp decrease in the velocity magnitude from the inlet region (distance to cooling unit = 0) to the door side due to short-circuiting of air in the container (Figure 3.17). These gaps allow cooled air to return through the overhead space to

the cooling unit unused, hence contributing to the low airflow in other regions. Nine out of the twenty loaded pallet stack receive low airflow (< 0.01 m/s) during transportation (Figure 3.16). There was up to 87% decrease in the average velocity of pallet stack near the cooling unit (P1, P2) to the pallet stack near the container door (P7, P8, P9). The airflow distribution in a refrigerated container is a heterogeneous one due to the difference in the volumetric flow rate of cooled air across the length of the container (Figure 3.17). The stacking pattern of the pallets, use of unvented packaging boxes also contributed to the heterogeneity of airflow distribution in the refrigerated container (Defraeye et al., 2015b).

At the free stream region between the door and the pallet stack, there was a low airflow region (air velocity <0.4) (Figure 3.18) which is within the same range as reported in previous studies (Getahun et al., 2017a). Vertical airflow in the pallets (P9 and P20) indicated it was simulated to evaluate the effect of the void plug on airflow within the rear pallets. For both pallets (P9 and P20), there was an improved vertical flow of air when the void plug was used to block airflow at the freestream (Figure 3.19). This further shows that coverage of the unutilised floor areas with fibreboard corrugated boxes can improve the vertical flow of air within the rear pallet stacks. The Vigneault number (Vigneault et al., 2004) in the rear pallet (P9) was determined to estimate the ventilation uniformity in the stacked pallet. Based on a sensitivity analysis, fifty measuring points of air-velocities were used as a data set within the rear pallet stack. Pallet stack (P9) with void plug has lower Vigneault number (0.39) while pallet stack (P9) without void plug has comparatively higher Vigneault number (0.42). This indicates that there is uniformity in airflow distribution within the rear pallet. This further shows that coverage of the unutilised floor areas with fibreboard corrugated boxes can improve the vertical flow and airflow uniformity within the rear pallet stacks. Berry et al. (2020) highlighted the significance of using void plug to block unutilised T-bar floor areas near the container door. The author suggested further research to evaluate how void plug designs impact airflow bypass in the refrigerated container.

3.5.3 Cooling patterns

Figure 3.20 shows the averaged experimental apple temperature and the surrounding air temperature in monitored pallets within the refrigerated container. A substantial difference between the fruit and its surrounding air temperature was noticeable, which was a result of the significant transfer of heat between the solid (fruit) and liquid phase (air). This result supports the use of local thermal non-equilibrium heat transfer model for the porous region (pallet) to accurately capture the heat transfer between the cooled air, apples and carry bag. Hoang et al. (2015)

and Gruyters (2019) used this heat transfer to simulate the transfer of heat in a postharvest cold chain application.

The measured and simulated fruit data were normalised using dimensionless temperature ratio (*Y*). See section 2.4.3.2 and equation (2.22) for more details. The numerical and experimental cooling curve for the monitored pallets shows a very close agreement with each other (Figure 3.21 and Figure 3.22). This demonstrates that the model was able to accurately capture the cooling pattern of fruit in the refrigerated container. The average prediction error of the cooling data for the first and second experimental scenarios is 11%. This is a significant improvement over the 18%, which was reported in Getahun et al. (2017a) study. Figure 3.21 shows the simulated and experimental temperature profile of measured pallets during the second experimental scenarios. Figure 3.22 shows the averaged simulated and experimental cooling curves for both the initial and the second full-scale experimental scenarios, where the first and second experimental durations lasted 16 hours and second 42 hours, respectively.

Table 3.5 shows a summary of HCT for the monitored pallet in the second experimental scenario. The variation in the half cooling time indicates the heterogeneity in cooling of fruit in the refrigerated container. The cooling rate difference between pallet stack shows a randomised cooling pattern. Some pallet stacks comparatively closer to the refrigeration unit (P6, P17) did not necessarily cool rapidly than stacks closer to the container door (P9, P19). This randomised cooling pattern has been reported by Getahun et al. (2017a), (Defraeye et al. (2015a) and Jedermann et al. (2014). Figure 3.23 and Figure 3.24 shows simulated temperature contour of palletised apple stack for both experimental scenarios (first and second). At the end of the cooling duration, pallet stacks in the container have different temperature even when they were all initialised at the same temperature at the beginning of the numerical simulation. Pallet stacks in regions of good airflow require less cooling time while pallet stacks in low airflow region require higher cooling time. The heterogeneity in the cooling pattern of fruit in the refrigerated container can be seen in both experimental scenarios (Figure 3.23 and Figure 3.24). A reasonable and logical cooling pattern was realised. This indicates that the developed model was able to predict the cooling pattern of fruit within the refrigerated container.

The spatial cooling heterogeneity of fruit in the refrigerated container will affect its quality preservation and reduce its shelf life (Defraeye et al., 2015a). Achieving cooling uniformity in palletized fruit has been a challenge. To address the heterogeneity challenge during transportation of fruit, the following strategies are proposed to improve the current practice

- Packaging systems (packaging design and stacking pattern) that optimize vertical airflow penetration should be utilised
- Airflow short-circuiting which cause bypass of airflow should be reduced by effectively utilising the container internal volume.

Successful implementation of these strategies will lead to saving of energy as the cooling capacity of the refrigerated will be effectively utilised (Defraeye et al., 2015a).

3.6 Conclusion

This study presented an experimentally validated CFD model of a fully packed refrigerated container with a realistic refrigeration unit. To realistically represent the cooling unit, axial fan performance was modelled with experimental data. Also, the dynamic control of the cooling unit was modelled with the temperature gradient data of the air supply and air return region. The developed model accurately characterises the airflow distribution and cooling pattern of fruit in the refrigerated container. A good agreement between numerical results and experimental data was obtained with a 17% modelling prediction error for airflow distribution and 11% for temperature prediction. The apple pallet stacks were modelled as a porous media, and the porous parameter (Darcy Forchmeicher coefficient, permeability coefficient) were obtained from relevant literature. The use of Local non-thermal equilibrium model (LTNE) heat transfer model was as a result of the substantial difference in the collected experimental data for the pulp and air temperature. The airflow distribution in the fully packed refrigerated container was largely non-uniform. This is due to the presence of gaps between the pallet stacks within the container, which allows the short-circuiting of cooled air back to the refrigeration unit. Void plugs were used to block airflow at the freestream region between the door and pallet stacks which improves the vertical airflow within the pallet stacks near the door. Also, the impact of middle gaps in the heterogeneity of airflow distribution was assessed. Future works will develop innovative loading strategies which will better utilise the refrigerated container volume and improve cooling.

3.7 Future work

The refrigeration unit can be better improved by incorporating a detailed algorithm system for the dynamic control of container operation modes (frozen modes, chilled mode, and defrosting mode). This will allow researchers to accurately measure the energy consumed throughout the container operation in transit. Also, the fruit and packaging boxes in pallet stacks can be explicitly modelled to characterise airflow and cooling pattern in a refrigerated container.

The flow resistances inside the packaging and loaded pallet stack should be accounted for separately in the porous media formulation. This will drastically reduce the prediction error caused by the porous media assumption.

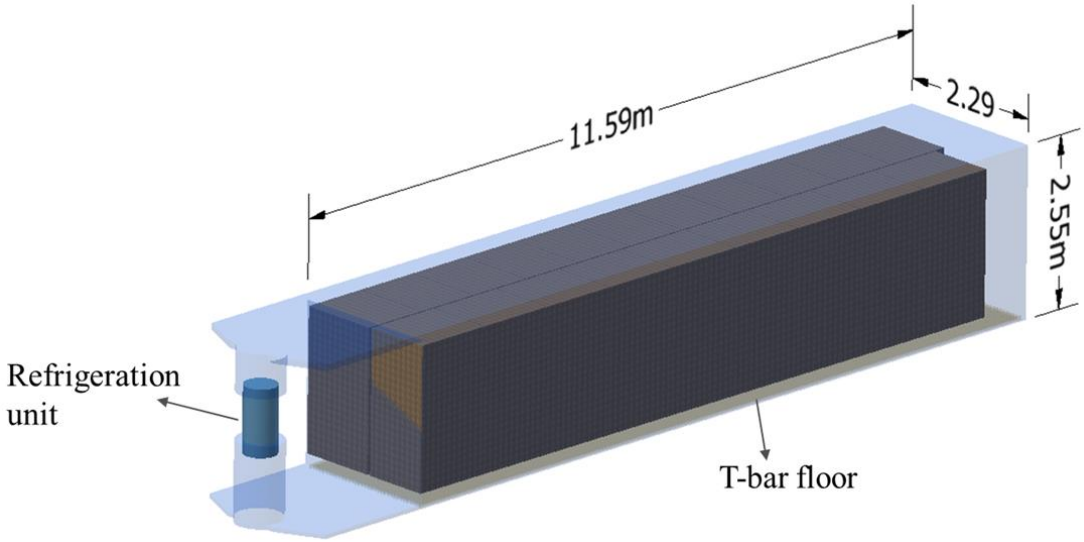

Figure 3.1: Fully loaded refrigerated container as used in the CFD model.

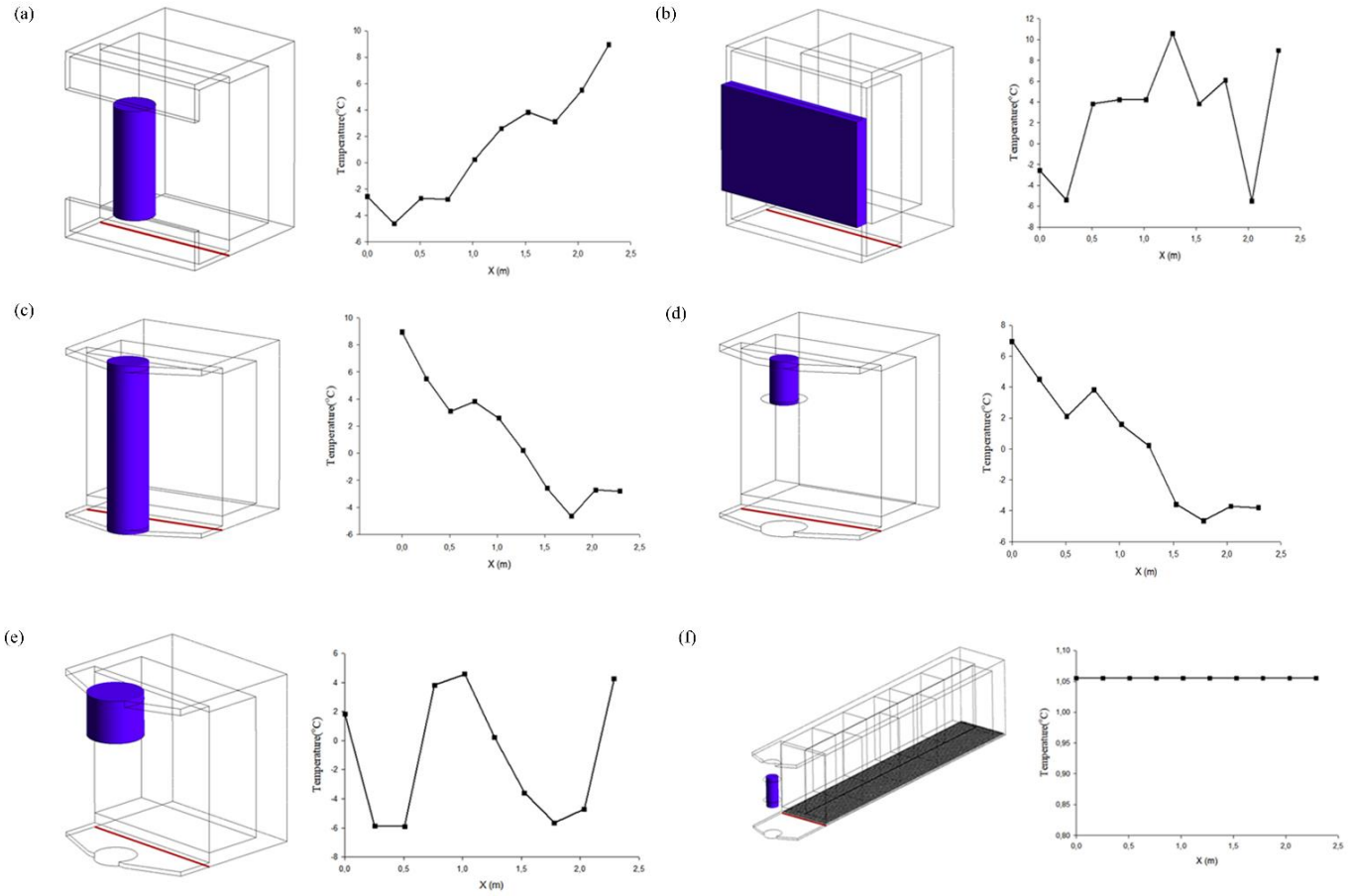

Figure 3.2: Simulations for the various refrigeration unit geometries that were tested. The blue domain represents a momentum source and energy sink term, so that airflow cycles through the system (top to bottom across blue domain). A heat source was included on one side of the container so that a temperature gradient is present along the x-axis. The red line represents an array of temperature samples, as plotted in the graph on the right. The designs in (a-e) do not effectively mix the air, whereas the design in (f) allowed for a uniform delivery of air.

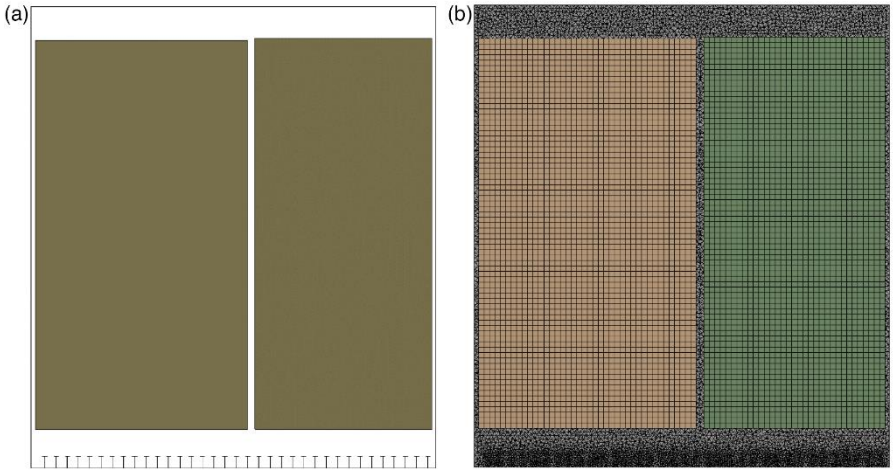

Figure 3.3: (a) Geometry and (b) mesh of computational domain across XY section (Z = 5 m).

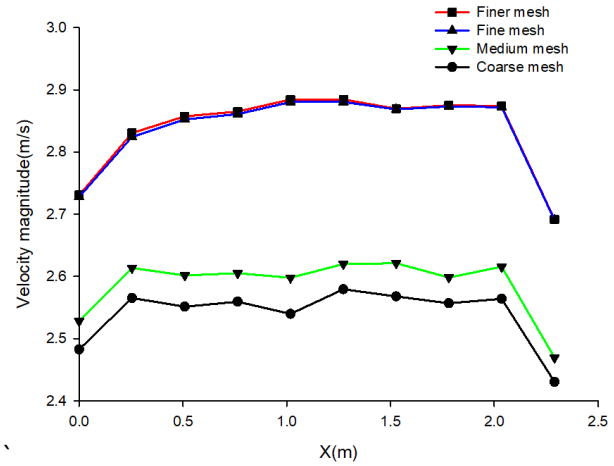

Figure 3.4: Mesh sensitivity analysis (air inlet region).

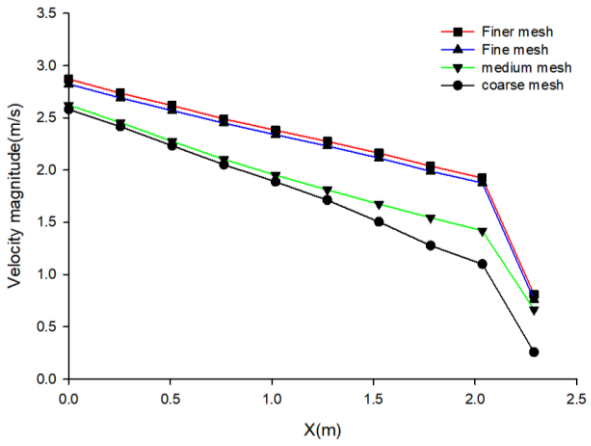

Figure 3.5: Mesh sensitivity analysis (T-bar floor region).

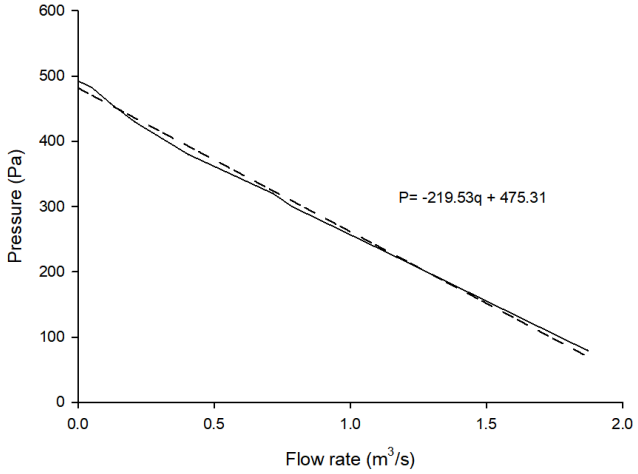

Figure 3.6: Axial performance curve.

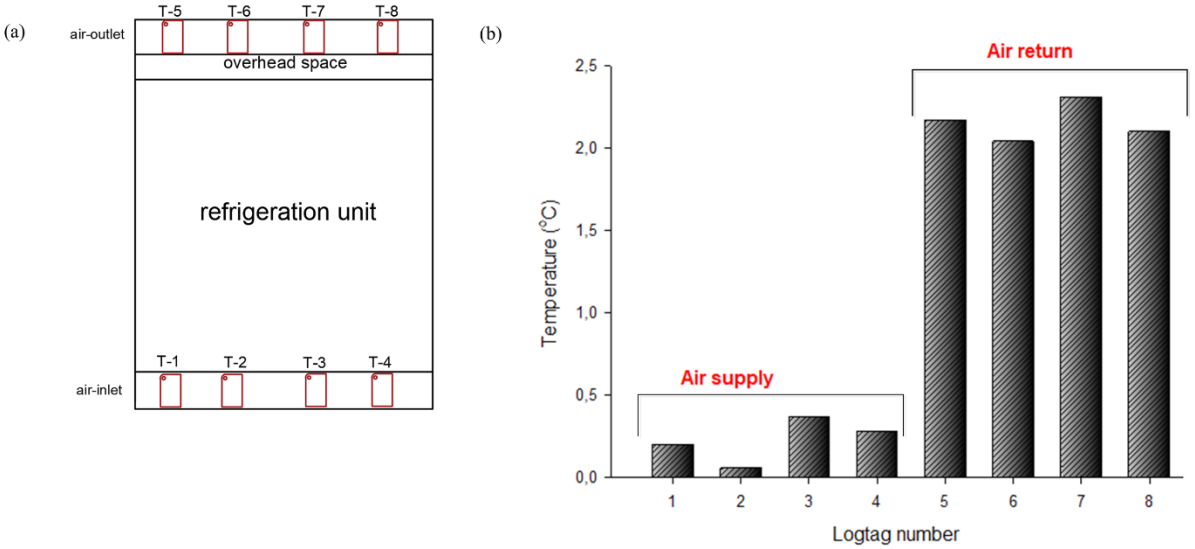

Figure 3.7: (a) Logtag positioning across the inlet and outlet region of the cooling unit. (b) Temperature gradient across the cooling unit.

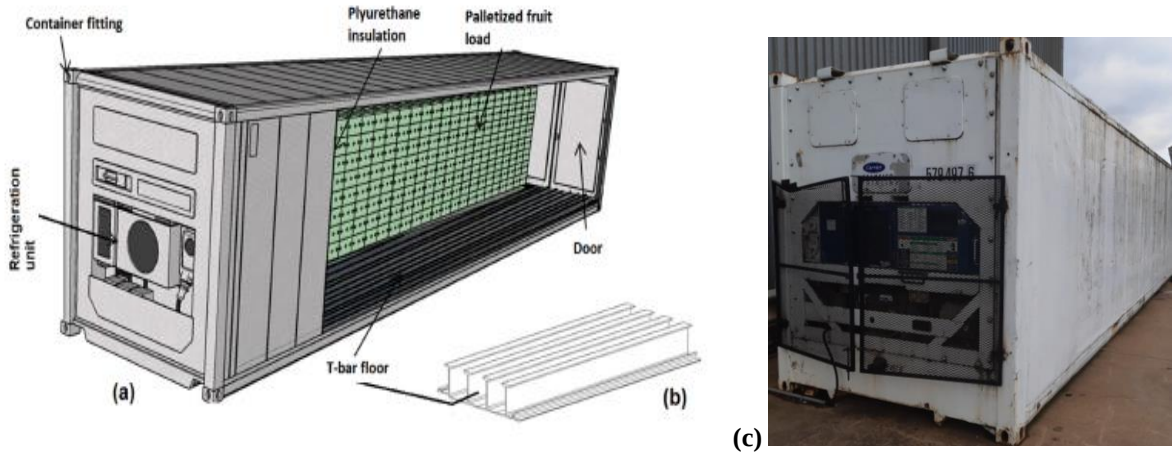

Figure 3.8: Refrigerated container with bottom air delivery system a) named selection of different parts b) T-bar floor design (Getahun et al., 2017a). c) Photo of the refrigerated container (Carrier Transicold) used in the validation experiments at Two-a-day packhouse.

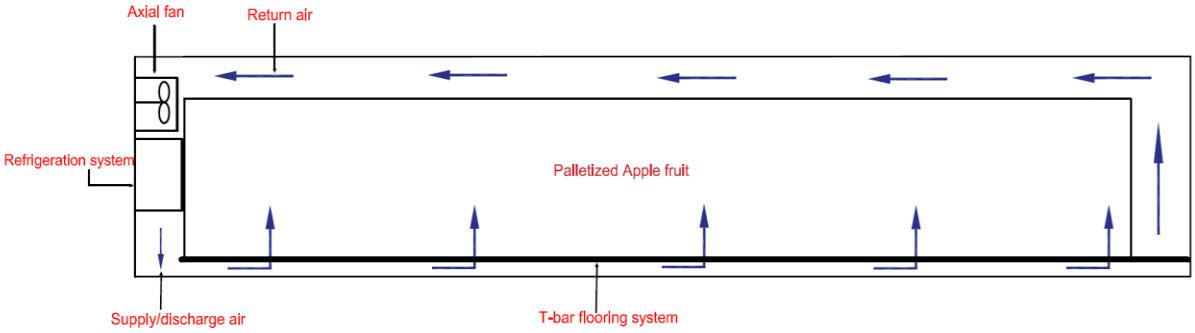

Figure 3.9: Schematic illustration of the airflow circulation inside a refrigerated container when using a bottom air delivery system.

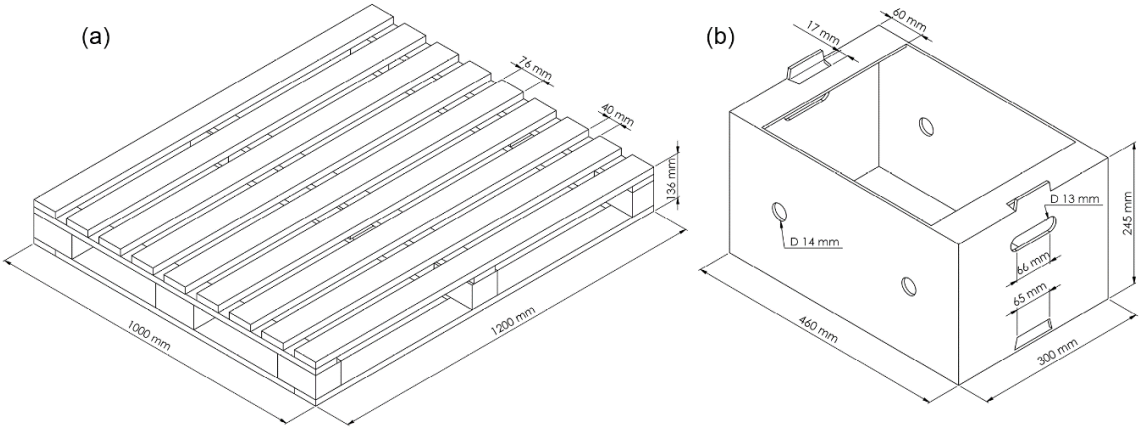

Figure 3.10: Schematic diagram of the pallet base (a) and the Econo-D carton (b) as used in the validation experiments.

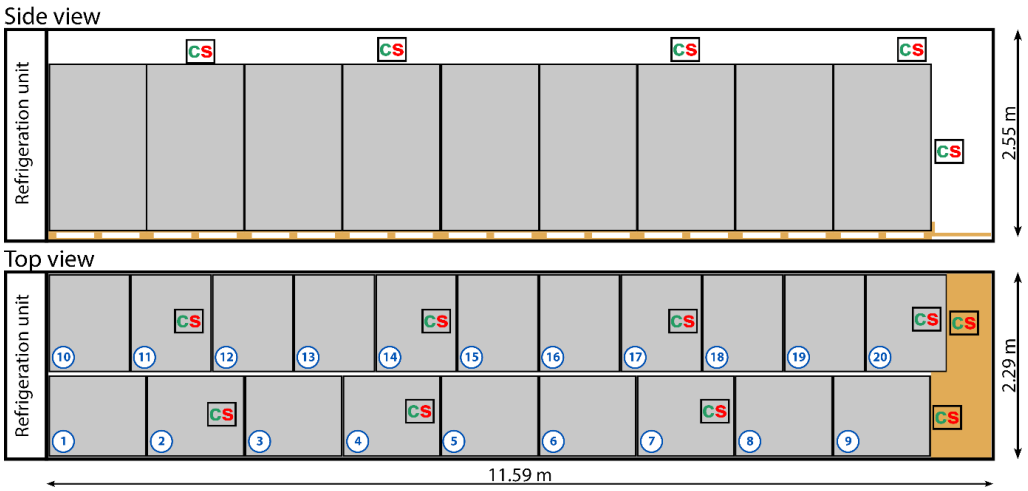

Figure 3.11: Schematic of the refrigerated container showing candlestick sensor placement in both experiments. Blue numbers in white circles show the pallet number; the "CS" boxes indicate the position of candlestick

sensors and the brown plane near the door represents the void plug, which was only present in the second experiment.

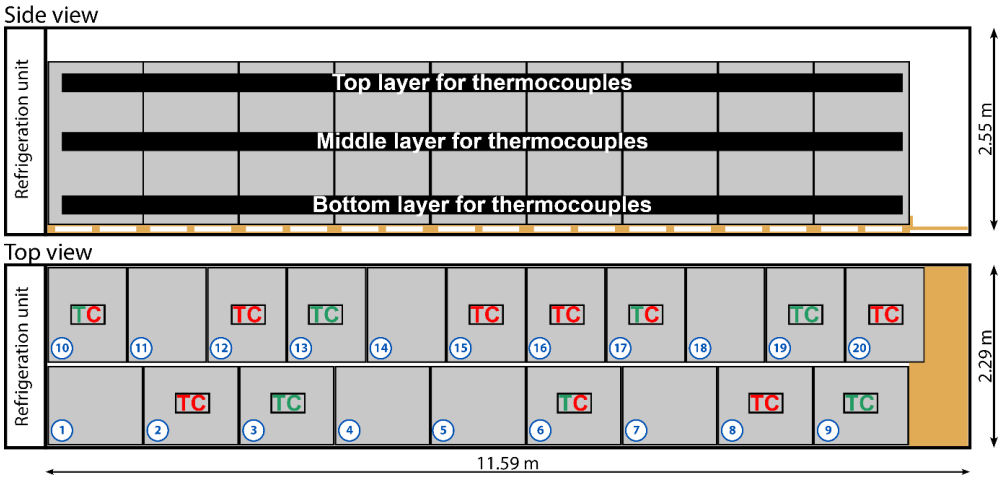

Figure 3.12: Top view schematic of a refrigerated container showing thermocouple wire position location for First and second experiments. Blue and white number indicate the pallet ID and the brown plane at the door represents the void plug, which was only present in the second experiment. The "TC" boxes indicate the position of thermocouple sensors, where red, green and red/green text relates to the positioning of probes in either the first, second or both experiments, respectively.

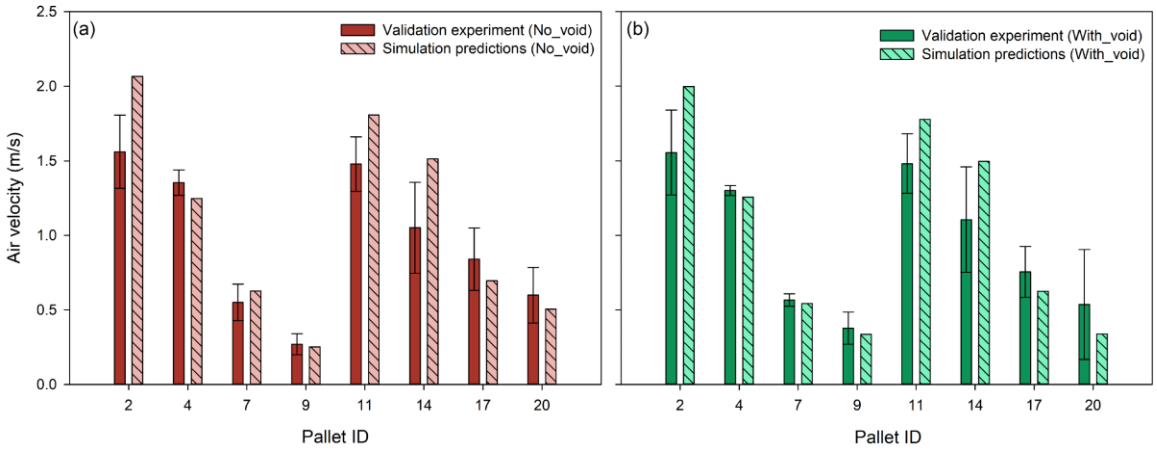

Figure 3.13: Numerical model results and Experimental results for the experimental scenarios (a) First scenario (No void plug was used) (b) Second scenario (void plug was used between the door and pallet stack).

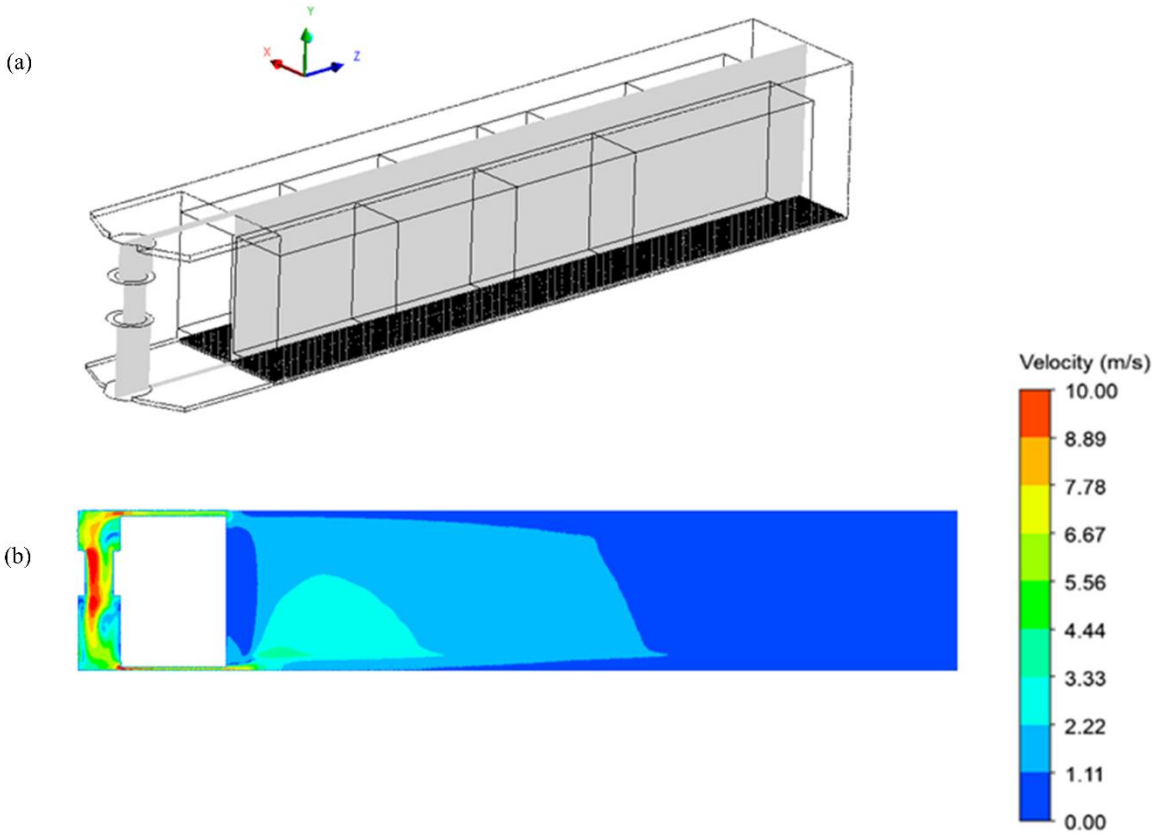

Figure 3.14: Velocity magnitude contour at the freestream region between pallet rows (a) Computational domain YZ plane (x= 1.04m) (b) contour plot.

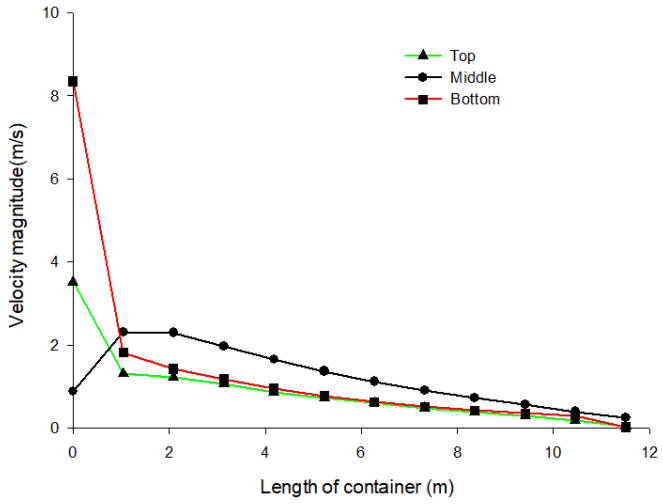

Figure 3.15: Velocity magnitude vertically across the height of the refrigerated container at the freestream region between the pallet stack (YZ plane x=1.04m).

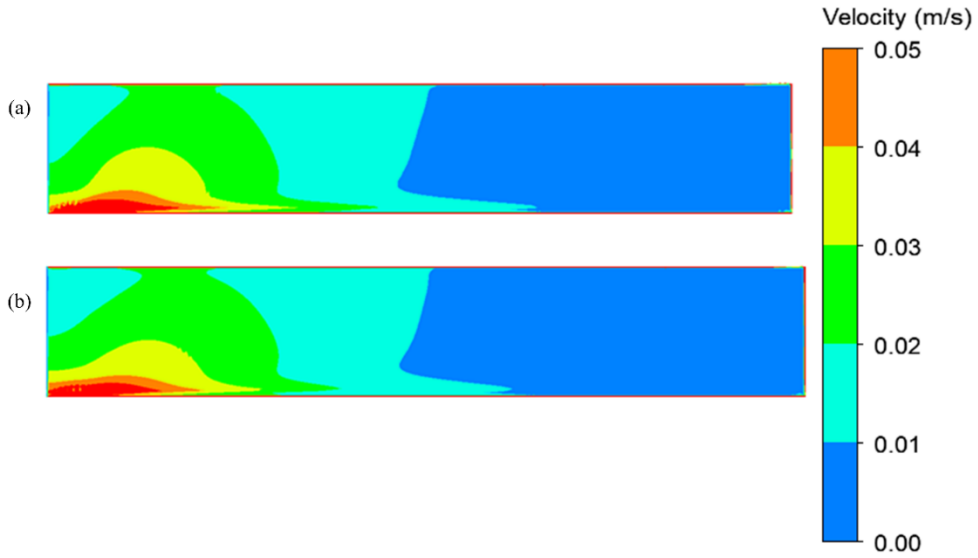

Figure 3.16: Velocity magnitude contour plot through the midline of the pallet stacks in row 1 (YZ plane, X = 0.5 m) (a) and row 2 (YZ plane, X= 1.7 m) (b).

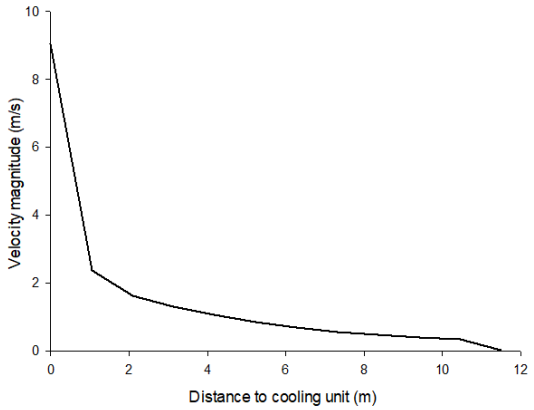

Figure 3.17: Simulated airflow distribution along the length of the container.

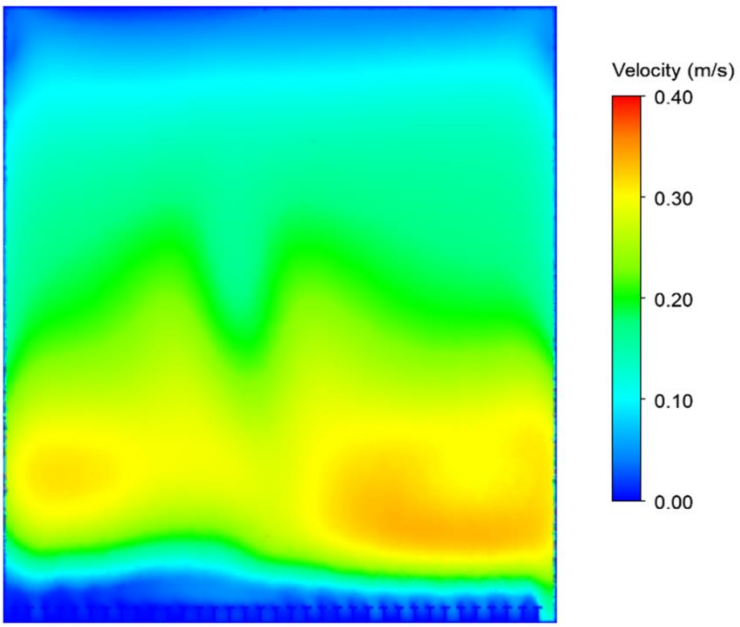

Figure 3.18: Simulated airflow profile at the freestream region between the door and pallet stacks.

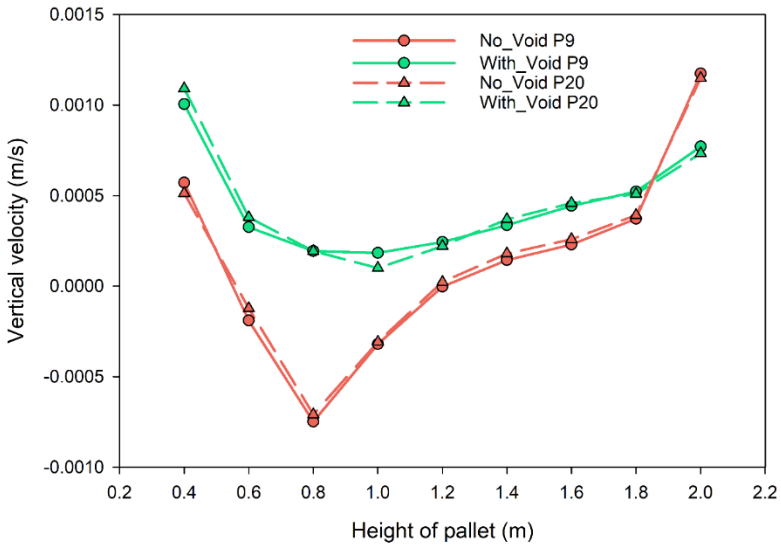

Figure 3.19: Simulated vertical airflow profile within pallets P9 and P20.

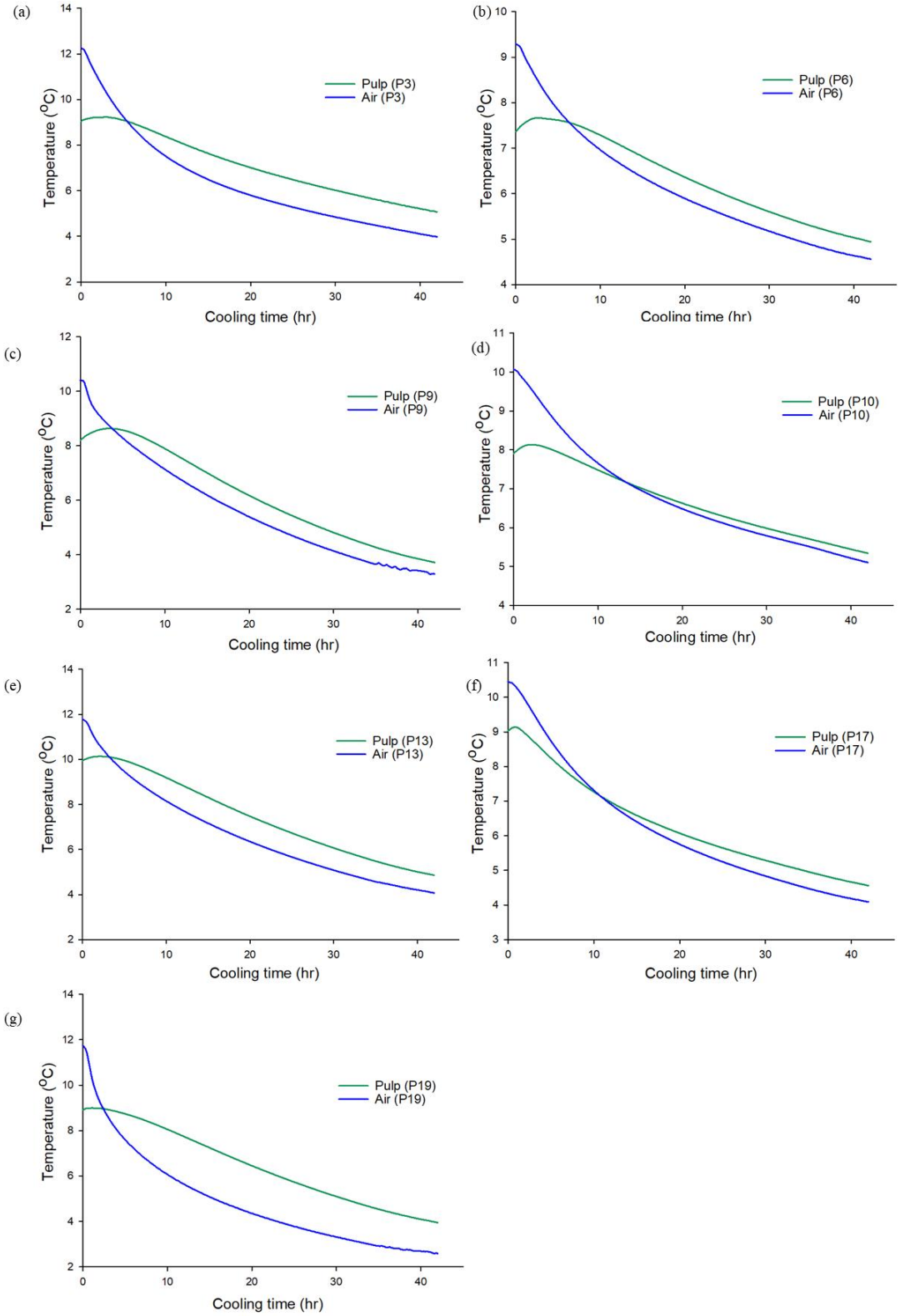

Figure 3.20: Experimental (measured) averaged pulp and air temperature profile for different pallets in a fully loaded refrigerated container (second experimental scenario (duration=42hr)) (a) P3 (b) P6 (c) P9 (d) P10 (e) P13 (f) P17 (g) P19.

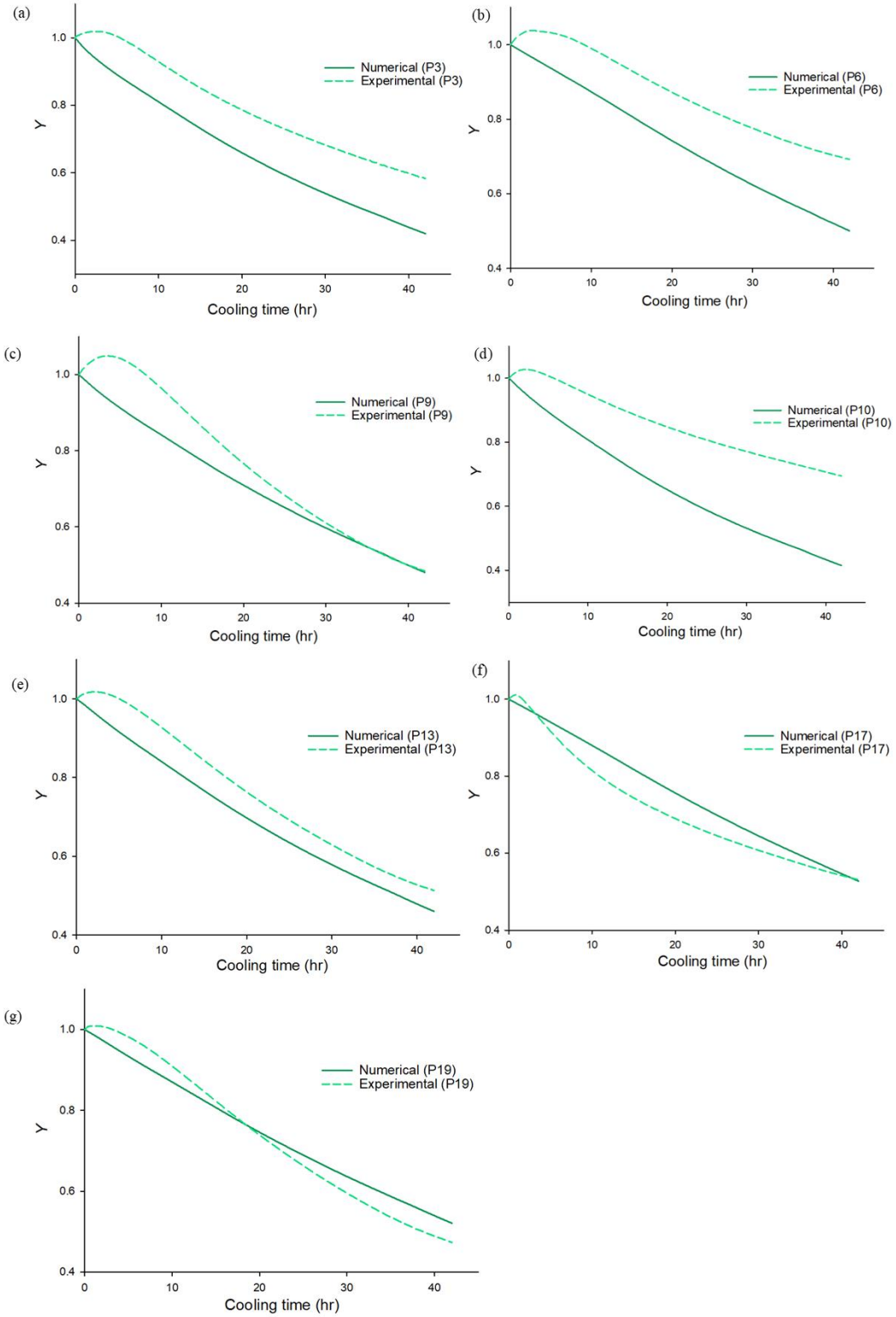

Figure 3.21:Numerical (solid line) and experimental (dashed line) cooling curve for monitored pallets (second experimental scenario (duration=42hr)) (a) P3 (b) P6 (c) P9 (d) P10 (e) P13 (f) P17 (g) P19.

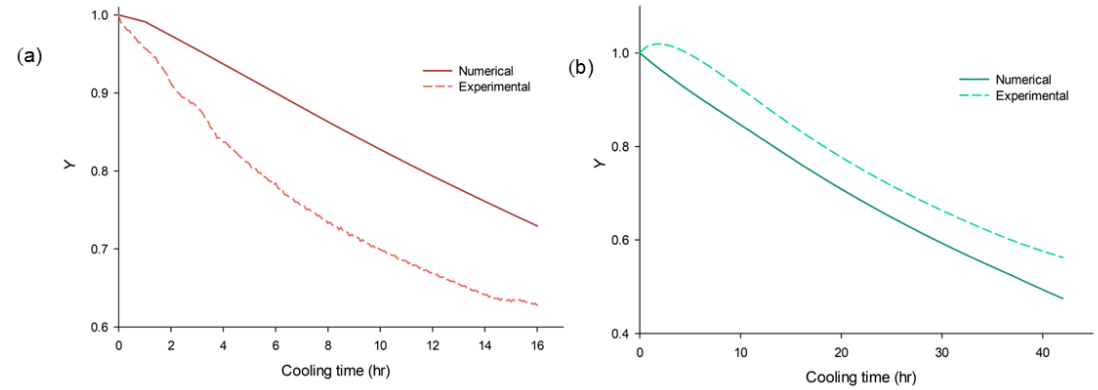

.

Figure 3.22: Averaged numerical (simulated) and experimental (measured) cooling curve of monitored pallets in the refrigerated container (a) First experimental scenario (duration=16hr) (b) Second experimental scenario (duration=42hr).

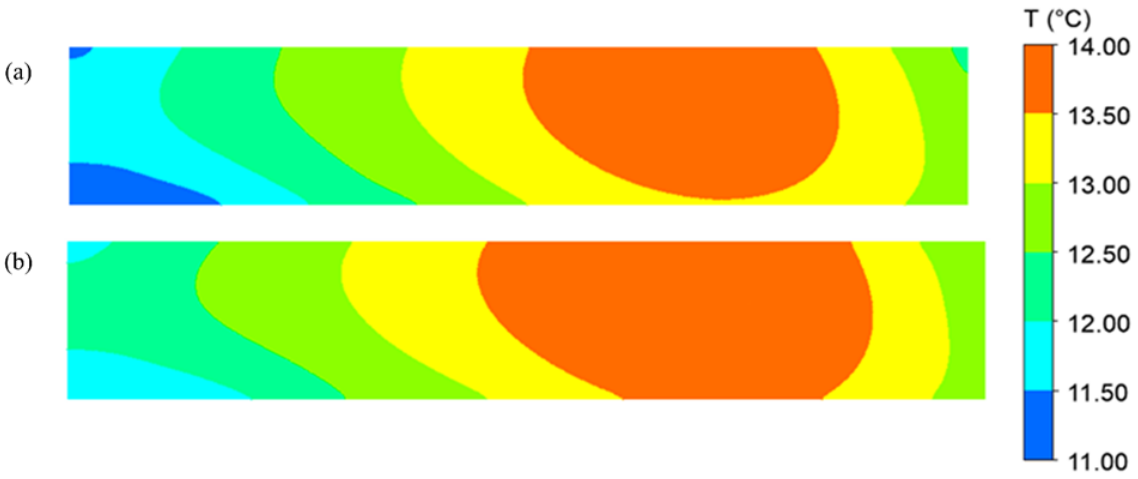

Figure 3.23: Simulated temperature profile of Apple pallet stack at the end of the cooling duration(16hr) for the first experimental scenario (a) row 1 (YZ plane, X = 0.5 m) (b) row 2 (YZ plane, X = 1.7 m).

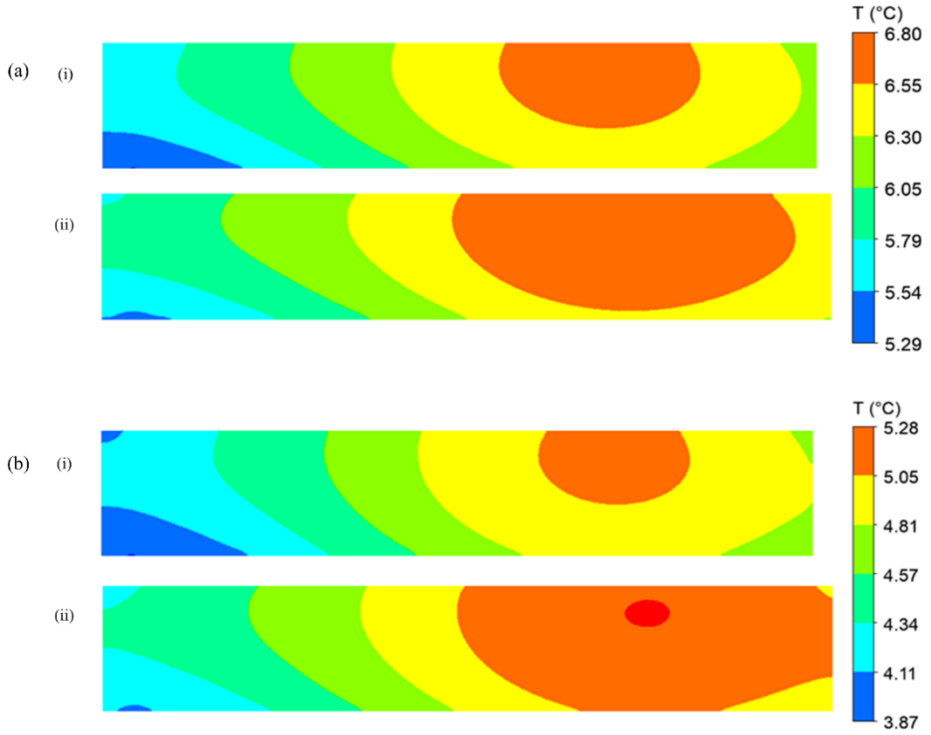

Figure 3.24: Simulated temperature profile of apple pallet stack at 24hr (a) and the end of the cooling duration (42hr) for the second experimental scenario (i) row 1 (YZ plane, X = 0.5 m) (ii) row 2 (YZ plane, X = 1.7 m).

Table 3.1:Computational domain geometrical parameters.

	Number	Dimensions (length × width × height (m))
Refrigerated container (interior)		11.59 m × 2.29 m × 2.55 m
Refrigerated container (exterior)		12.20 m × 2.44 m × 2.90 m
Pallet Row 1	11	1.2 m × 2.15 m × 11 m
A Pallet stack in Row 1	1	1.2 m × 2.15 m × 1 m
Pallet Row 2	9	1 m × 2.15 m × 10.8 m
A Pallet stack in Row 2	1	1 m × 2.15 m × 1.2 m

Table 3.2: Directional loss properties of a pallet stack.

Pallet Flow direction	$1/\kappa$ (m^{-2})	β (m^{-1})
x-direction	600 000	41 438
y-Top half	3 100 000	77 072
y-Bottom half	66 000 000	113 174
z-direction	1 700 000	2 110

Table 3.3: Physical properties of Apple (Lisowa et al., 2001).

Diameter (m)	0.084
Density (kg m^{-3})	898
Thermal conductivity (W $m^{-1}K^{-1}$)	0.463
Specific heat capacity (J $kg^{-1}K^{-1}$)	3829

Table 3.4: Number of cells of different meshing type for mesh sensitivity analysis.

Meshing type	Number of cells
Coarse mesh	1 005 967
medium mesh	5 202 620
Fine mesh	21 426 996
Finer mesh	27 337 776

Table 3.5: Summary of half cooling time (HCT) for pallets monitored in the second experimental scenario(duration=42hr).

Pallet numbering	HCT (hr)	
	Numerical	Experimental
P3	34.2	50.11
P6	42.25	70.22
P9	40.73	39.54
P10	32.6	73.5
P13	36.9	43.28
P17	47.62	43.79
P19	44.14	38.85

Chapter 4. Conceptual Packaging Systems for Improved Container Space Utilisation and Cooling

4.1 Introduction

Transport and logistics are integral components in South African (SA) fruit export supply chain. Over the years, there has been a continual increase in the transport and freight expenses which are significant portions of the export supply chain total cost. The rising freights costs, and growing global warming concerns (high carbon footprint) have emphasised the need for efficient and effective export of fruit (Berry, 2017; Louw and Nel, 2019). The most viable solution is to optimise the refrigerated container (RC) volume by utilising innovative packaging systems. Currently, cartons are stacked on standard 1SO pallet (1.0 × 1.2 m), this leaves over 10% of the refrigerated container floor area and 25% of the container volume unused. A new packaging system which consists of improved carton and pallet design could potentially allow the industry to use up to 2800 fewer RC yearly and thus reduce freight costs by approximately 18 million USD (Berry, 2017).

Previous research has extensively analysed potential saving opportunities of high cube refrigerated container used in the pome and stone fruit industries. Louw and Nel (2019) used optimisation software such as pallet manager and cargo manager to investigate improved stacking patterns, sizes of pallets and cartons. This yielded the following recommendations: (i) use of slip-sheet instead of pallet (ii) use of specialised pallet (new size) to accommodate new packaging systems (ii) optimal arrangements of fruits in packaging boxes. The results also showed that pome fruit have a higher potential for increasing volume usage when compared to stone fruit (Louw and Nel, 2019). Stone fruit has lesser room for volume improvement because their cargo are currently within close range to the maximum payload limit (Louw and Nel, 2019). Berry (2017) explicitly modelled cooling in the current (Standard A, B, C) and new (Tes, Hex) packaging systems for pome fruit. From both a cooling and packaging density perspective, the Hex and Tes packaging systems showed significant benefits when compared to the standard packaging systems (Berry, 2017).

A major benefit in developing and implementing new packaging system for refrigerated container space utilisation is that it allows for cooling heterogeneity challenges to be addressed during the transportation of fruit (Berry, 2017). The resolution of the container volume utilisation and improved cooling performance will enhance the quality preservation of fruit. This study aims included the evaluation of conceptual packaging systems inside a fully packed refrigerated container for space utilisation and cooling efficiency. A 3D computational fluid dynamics (CFD) validated model, with realistic refrigeration unit was used to characterise the airflow and transfer of heat within the packaging systems inside the refrigerated container. In this study, the packaging systems were modelled as a porous media and a multi-parameter analysis is used to evaluate the performance of the packaging systems inside the refrigerated container.

4.2 Materials and methods

The new packaging system design takes into consideration the realistic factors that will enhance the functionality and practicability of an effective container for space utilisation and cooling efficiency (Berry, 2017): (i) The proposed pallet base should be similar to the currently used pallet base for ease in loading, handling and compatibility with equipment's (forklifts, doorways); (ii) The stability of the pallet stack should be improved by including interlocking patterns to allow cartons to lean on each other for support; and (iii) The pallet stack should further enable the alignment of carton vent holes for improved airflow distribution within the refrigerated container. The proposed packaging system design offers tremendous benefit (finance and practicality) when compared with the initial investment required (Berry, 2017).

4.2.1 Packaging systems

4.2.1.1 Standard packaging system

An optimal pallet of 1 166 × 999 mm is used in standard packaging system to eliminate wasted space. Currently, the carton design of 500 × 333 × 270 mm (Figure 4.1a) and standard pallet of 1 200 × 1 000 mm (Figure 2.6) are used in the export of apple fruits. The current pallet stack loading configuration leaves an unused gap of 35 mm along the length of the pallet (Berry, 2017). The optimal pallet used for this packaging system takes this into consideration. Three different loading strategies of the standard packaging system are evaluated in this study (Figure 4.2). Standard A and B design use 87.7% of the RFC floor area while loading 20 pallets (7 cartons per layer (Figure 4.3a) while Standard C design enables loading of 21 pallets using 92.1% of the RFC floor area. Figure 4.2 shows the pallet stack loading configuration for the standard packaging systems, and Figure 4.3 shows the packaging system configurations on the pallet.

4.2.1.2 Hexagonal packaging system

Hexagonal (Hex) packaging system is an alternative loading approach proposed by Berry (2017) to improve the stacking efficacy of cartons and utilisation of the RFC floor area. This packaging system utilises an entirely new carton design (Hex carton) which has an isosceles trapezoid shape. Figure 4.1(b & e) shows the Hexagonal carton design and fruit-tray packing configuration inside the carton. The Hex pallet stack configuration allows the loading of 22 pallets (6 carton per layer (Figure 4.3b) and RFC floor usage of 97.4%. The pallet stack configuration leaves a 2 cm gap along the side of the pallet to aid loading (Berry, 2017). The peculiar tessellating structure of the Hex carton design ease the alignment of vent holes between the individual cartons and interlocking pallet stacks between the loaded pallets (T. M. Berry, 2017).

4.2.1.3 Tes packaging system

Tes packaging system uses an innovative pallet design (1 157 × 1 134 mm (Figure 4.3c) and carton design. The Tes pallet stack configuration allows the loading of 20 pallets (9 cartons per layer) and RFC floor usage of 99%. 1% of the RFC floor is left unoccupied to ease the loading process (Berry, 2017). Figure 4.1c shows the geometry of Tes Carton design. Tes

carton has non-symmetrical vent holes to enable vent alignment during stacking on the pallet (Berry, 2017).

4.2.2 Numerical simulation

4.2.2.1 Computational domain

The computational domain for the refrigerated container internal dimension is 11.59 m long, 2.29 m wide and 2.55 m high (internal volume: 67.6 m^3). Different packaging system configurations are loaded in the container (Figure 3.1). Air gaps are not included between the pallet stack rows for the evaluated packaging system as this causes significant bypass of air in the refrigerated container.

4.2.2.2 Simulation set-up

All numerical simulation were run using ANSYS CFX 19.1 CFD code and validated model of the refrigerated container. Airflow characterisation and distribution in the refrigerated container was obtained by first simulating steady-state simulations. The numerical models was developed using various assumptions and simulation set-ups described below;

- Axial fans were implicitly incorporated in the model by conducting an axial performance experiment. The fan system equation was generated from the experimentally obtained performance curve. The geometrical parameters of the fan (length, radius), flow rate and fan system equation were integrated as a momentum source using CFX expression language (CEL).
- The packaging systems was modelled as a two-phase porous media and its directional loss properties are obtained from literature (Getahun et al, 2017a) with no modification.
- The T-bar floor design of the refrigerated container was modelled as an adiabatic no-slip boundary and smooth wall.
- Turbulence was modelled using SST κ-ω turbulence.
- A local thermal non-equilibrium model (LNTE) was used to model the instantaneous transfer of heat from the packaged apples at the beginning of the cooling. The interfacial area density and heat transfer coefficient were correctly defined in the model.
- Humidification control system were not incorporated in this model because moisture condensation and evaporation that occurs inside a refrigerated container during distant transportation of fruit was assumed insignificant.
- High-resolution advection scheme and turbulence numerics were used to run all numerical simulations.
- Volume porosity of the pallet stack was assumed to be uniform spatially and temporarily (Volume porosity ≈ 0.6).

- The physical properties of the apple fruits specified are obtained from the literature (Lisowa et al., 2001).
- Generated heat by the axial fans was assumed to be totally removed by the evaporator coil.
- The temperature of the apple fruits were initialised at 5 °C at the beginning of the cooling process.

Different mesh sensitivity analysis were performed for all the pallet stack loading strategies to determine the best combination of mesh element sizes that accurately predict flow in the refrigerated container with minimum computational load requirements. The total computational mesh element generated for all packaging systems are presented in Table 4.1.

All numerical computations were performed using the University of Stellenbosch's high-performance computing clusters (Rhasatsha).

4.2.3 Performance evaluation parameters

4.2.3.1 Cooling heterogeneity (uniformity)

Convective heat transfer coefficient (CHTC; h) is a direct measure to assess cooling heterogeneity on fruit surfaces within pallet stacks. CHTC ($Wm^{-2}K^{-1}$) is expressed mathematically as the ratio of the convective heat flux normal to the surface (q_{cw}; $[Js^{-1}K^{-1}]$) to the difference between the fruit surface temperature (T_w [K]) and reference temperature (T_{ref} [K]) often set as the cooling air temperature

$$h_{conv} = q_{cw}/(T_w - T_{ref}) \quad (4.1)$$

The selected reference temperature has a strong influence in determining CHTC for different cold chain applications (FAC, RFC, etc.). In this study, the packaging systems were modelled as a porous media and the convective heat transfer coefficient (h_{conv}) is correlated using Eqn. (2.11). CHTC is used to assess cooling heterogeneity by determining the relative standard deviation (%; RSD) across the surface of the fruit. Fifty CHTC monitoring points per pallet stack are used as data set in calculating the relative standard deviation. Low RSD represents homogenous cooling while high RSD represents heterogeneous cooling.

4.2.3.2 Ventilation uniformity

Ventilation uniformity in the packaging can be evaluated by determining the coefficient of variance (C_u) of the air-velocities at different measuring points. This parameter displays the variance of the instantaneous air velocities at different positions to the mean value within a pallet stack. C_u is mathematically defined as the ratio of the standard deviation (σ) of air-velocities to the average value ($\bar{U}$) at different monitoring points.

$$C_u = \frac{\sigma}{\bar{U}} = \frac{\sqrt{\frac{1}{N}\sum_{i=1}^{N}(U - \bar{U})^2}}{\bar{U}} \quad (4.2)$$

In this study, 50 monitoring points of air-velocities are used as data set in each pallet stack. Low value of C_u indicates uniform airflow through a porous media while a high value of the C_u means non-uniform air distribution. Also, the cooling uniformity within a pallet stack can

be evaluated by quantifying the Vigneault number (Vigneault et al., 2004) and the heterogeneity index for air velocities (Dehghannya et al., 2008).

4.3 Results and discussion

4.3.1 Airflow characterisation and profile

The simulated airflow profiles for the packaging systems are shown in Figure 4.4. The Standard packaging systems (A, B, and C) shows similar airflow profiles. The airflow rate nonlinearly decreases as the pallet stacks are positioned farther from the refrigeration unit. Pallet stacks near the refrigeration unit receive a high volumetric flow rate of air while pallets near the container door receive low volumetric airflow rates. Generally, 0.01 m/s is considered as reasonably low velocity for cooling of pallet stack in a refrigerated container. In the Standard A design, 9 out of the 20 loaded pallet stack receive low air velocity, which is primarily due to the bypass of airflow at the freestream region between the pallet stack and door. There was up to 95% decrease in the average velocity from the pallet stack near the refrigeration unit (P1) to the pallet stack near the door unit (P9, P11). About 50% of the loaded pallet stack in the standard B design receive low air velocities. For Standard C design, there was up to 97% decrease in the average velocity from P1 to P11 and 11 out of the loaded 21 pallets receive low airflow velocities. The average range between minimum and maximum air velocity for each of the packaging systems are presented in Table 4.2.

As illustrated in Table 4.2, all the Standard packaging systems have a comparatively higher air velocity range than the Hex and Tes design. This large deviation is due to the considerable gradient-flow structure in standard loading strategies. The unutilised floor area in Standard A and B packaging system allowed a substantial quantity of air bypass from the pallet stack in the refrigerated container. A logical trend was noticeable from the simulations, the higher the unutilised floor area, the larger the short-circuiting of airflow in the container. This observation is, naturally, obvious, but provides much needed quantitative evidence to the industry attention.

Figure 4.5 shows the simulated airflow profile at the freestream region between the container door and pallet stack in the Standard A and B packaging systems. From the figure, the lower air velocity range of the Standard packaging systems can be correlated to a higher air velocity gradient at the freestream regions. Even though, Standard C utilise 92.1% of the RFC floor area, the space between the pallet rows during re-orientation of the pallet stack ease the short-circuiting of airflow in the refrigerated container. The unused RFC floor area in standard packaging designs (A and B) explains the large bypass of cooled air from the pallet stacks in these loading strategies. The nonlinear decrease in airflow rate in the Standard packaging systems will lead to the development of warm spots in areas of low ventilation and thus accelerated deterioration of the fruit quality.

The void plug has been found to be useful commercially in obstructing the bypass of air at the freestream region of the container (Berry et al., 2020) and in improving the vertical airflow in pallet stacks near the container door. Figure 4.6 shows velocity magnitude contour graph of

the pallet row 1 for each packaging system. Large regions of the Standard packaging systems are under low ventilation (< 0.01 m/s). The different Standard packaging designs shows similar airflow distribution with varying indices of heterogeneity. In contrast, the Hex and Tes designs show improved airflow profiles compared to the Standard packaging systems. The airflow profile shows a more gradual gradient across all the pallet stacks for the Hex and Tes design, while a high gradient of flow was observed for the Standard packaging systems (Figure 4.5). For both rows of the Tes and Hex design, the average velocity deviation of pallet stacks near the refrigeration unit and the container door are very low. This indicates uniformity in airflow distribution within pallet stacks in Tes and Hex design. All the pallets in the Hex and Tes loading strategies receive adequate airflow necessary for cooling of packaged fruit in the refrigerated container. Tes design shows significantly improved performance in airflow distribution in comparison to the Hex design as the coefficient of variance is lower. The average coefficient of variance for air velocities is 0.46 for the Tes packaging system and 0.51 for Hex packaging system. The lower the coefficient of variance in the air velocities, the more the uniformity in airflow distribution within the pallet stacks in the refrigerated container.

4.3.2 Airflow pattern

Figure 4.7 shows the simulated airflow pattern within the pallet stacks of the packaging systems. Refrigerated containers with bottom air delivery system depend on the vertical flow of cooled air through the pallet stacks for cooling. Although, some horizontal airflow that orient to the container length can occur (Berry, 2017; Jiménez-Ariza et al., 2014; Rodríguez-Bermejo et al., 2007; Smale et al., 2006). The standard packaging systems show predominantly horizontal airflow patterns (Figure 9). The bottom region of pallet stack in Hex design shows vertical flow while the remaining region show dominant horizontal airflow pattern. There is a mixture of vertical and horizontal airflow within the pallet stacks for Hex design (Figure 4.7). Vertical airflow pattern within the pallet stack in Tes design is very noticeable. This shows the vertical air velocity is comparatively much higher than the horizontal velocities that occur the length and width of the container. Efficient utilisation of Tes design RFC floor area will allow adequate cooling of the packaged fruit as the bypass of air in the container has been restricted to the barest minimum. The significant bypass of air in standard packaging systems contribute to factors that alter the preferential flow path of cooled air which will decrease fruit cooling rates. The Tes design shows superior performance in the simulated airflow pattern within the palles. In this study, uniform directional loss properties were used for all the packaging system. The change in airflow pattern within the pallet stack is largely due to the utilisation of the container space and stacking arrangement of the packaged fruit.

4.3.3 Cooling heterogeneity

The CHTC RSD for the packaging systems are shown in Table 4.3. The standard packaging systems (A, B and C) have high relative standard deviation while Tes/Hex shows comparatively lower values. This indicates heterogeneous cooling for the standard packaging systems (A, B and C) as the average RSD values are comparatively high to the Hex and Tes packaging system. Uniform cooling of fruit in the refrigerated container is required to

minimise the risk of chilling injury (Defraeye et al., 2013). The average RSD values of the standard packaging systems is 47% higher than Hex designs and 51% higher than the Tes designs. This result is consistent with Berry (2017) findings in the study of packaging configurations in the refrigerated container.For the Tes and Hex packaging systems, cooling of fruit will be homogenous, and the quality of the fruit will be better preserved.

The energy density rendering of the evaluated packaging systems is shown in Figure 4.8. Energy density is an indication of the rate of heat removal from packaged fruit and can be used as an index of accessing the uniformity in cooling of the pallet stack in the refrigerated container. The field heat removal rate is higher in regions of larger energy density while regions with low energy show lower rates of heat removal from the fruit. The Standard packaging systems all show the same energy density pattern with different heterogeneity indices (Figure 4.8 (a, b, c)). Pallet stacks near the refrigeration unit have high energy density while pallet stacks far from the refrigeration unit have low energy density in the standard arrangements. Large energy density gradients were observed for Standard packaging systems, while the Hex and Tes design show a relatively uniform cooling gradient across the pallets (Figure 4.8 (d, e)). The main consequence of improved packaging system in optimising cooling process to reduce field heat is reduction in cooling time. This then reduces respiration and prevent senescence during distant transportation of fruit (Defraeye et al., 2013).

4.4 Conclusion

This study evaluated the performance of conceptual packaging systems in a fully loaded refrigerated container with respect to space utilisation and cooling efficiency. In comparison with the Standard packaging systems, the Tes and Hex designs showed significant improvement in airflow distribution within the pallet stacks and homogeneity in cooling. The Hex design showed better performance in container utilisation and cooling efficiency than the Standard packaging systems. From a multi-parameter perspective, Tes design generally outperformed all other packaging design. it had the highest RFC floor usage of 99% and lowest average CHTC RSD. The airflow distribution was uniformly distributed with no low ventilation region, and it showed a dominant vertical airflow pattern within the pallet stacks, which is the preferential pathway for cooling in a refrigerated container. These cooling performance characterised indicate that fruit quality would thus be better preserved, and container space would also be optimised when using the Tes design. This study also showed a direct correlation between container space utilisation and cooling uniformity such that increase in refrigeration container space utilisation corresponded with higher fruit cooling performance.

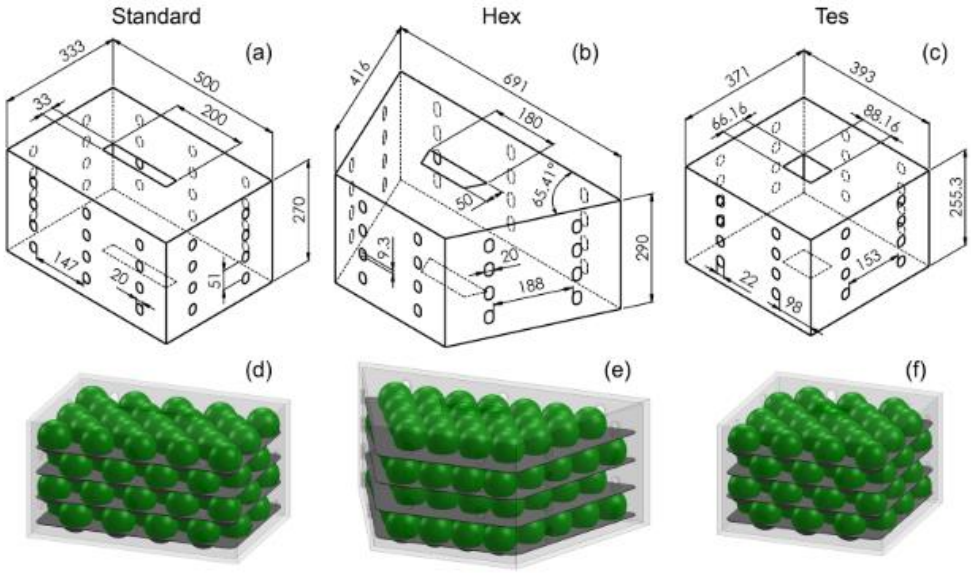

Figure 4.1: Carton design and fruit-tray packing configuration for packaging systems. (a & d) Standard (b & e) Hex (c & f) Tes (Berry, 2017).

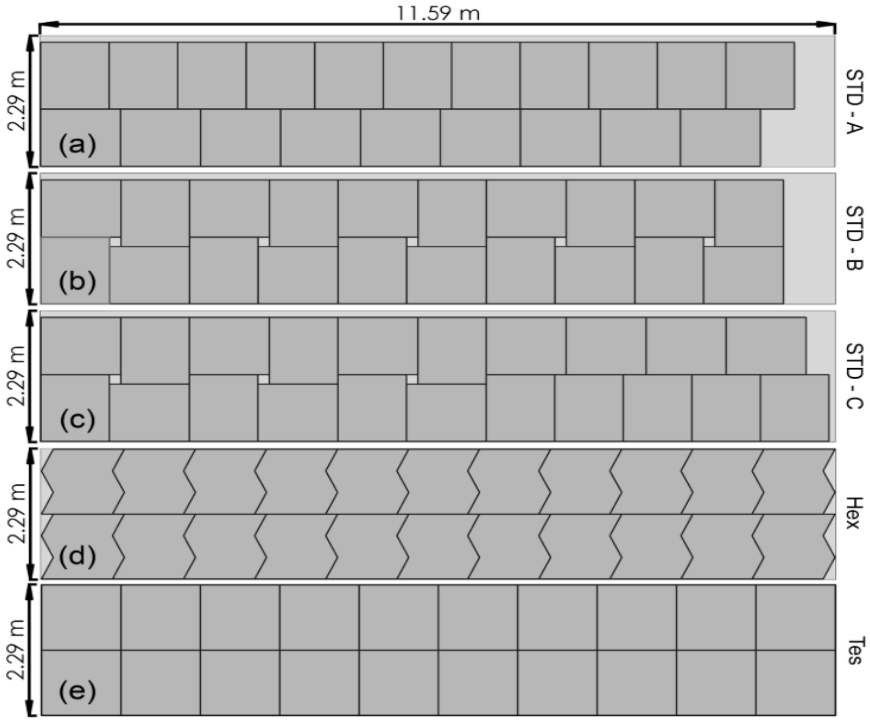

Figure 4.2: Pallet stack loading strategies in the Refrigerated container (Top view) (a, b &c) Standard (d) Hex (e) Tes packaging system (Berry, 2017).

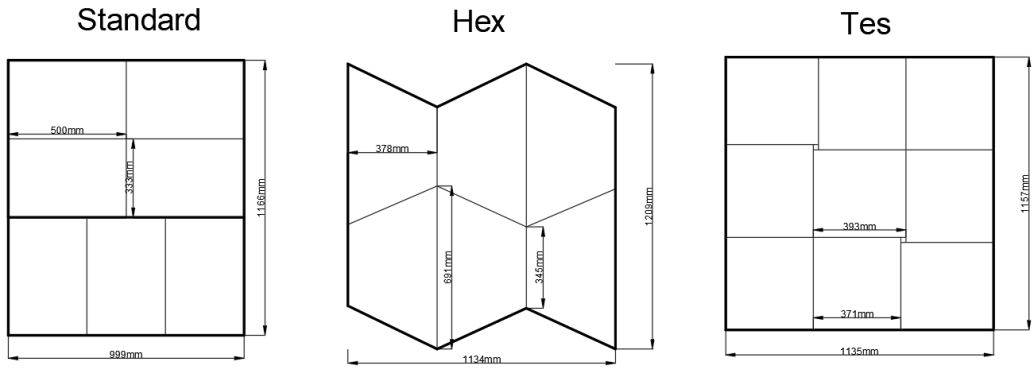

Figure 4.3: Packaging system configurations showing a) 7 b) 6 c) 9 cartons per layer.

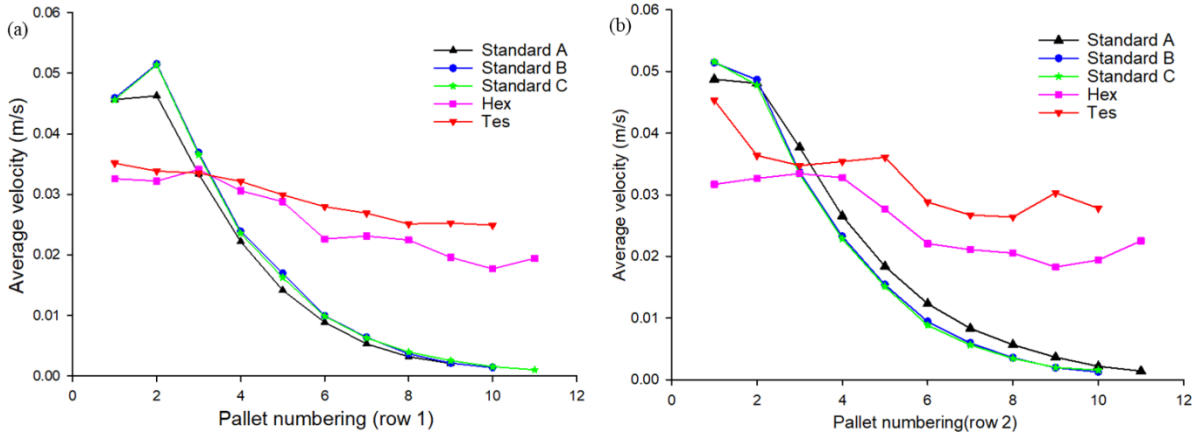

Figure 4.4: Simulated airflow profile for the packaging systems (a) row 1 (b) row 2

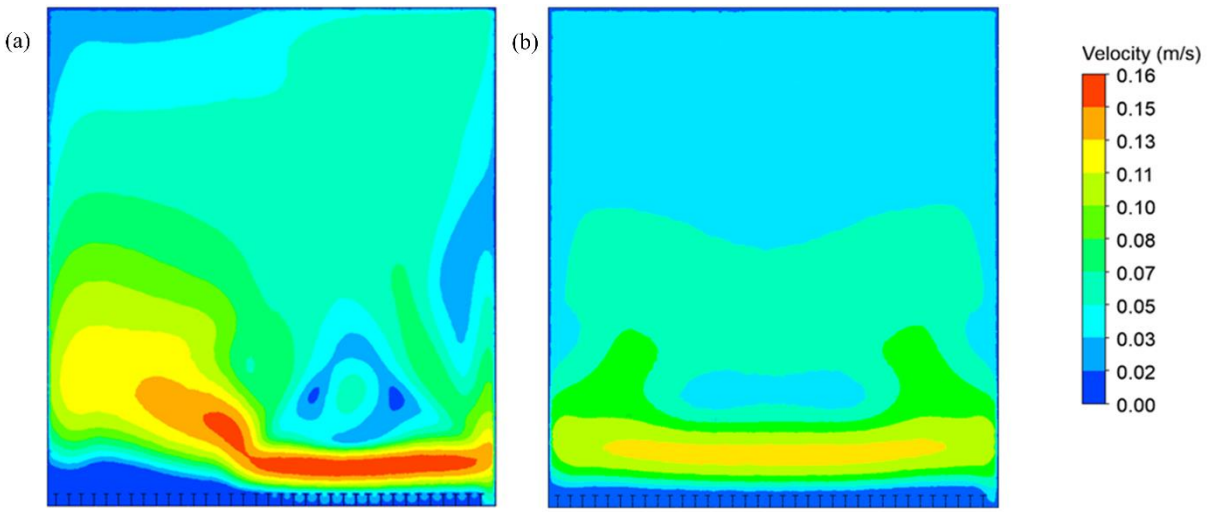

Figure 4.5: Simulated airflow profile between the pallet stack and the container door in Standard A (a) and Standard B (b) packaging system.

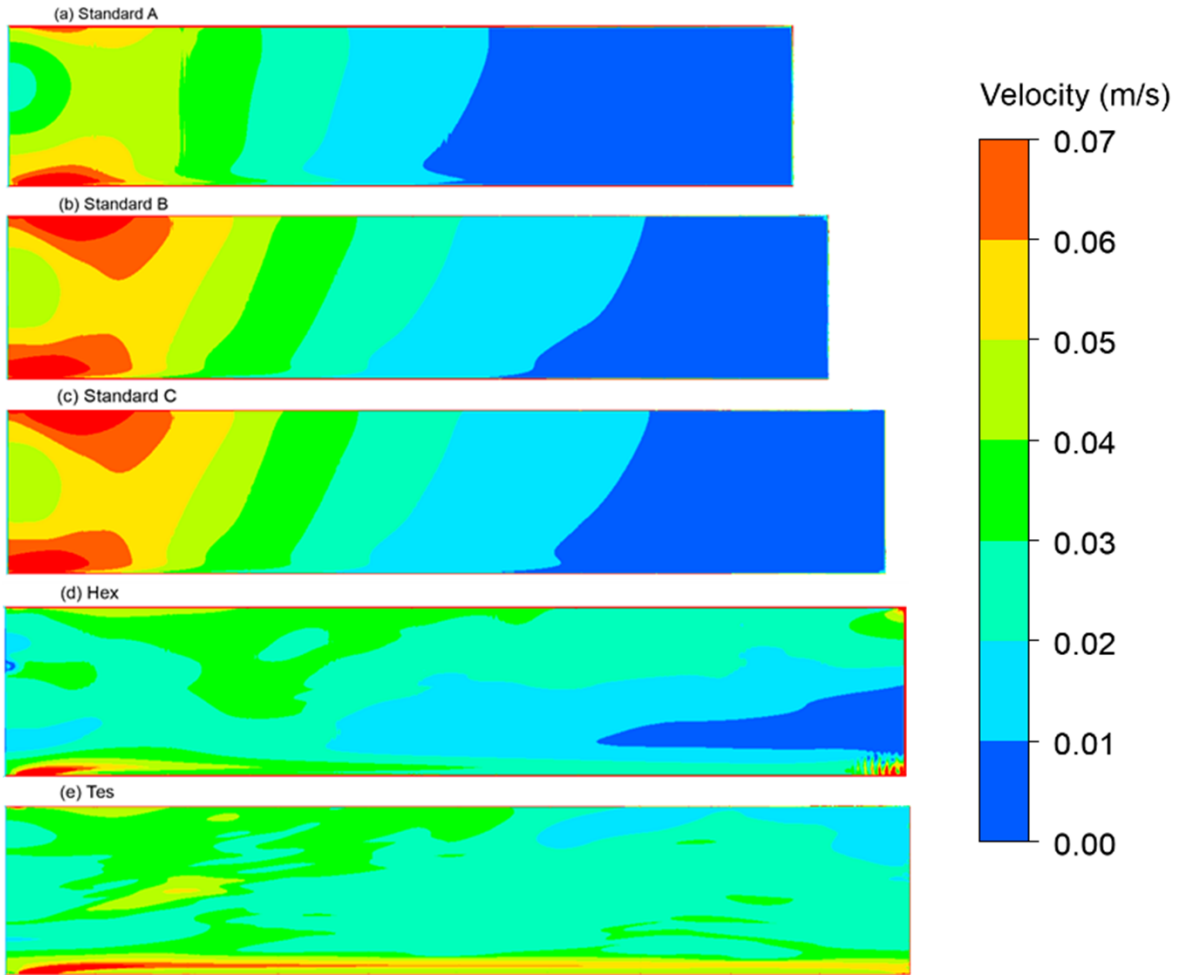

Figure 4.6: Velocity magnitude contour plot within pallet stacks in row 1(YZ plane, X = 0.5 m) of the packaging systems: (a) Standard A (b) Standard B (c) Standard C (d) Hex (e) Tes.

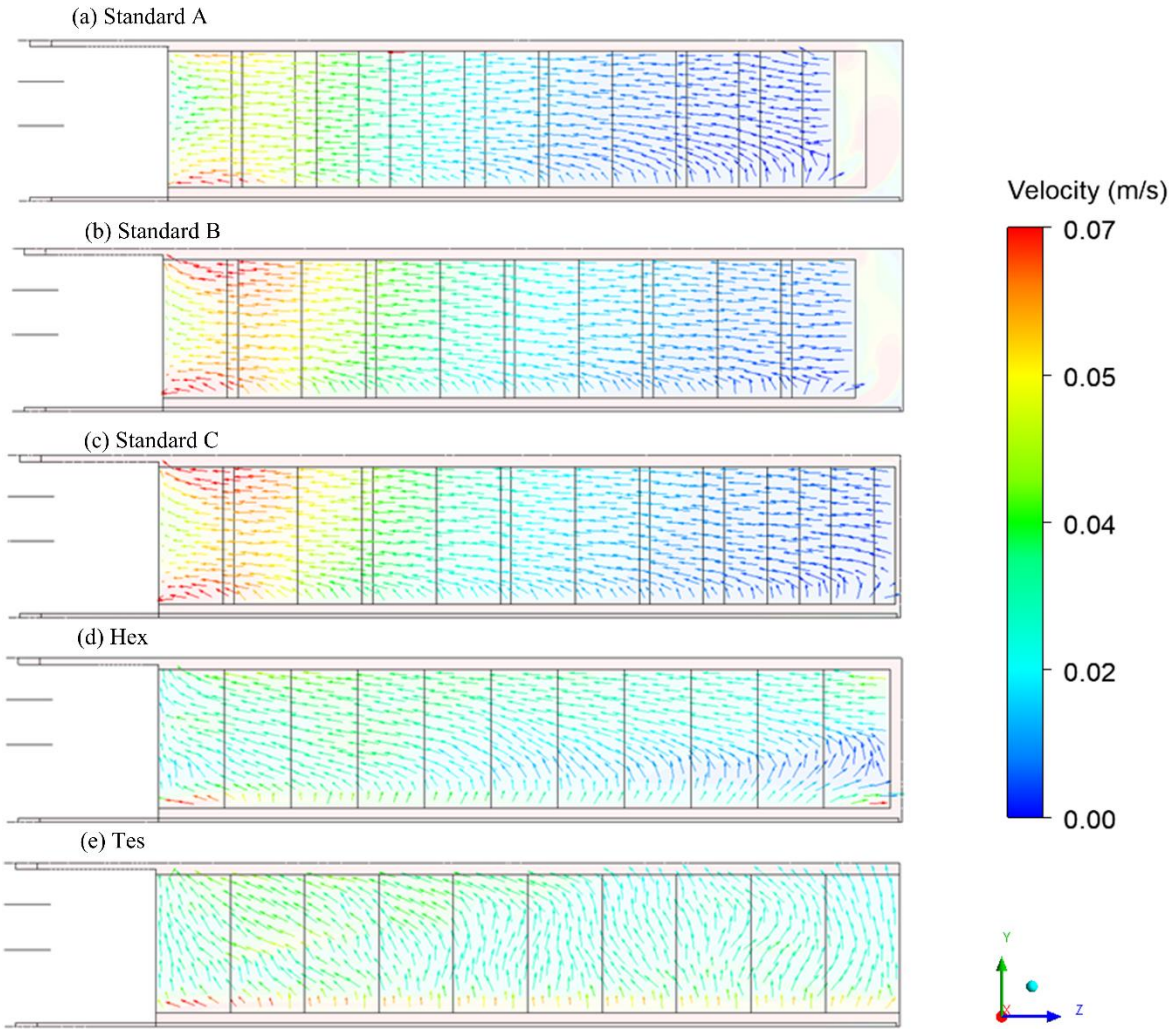

Figure 4.7: Simulated airflow pattern within the pallet stacks in row 1 (YZ plane, X = 0.5 m) of the packaging systems (a) Standard A (b) Standard B (c) Standard C (d) Hex (e) Tes.

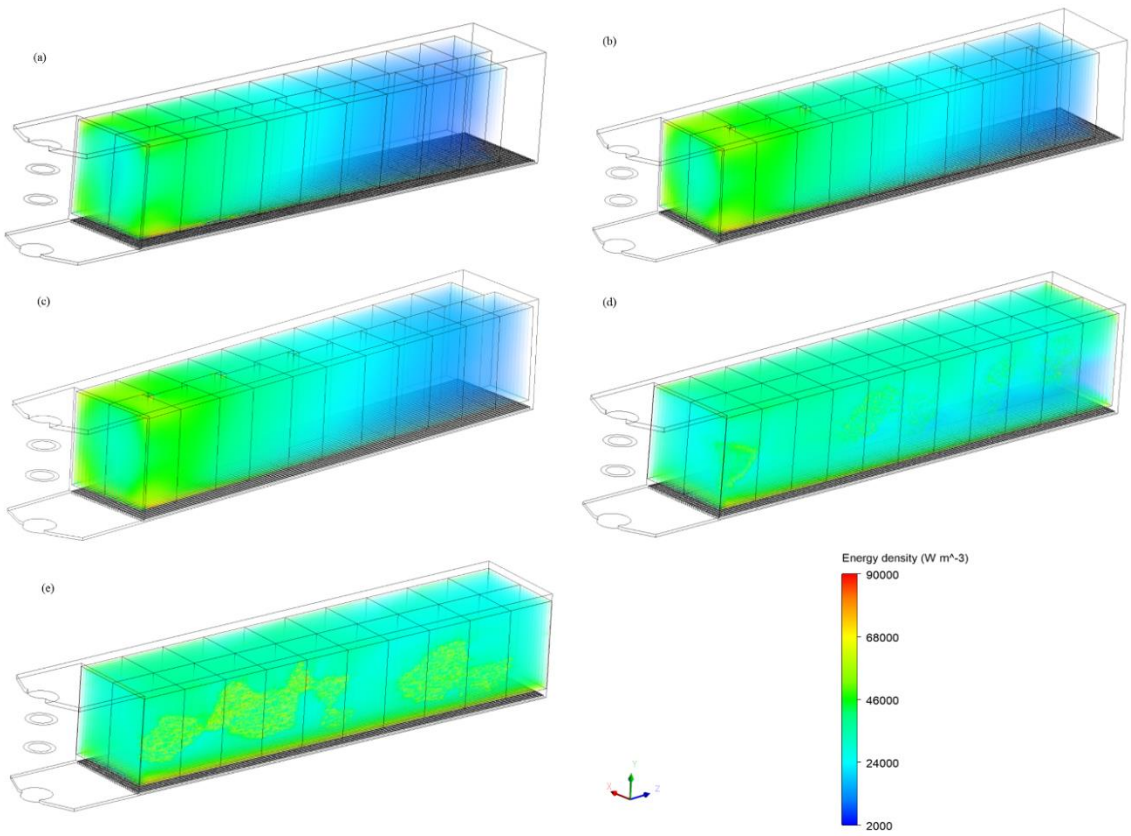

Figure 4.8: Energy density volume rendering of the packaging systems (a) Standard A (b) Standard B (c) Standard C (d) Hex (e) Tes.

Table 4.1: Number of computational mesh generated for the packaging systems.

Packaging system	Computational mesh size
Standard A	23 142 376
Standard B	31 628 939
Standard C	30 591 295
Hex	25 067 533
Tes	24 662 387

Table 4.2: Cooling air velocity range for the evaluated packaging systems.

Packaging system	Air velocity range (m/s)
Standard A	0.047
Standard B	0.05
Standard C	0.051
Hex	0.016
Tes	0.019

Table 4.3: Summary of CHTC Relative standard deviation for the packaging systems.

Packaging system	CHTC Relative Standard deviation (%)
Standard A	53.7
Standard B	60.8
Standard C	66.24
Hex	13.14
Tes	9.4

Chapter 5. Identification of Pallet Stack Ventilation Requirements for Improved Cooling

5.1 Introduction

Quality preservation of packaged fresh-produce during long-distance transport is critically dependent on adequately controlling airflow, heat and mass transfer processes within the refrigerated container (Van Der Sman, 2002). In horticultural cold chain systems, convective transfer of heat between products and the surrounding air is dominant. The cooling rate of horticultural products is primarily influenced by the intricate pattern of airflow in the cooling system (Smale et al., 2006). If not correctly managed, these airflow patterns can lead to the development of hot or cold spots in the refrigerated container which in turn lead to injuries induced by chilling and freezing, high rate of respiration and transpiration (Berry, 2017). Also, inadequate ventilation of the packaging system can lead to insufficient cooling and thus accelerated deterioration of fruit quality. Refrigerated containers rely on the flow of cold air around horticultural produce to achieve cooling, prevent senescence and to rapidly remove respiratory heat (Smale, 2004). Airflow distribution within several cold storage systems (cold room, refrigerated containers) are highly heterogeneous. The non-homogeneous delivery of air within the refrigerated container causes non-uniform cooling of horticultural produce (G. Alvarez & Flick, 1999; Getahun, 2016). Packaging design (vent area and positioning) and stacking arrangement of packages on a pallet base is thus of critical importance, as it influences the airflow distribution in the refrigerated container (Getahun et al., 2018).

Ventilation holes are typically added to horticultural package designs to optimise air penetration to the fruit and improve the airflow distribution in packaging boxes (Pathare et al., 2012). The sizing and positioning of ventilation holes on packaging boxes have direct significance on the uniformity of airflow and cooling efficiency of fruit in cold storage systems (Berry, 2015; Ngcobo et al., 2012; Pathare et al., 2012). During long-distance transportation, horticultural products are highly vulnerable to damage caused by different mechanical forces such as compression, shock, vibration and impact (Fadiji et al., 2016; Sittipod et al., 2009). Therefore, the mechanical strength of packaging is a significant consideration in vent hole design as it is necessary to determine the appropriate size and positioning of vent holes that will not result in mechanical failure and thus fruit damage (Berry et al., 2015; Defraeye et al., 2015; Pathare et al., 2012). In recent years, much research has been directed towards optimising the design for carton ventilation and correspondingly, its effect on airflow distribution under forced air cooling and refrigerated transportation. Various total ventilation areas (TVA) have been recommended as a compromise between the structural integrity of packages and cooling efficiency of fruit. Kader (2002) suggested a total vent area of 5-6% for corrugated fibreboard carton. De Castro et al. (2005) demonstrated that a total vent area between 8-16% is best for cooling air efficiency and energy use optimisation. Also, it has been reported that TVAs beyond 7-8% will not increase fruit cooling rates. Getahun et al. (2017b) examined the contribution of bottom area ventilation to packaging

designs used in South African export of apple fruit. The author demonstrates that adding 3.5% to the bottom area of Econo-D packaging box increase airflow (vertical) by ten-fold and decreased the cooling time (SECT) by 37%.

In addition to package design, stacking arrangement of packages has a significant influence on the intensity and airflow pattern in a refrigerated container (Alvarez & Flick, 1999; Ngcobo, 2013; Van Der Sman, 2002). The quantity of air reaching the fruit when stacked depends on the following factors: (i) package design, (ii) number and arrangement of fruit in a package box, and (iii) pallet stacking pattern (Getahun et al., 2017b). Misalignment of vent holes and obstruction of air by internal packaging accessories (trays, carry bag, plastic liners) contribute to the pallet stack airflow resistance (De Castro and Vigneault, 2005; Getahun et al., 2017b; Vigneault et al., 2009) and also affect the preferential airflow pathway necessary for cooling in the container (Delele et al., 2008; Ngcobo, 2013). Refrigerated containers with bottom air-delivery configurations rely on the flow of cold air vertically (bottom to top) for cooling. However, undesirable horizontal airflow can still occur (Berry, 2017; Jiménez-Ariza et al., 2014; Rodríguez-Bermejo et al., 2007; Smale et al., 2006). Higher ratios of horizontal flow (versus vertical flow rates) takes place as a result of insufficient ventilation across the vertical axis. This is attributed to limited or more frequently obstructed ventilation after the cartons have been stacked into a pallet.

Previous research has demonstrated the influence of package design and flow resistance (vertical and horizontal) on airflow distribution and cooling rate of fruit (Getahun et al., 2017b). The decrease in the vertical flow resistance values can lead to an increase in airflow velocities and a reduction in cooling time of loaded fruit in the container. To the best of the author's knowledge, no previous work has been done to determine an optimal pallet stack ventilation value that will enable improved vertical airflow distribution necessary for better cooling of fruit in a refrigerated container. This study aims to explore the relationship between pallet stack permeability and the ratio of vertical to horizontal airflow during refrigerated cooling. A validated 3D computational fluid dynamics (CFD) model with realistic refrigeration unit was used to evaluate this phenomenon.

5.2 Materials and methods

5.2.1 Computational domain

The refrigerated container internal dimension is 11.59 m long, 2.29 m wide and 2.55 m high (internal volume: 67.6m^3). The geometry was set up to hold twenty pallets arranged in two rows in the container. No Air gap was included between the rows as this contributes to heterogeneity of airflow in the container. Void plugs were added to the freestream region between the door and the pallet stacks to restrict the bypass of air in the container. The Standard-A packaging system configuration was used in this study. Figure 5.1shows (a) top and (b) side view of the container internal computational domain with void plugs at the freestream region between the door and pallet stack.

5.2.2 Pallet modelling

The pallet stack was modelled as a two-phase porous model, and the appropriate interfacial area density and heat transfer coefficient were specified. The maximum directional loss properties used in this study were numerically determined by relating the pressure drop over the pallet stack to the rate of flow (Berry, 2017). This relation is expressed using Darcy-Forchheimer equation that accounts for the inertial effects only;

$$\Delta P = \xi U^2 \tag{5.1}$$

where ξ (kgm^{-4}) represent the pressure loss coefficient (PLC).

Berry (2017) explicitly modelled the packaging boxes, pallet stacks and internal packaging accessories to determine the streamwise and transverse pressure loss coefficient of the pallet stack to airflow. Figure 5.2 shows the directional loss properties of the standard packaging system.

5.2.3 Simulation set-up

Please refer to section 4.2.2.2 for the simulation set-ups and assumptions used in developing the numerical model.

5.3 Results and discussion

Based on a sensitivity analysis, vertical and horizontal air velocities were monitored at 100 evenly spaced positions within the simulated pallet domains. For all numerical simulations, the horizontal pressure loss coefficient for the pallet stack was maintained at a constant value (2 389 kgm^{-4}) while the vertical pressure loss coefficient was varied between 200 kgm^{-4} and 26 915 kgm^{-4}. The airflow pattern of each simulation was then monitored to determine at what value the transition from vertical flow to horizontal flow occurs in the pallet stack.

5.3.1 Airflow characterisation within the pallet stack

Table 5.1 shows the averaged simulated vertical (U_v) and horizontal velocities (U_w, U_u) for the examined range of vertical pressure loss coefficients. Airflow distribution in a fully loaded refrigerated container occurs vertically through stacked horticultural produce (U_v) and horizontally through the container length (U_w) and width (U_u). Vertical airflow in a refrigerated container is the preferential pathway for cooling of fruit, but as a result of high vertical pressure loss coefficient, air will flow along the route with least resistance, which under the right conditions is along the container length.

Figure 5.3 shows the average air velocity and air velocity ratio profile for the examined range of vertical pressure loss coefficients. Noticeable trends are visible in Table 5.1 and Figure 5.3, for low vertical pressure loss coefficients (200 kgm^{-4}, 1000 kgm^{-4}, 2000 kgm^{-4}) the vertical air velocity (U_v) is comparatively higher than the horizontal air velocities (U_w, U_u). Hence, the ratio of the mean air velocities of all pallets (U_v/U_w, U_v/U_u) are comparatively higher for the pressure loss coefficients as mentioned earlier. This indicates that the airflow pattern within

the pallet stack is predominantly vertical for these pressure loss coefficients (Figure 5.4). In a refrigerated container, the air absorbs field heat from packaged fruit rapidly. In horizontal airflow cases where there is a dominant flow of air along the container length, the air becomes saturated with heat from the fruit long before it exits the packaging and returns to the refrigeration unit. Dominant vertical airflow within the pallet stack, therefore, provides the air with a higher refresh rate of cold air.

As the vertical pressure loss coefficient increases, the Uv decreases significantly, which in turn increases the U_w and U_u (Table 5.1, Figure 5.3). Up till 5500 kgm^{-4}, the mean Uv is higher than 0.01m/s, which is generally considered as a relatively low air velocity for refrigerated container cooling. The transition from vertical airflow pattern within the pallet stack occurred when the vertical pressure loss coefficient was increased to 7500 kgm^{-4}. At this critical resistance value, U_v/U_w and U_v/U_u are comparatively low, since U_w is approximately two folds higher than the U_v. Figure 5.5 shows the simulated horizontal and vertical airflow profile of pallet stacks when the vertical pressure loss coefficient is 7500 kgm^{-4}. The graph clearly shows the variation between the U_w and U_v for all pallet IDs. U_w and U_v decreases across the container length as the distance of the pallet stacks to the refrigeration unit increases (Figure 5.5). At the higher vertical pressure loss coefficients (9000 kgm^{-4}, 11000 kgm^{-4}, 13000 kgm^{-4}, 26915 kgm^{-4}), the airflow pattern is predominantly horizontal (Figure 5.4). The horizontal velocities (U_w and U_u) are higher than the vertical air velocity (U_v) at these resistance value.

5.3.2 Vertical airflow profile across the pallet stack height

Table 5.2 shows the average vertical air velocity across the pallet height for all the pallets when applying the respective ranges of vertical pressure loss coefficients. The effect of vertical pressure loss coefficient on the vertical air velocity across the pallet height was clearly established. Increasing the airflow resistance of a pallet stack generally decreases the vertical air velocities. Lower vertical pressure loss coefficients (200 kgm^{-4}, 1000 kgm^{-4}, 2000 kgm^{-4}) yield high vertical velocity magnitude whereas higher pressure loss coefficients (9000 kgm^{-4}, 11000 kgm^{-4}, 13000 kgm^{-4}, 26915 kgm^{-4}) yield lower vertical velocities. The critical point that shows the transition from a high vertical velocity across the pallet height occurs when the air velocity ratio (U_v/U_w) is approximately 0.4 (Table 5.1).

Figure 5.6 shows the simulated vertical airflow profiles across the pallet stack height for the ranges of vertical pressure loss coefficient. Pallet stacks near the refrigeration unit (P1, 2, 3 (Figure 5.1) receive high volumetric airflow rate, hence will cool faster. In contrast, the pallet stacks furthest from the refrigeration unit receive lower air velocities. The vertical airflow profile (Figure 5.6(a, b)) of lower pressure loss coefficients (200 kgm^{-4}, 1000 kgm^{-4}) shows an approximately uniform vertical air movement across the pallet stack height. The difference in the vertical velocity across the height of the pallet stack is comparatively low. Figure 5.6(c,d,…k) shows similar velocity profile with different heterogeneity indices.

The air jet from the refrigeration unit separates into primary and secondary airflow distributions. The primary airflow distribution refers to air movement along the container wall and floor, which is due to Coanda effect (Senguttuvan et al., 2020). The Coanda effect refers to the tendency of a fluid jet to “stick” or flow along to the container wall (Crivoi and

Doroftei, 2016). The secondary airflow distribution occurs vertically (bottom to top) across the pallet stack to cool packaged fruit in the refrigerated container. The vertical airflow profile of the pallet stack closest to the refrigeration unit (P1) for all vertical pressure loss coefficients show a concave curve when the pallet stack height is between 0.5 m and 1.5 m (Figure 5.6).

Figure 5.7 shows the vertical velocity contour at different vertical planes across the container length. As illustrated (Figure 5.7), this phenomena occurs only in pallets nearest to the refrigeration unit in both rows. This region is characterised by the substantial perpendicular movement of air. In the internal computational domain set-up, gaps between pallet stack rows were not included to limit the short-circuiting of air in the refrigerated container. The vertical repression of the velocity profile across the middle region of P1 can be attributed to the exclusion of these gaps.

5.4 Conclusion

An optimal pallet stack ventilation value was identified in this study by evaluating the pattern of airflow distribution and vertical airflow profiles within packaging systems using a range of directional loss properties. This study revealed the significant influence of packaging system flow resistance on the intensity and pattern of flow within a refrigerated container. Vertical air velocity for low pressure loss coefficients were comparatively higher than the horizontal velocities while horizontal air velocities for high vertical pressure loss coefficients were higher than the vertical velocity. Overall, vertical airflow pattern was dominant within the pallet stack when the vertical pressure loss coefficient was low. At the same time, horizontal airflow pattern was dominant when the pallet stack vertical pressure loss coefficient was high. In refrigerated containers, the dominance of horizontal airflow pattern within the pallet stacks causes low refresh rate of cold air. This significantly increases the fruit cooling time and affects the cooling efficiency of fruit. This pattern of airflow in packaging systems can substantially impact the quality preservation of fruit during distant transportation/shipping. Efficient package design and loading arrangement of pallet stack will reduce the vertical flow directional loss properties and optimise vertical airflow penetration into packaging systems. This will, in turn, improve the airflow distribution in the refrigerated container. This study identified the need to determine the directional loss properties at the critical point where the airflow pattern in packaging systems changes from vertical to horizontal. Also, this study has presented much needed baseline knowledge to support further research on future ventilation designs that will enhance the maintenance of fruit quality during refrigerated transport.

5.5 Future work

The directional loss properties of the pallet stacks used in this study are not exhaustive. The transverse (horizontal) pressure loss coefficient was constant for all simulation scenarios, while the streamwise (vertical) pressure loss coefficient was systematically varied within a numerically obtained maximum limit. Future studies should aim to explore more variation of the directional loss properties within this range. Many variables such as the loading arrangement of pallet stacks, the container layout/type and floor design will affect the quantity of air penetrated into palletised fruit. For example, Getahun et al. (2018) numerically

investigated the effect of different floor design on the airflow distribution in a refrigerated container. In comparison to the Flat floor design, T-bar floor structure shows an increased quantity of vertical airflow in the refrigerated container. Further numerical studies should fully capture all the factors that can significantly impact the pattern of flow in the refrigerated container. This will yield a more holistic characterization of airflow patterns within the pallets.

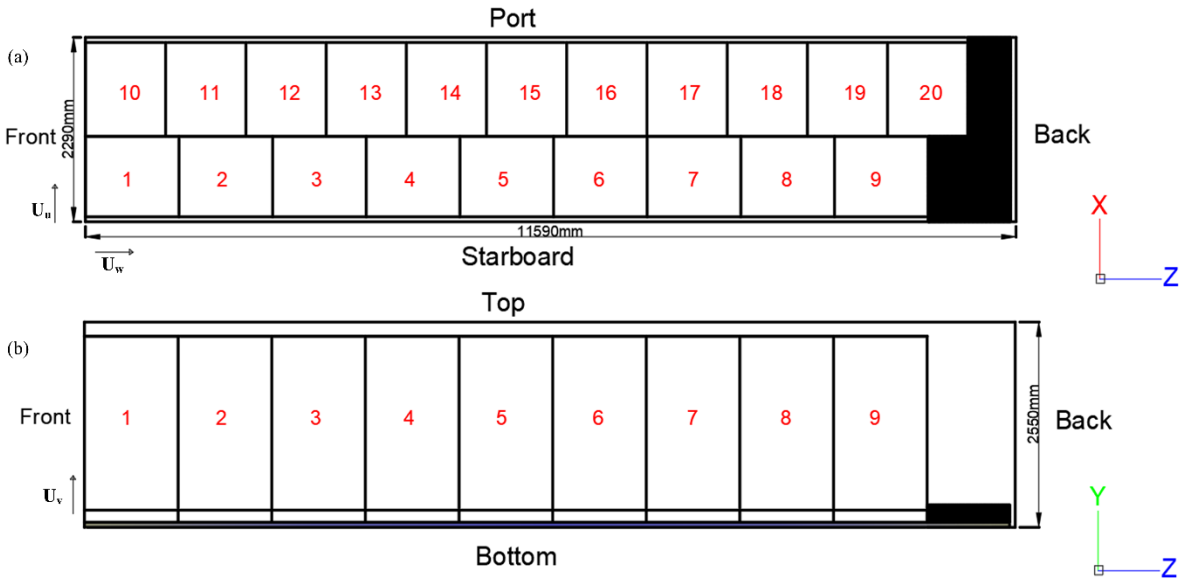

Figure 5.1: Top and (b) Side view of the refrigerated container internal computational domain showing air velocity vectors acting perpendicular to the container length (U_u), vertically across the container height (U_v) and parallel to the container length (U_w).

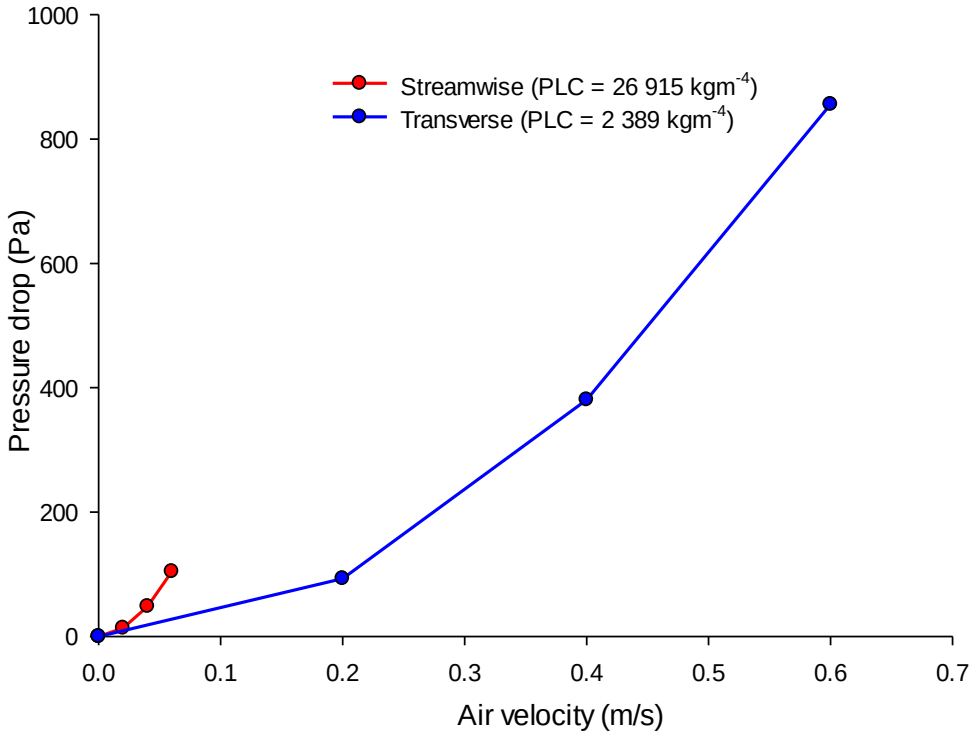

Figure 5.2: Numerically obtained pressure drop against air velocity showing the pressure loss coefficient (PLC) for streamwise (vertical) and transverse (horizontal) direction of the Standard A packaging system (Berry, 2017).

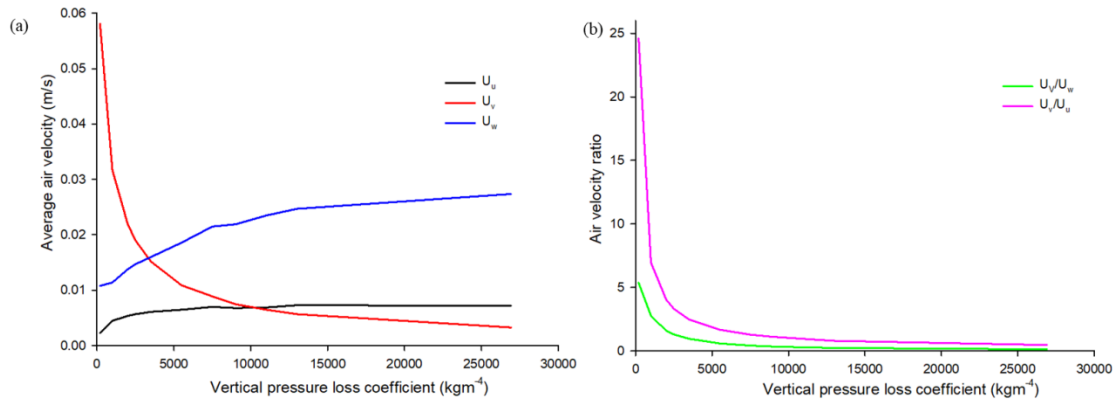

Figure 5.3: Simulated average air velocity (a) and air velocity ratio (b) profile for the examined range of pressure loss coefficients.

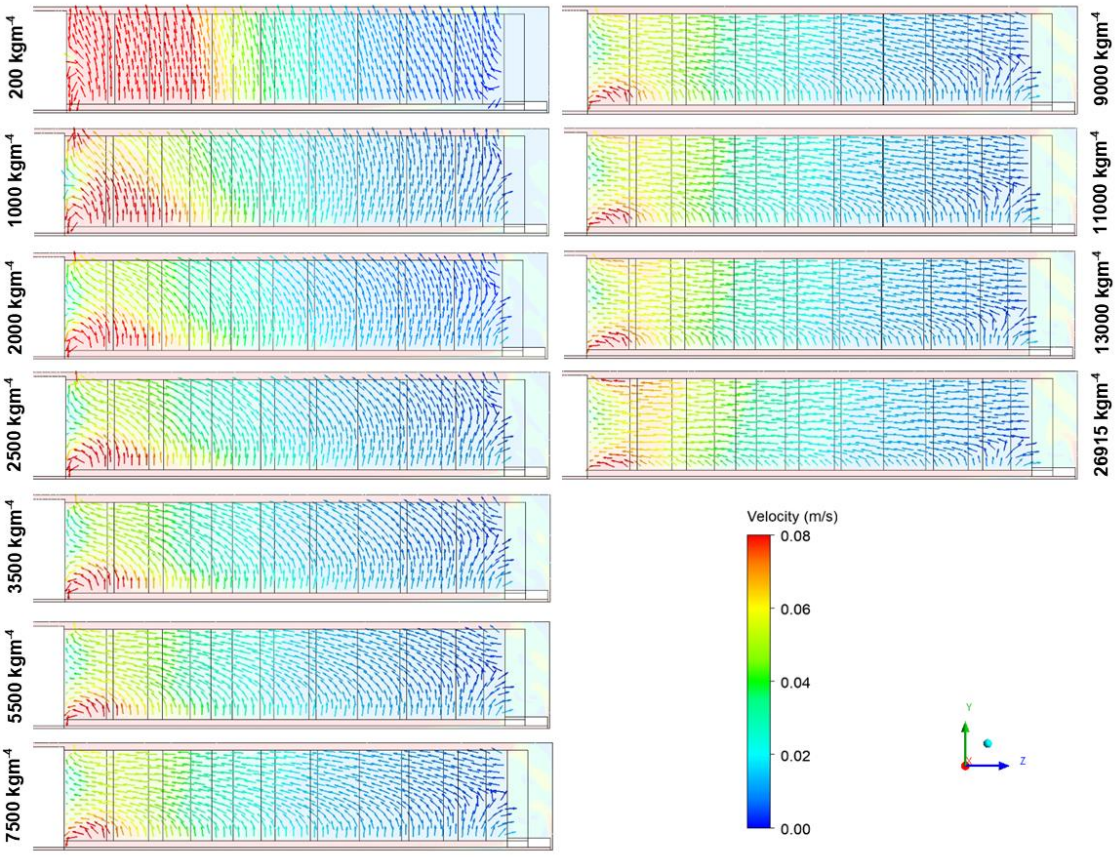

Figure 5.4: Simulated airflow pattern and velocity magnitude contour on YZ plane (X= 0.5 m) using different ranges of streamwise (vertical) pressure loss coefficients.

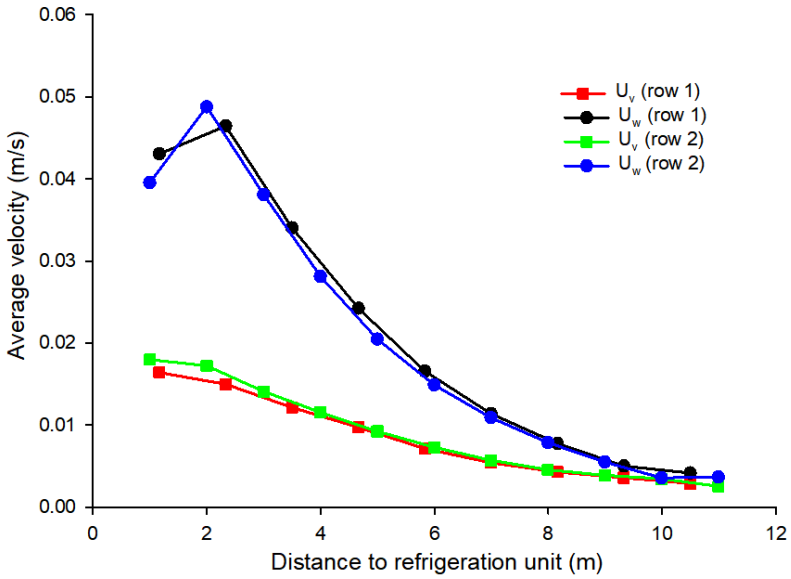

Figure 5.5: Simulated horizontal and vertical airflow profile of pallet stack when the vertical pressure loss coefficient is 7500 kgm^{-4}.

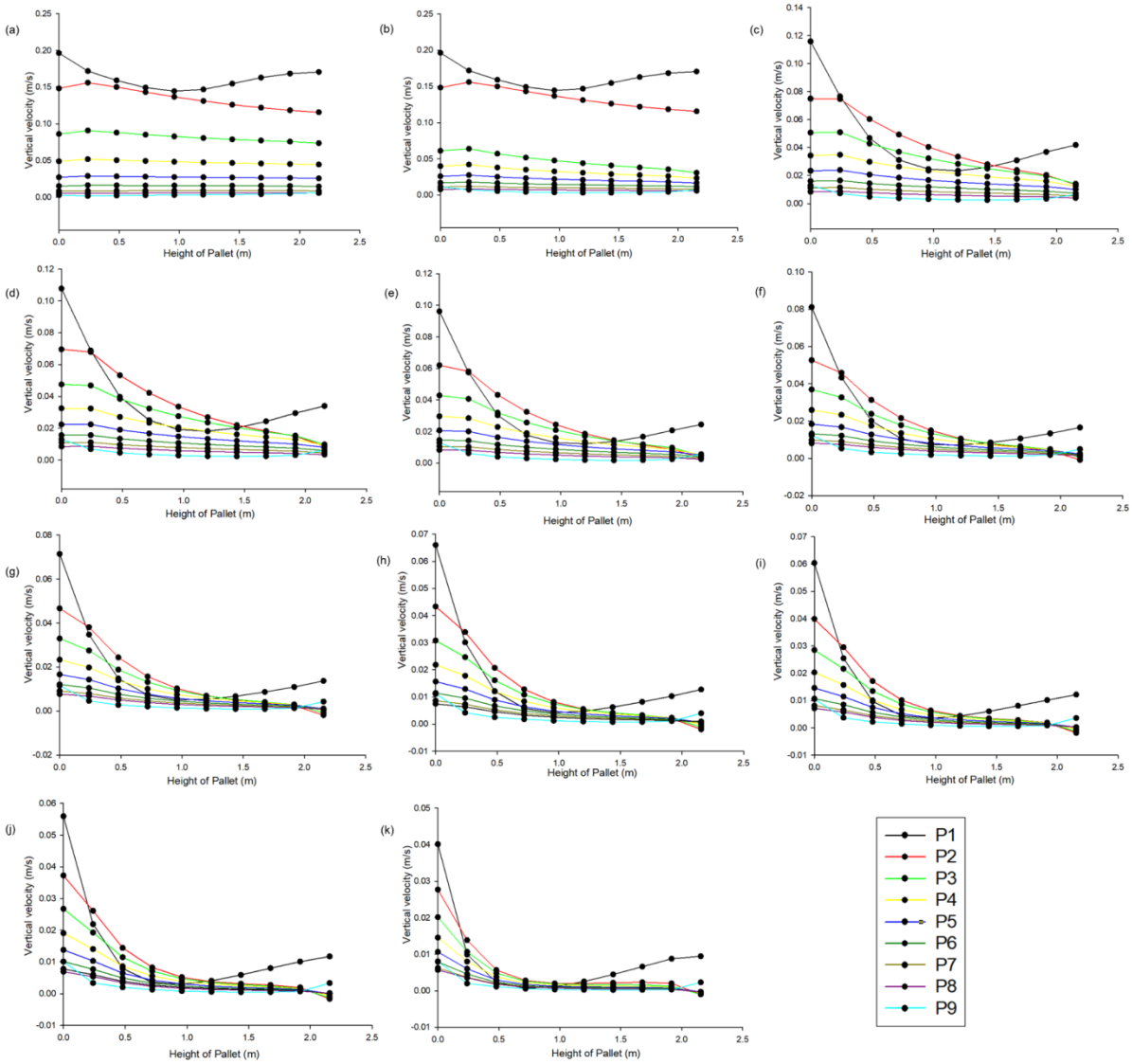

Figure 5.6: Simulated vertical airflow profile across the pallet stack height using the examined range of streamwise (vertical) pressure loss coefficient (a) 200 kgm^{-4} (b) 1000 kgm^{-4} (c) 2000 kgm^{-4} (d) 2500 kgm^{-4} (e) 3500 kgm^{-4} (f) 5500 kgm^{-4} (g) 7500 kgm^{-4} (h) 7500 kg m^{-4} (h) 9000 kgm^{-4} (i) 9000 kgm^{-4} (j) 13000 kgm^{-4} (k) 26915 kgm^{-4}.

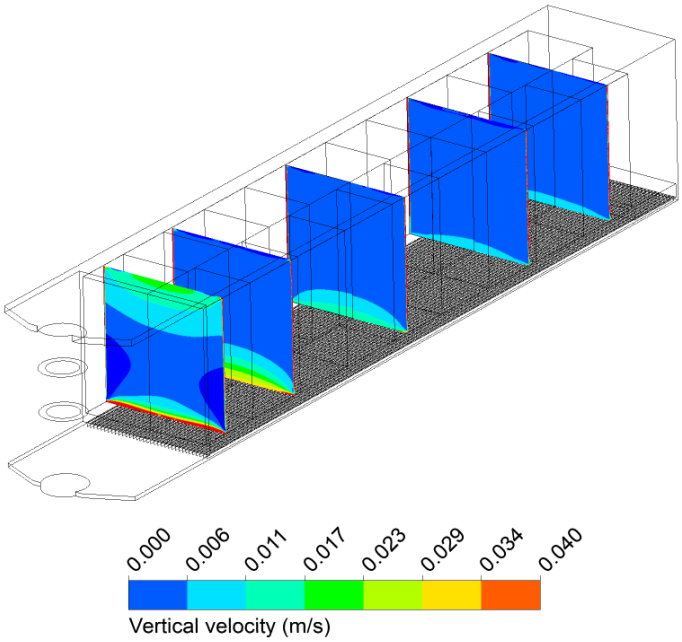

Figure 5.7: Vertical velocity contour on several XY plane (Z = 0.5 m, 2.2 m, 5 m, 8 m, 10 m) bisecting the pallet stack rows when the vertical pressure loss coefficient is 26 915 kgm^{-4}.

Table 5.1: Averaged Simulated vertical and horizontal air velocities for the examined range of streamwise (vertical) pressure loss coefficients. U_u, U_v and U_w are the horizontal (perpendicular to length), vertical and horizontal (parallel to length) air velocity vectors.

Vertical pressure loss coefficient (kgm^{-4})	U_v/U_w	U_v/U_u	U_v (m/s)	U_w (m/s)	U_u (m/s)
200	5.359	24.609	0.0581	0.0108	0.0023
1000	2.765	6.954	0.0317	0.0114	0.0045
2000	1.58	4.033	0.0219	0.0138	0.0054
2500	1.297	3.307	0.019	0.0147	0.0057
3500	0.947	2.465	0.0152	0.016	0.0061
5500	0.587	1.672	0.0109	0.0186	0.0065
7500	0.417	1.273	0.0089	0.0215	0.007
9000	0.344	1.103	0.0075	0.0219	0.0068
11000	0.278	0.94	0.0065	0.0235	0.0069
13000	0.234	0.786	0.0057	0.0247	0.0073
26915	0.12	0.455	0.0033	0.0274	0.0072

Table 5.2: Simulated average vertical air velocities across the pallet stack height for the examined range of streamwise (vertical) pressure loss coefficients.

Vertical pressure loss coefficient (kgm^{-4})	Vertical velocity across pallet height (U_v (m/s))
200	0.0520
1000	0.0371
2000	0.0203
2500	0.0177
3500	0.0143
5500	0.0104
7500	0.0083
9000	0.0073
11000	0.0064
13000	0.0057
26915	0.0035

Chapter 6. General Conclusion

Refrigerated containers are used for the transportation of horticultural produce to distant export markets. To minimise postharvest losses during transport and extended storage duration, it is important for the packaged fruit to receive adequate cooling airflow to maintain the cold chains. However, airflow distribution in refrigerated containers is predominantly heterogeneous. Pallet stacks near the refrigeration unit receive large volumetric airflow rates, while pallet stacks near the container door receive low airflow rates. The air velocity within pallet stacks decreases across the container length as the distance to the refrigeration unit increases. The influence of gaps between pallet rows on the heterogeneity of airflow inside the refrigerated container was assessed. Freestream region in the container causes short-circuiting of air and reduces the intensity of air penetration in the container. The effect of void plugs on airflow in the back (near the door) pallets were also evaluated. The result accentuates the importance of void plug usage as an effective method of constricting bypass of airflow in the refrigerated container and improving the vertical airflow within pallets.

Non-uniform cooling of packaged fruit in the refrigerated container causes the deterioration of fruit quality and a reduction in shelf life. In chapter 4 of this thesis, conceptual loading approaches were evaluated concerning the container space utilisation and cooling efficiency. The performance of the packaging systems were evaluated using a multi-parameter analysis. The Tes designs showed superior performance over the other evaluated packaging systems. The Tes Packaging system design had the lowest coefficient of variance for air-velocities and the lowest cooling heterogeneity index. The results thus show a significant benefit in cooling performance, if a packaging system that utilises more of the containers floor area is adopted by the industry. Chapter 5 examined different ranges of streamwise (vertical) to determine the critical point where the transition from vertical airflow to horizontal airflow occurs. The results showed that the ratio between ventilation area on the sides versus the top/bottom of cartons must be selected with care to ensure a preferential pattern of airflow in refrigerated containers. The preferential pathway for cooling of stacked fruit in a refrigerated container is vertical airflow, but due to high vertical pressure loss coefficients, air flows through the container length. This research has demonstrated potential improvements that are possible in refrigerated container cooling performance towards improved quality preservation of fruit. Future research should employ explicit modelling of package material inorder to evaluate the computational structural dynamics of the packaging systems. Plastics wastage contributes greatly to the pollution of the environment and depletion of the ozone layer and this has contributed to global demand to reduce the use of plastics in the horticultural cold chains. Therefore, future research should comprehensively evaluate the performance of plastic packaging in fruit cold chain systems with the strategic goal of reducing the amount of plastics used.

References

Africa, F. S. (2015). *A Socio Economic Impact Study Of The South African Fruit Export Industry - With Special Emphasis On The Role Of Transnet SOC And Its Subsidiaries - In The Sustainability Of The Fruit Export Industry*.

AIAA. (1998). Guide for the verification and validation of computational fluid dynamics simulations. *American Institute of Aeronautics and Astronautics, G-077-1998(AIAA G-077-1998), 1–29*.

Alvarez, G., & Flick, D. (1999). Analysis of heterogeneous cooling of agricultural products inside bins. Part II: Thermal study. *Journal of Food Engineering*, *39*(3), 239–245. https://doi.org/10.1016/S0260-8774(98)00166-6

Alvarez, Graciela, Bournet, P. E., & Flick, D. (2003). Two-dimensional simulation of turbulent flow and transfer through stacked spheres. *International Journal of Heat and Mass Transfer*, *46*(13), 2459–2469. https://doi.org/10.1016/S0017-9310(02)00546-X

Ambaw, A., Delele, M. A., Defraeye, T., Ho, Q. T., Opara, L. U., Nicolaï, B. M., & Verboven, P. (2013a). The use of CFD to characterize and design post-harvest storage facilities: Past, present and future. *Computers and Electronics in Agriculture*, *93*, 184–194. https://doi.org/10.1016/j.compag.2012.05.009

Ambaw, A, Mukama, M., & Opara, U. L. (2017). Analysis of the effects of package design on the rate and uniformity of cooling of stacked pomegranates : Numerical and experimental studies. *Computers and Electronics in Agriculture*, *136*, 13–24. https://doi.org/10.1016/j.compag.2017.02.015

Ambaw, Alemayehu, Verboven, P., Defraeye, T., Tijskens, E., Schenk, A., Opara, U. L., & Nicolai, B. M. (2013b). Porous medium modeling and parameter sensitivity analysis of 1-MCP distribution in boxes with apple fruit. *Journal of Food Engineering*, *119*(1), 13–21. https://doi.org/10.1016/j.jfoodeng.2013.05.007

Ambaw, Alemayehu, Verboven, P., Delele, M. A., Defraeye, T., Tijskens, E., Schenk, A., … Nicolai, B. M. (2014). CFD-Based Analysis of 1-MCP Distribution in Commercial Cool Store Rooms: Porous Medium Model Application. *Food and Bioprocess Technology*, *7*(7), 1903–1916. https://doi.org/10.1007/s11947-013-1190-9

Ambaw, Alemayehu, Verboven, P., Tijskens, E., Schenk, A., & Nicolai, B. M. (2013). CFD Modelling of the 3D Spatial and Temporal Distribution of 1-methylcyclopropene in a Fruit Storage Container, *Food and Bioprocess Technology 6 (9)*,2235–2250. https://doi.org/10.1007/s11947-012-0913-7

Anderson, J. D., & Wendt, J. (1995). *Computational fluid dynamics* (Vol. 206). New York: McGraw-Hill.

ASHRAE. (2010). *ASHRAE handbook of refrigeration: Systems and applications (SI Ed.)*. Atlanta.

Berry, T. M. (2017). *Optimisation of multi-scale ventilated package design for next-generation cold chain strategies of horticultural produce*. PhD Thesis. Stellenbosch University.

Berry, T M, Defraeye, T., Ambaw, A., Coetzee, C., & Opara, U. L. (2018). Horticultural packaging systems of the future: Improving reefer container usage. *Acta Horticulturae*

Vol. 1201, pp. 221–228. https://doi.org/10.17660/ActaHortic.2018.1201.30

Berry, Tarl M., Defraeye, T., Nicolaï, B. M., & Opara, U. L. (2016). Multiparameter Analysis of Cooling Efficiency of Ventilated Fruit Cartons using CFD: Impact of Vent Hole Design and Internal Packaging. *Food and Bioprocess Technology*, *9*(9), 1481–1493. https://doi.org/10.1007/s11947-016-1733-y

Berry, Tarl Michael, Delele, M. A., Opara, U. L., & Griessel, H. (2015). Geometric Design Characterisation of Ventilated Multi-scale Packaging Used in the South African Pome Fruit Industry. *Agricultural Mechanization in Asia, Africa, and Latin America*, *46*(3), 1–19.

Bouwer, K. & Dodd, M. 2016. Interviews, reefer volume utilisation. [Interview]. 11 March 2016.

Buehlmann, U., Bumgardner, M., & Fluharty, T. (2009). Ban on landfilling of wooden pallets in North Carolina: an assessment of recycling and industry capacity. *Journal of Cleaner Production*, *17*(2), 271–275. https://doi.org/10.1016/j.jclepro.2008.06.002

Caleb, O. J., Mahajan, P. V., Al-Said, F. A. J., & Opara, U. L. (2013). Modified Atmosphere Packaging Technology of Fresh and Fresh-cut Produce and the Microbial Consequences-A Review. *Food and Bioprocess Technology*, *6*(2), 303–329. https://doi.org/10.1007/s11947-012-0932-4

Chourasia, M. K., & Goswami, T. K. (2007). Steady state CFD modeling of airflow, heat transfer and moisture loss in a commercial potato cold store. *International Journal of Refrigeration*, *30*(4), 672–689. https://doi.org/10.1016/j.ijrefrig.2006.10.002

Crivoi, O., & Doroftei, I. (2016). Some experimental results on Coanda effect with application to a flying vehicle. *IOP Conference Series: Materials Science and Engineering*, *147*(1). https://doi.org/10.1088/1757-899X/147/1/012082

Datta, A. K. (2007). Porous media approaches to studying simultaneous heat and mass transfer in food processes. I: Problem formulations. *Journal of Food Engineering*, *80*(1), 80–95. https://doi.org/10.1016/j.jfoodeng.2006.05.013

De Castro, L. R., Vigneault, C., & Cortez, L. A. B. (2005). Cooling performance of horticultural produce in containers with peripheral openings. *Postharvest Biology and Technology*, *38*(3), 254–261. https://doi.org/10.1016/j.postharvbio.2005.07.004

Defraeye, T., Blocken, B., Derome, D., Nicolai, B., & Carmeliet, J. (2012). Convective heat and mass transfer modelling at air-porous material interfaces: Overview of existing methods and relevance. *Chemical Engineering Science*, *74*(0), 49–58. https://doi.org/10.1016/j.ces.2012.02.032

Defraeye, T., Blocken, B., Koninckx, E., Hespel, P., & Carmeliet, J. (2010). Computational fluid dynamics analysis of cyclist aerodynamics: Performance of different turbulence-modelling and boundary-layer modelling approaches. *Journal of Biomechanics*, *43*(12), 2281–2287. https://doi.org/10.1016/j.jbiomech.2010.04.038

Defraeye, T., Cronjé, P., Berry, T., Opara, U. L., East, A., Hertog, M., … Nicolai, B. (2015a). Towards integrated performance evaluation of future packaging for fresh produce in the cold chain. *Trends in Food Science and Technology*, *44*(2), 201–225. https://doi.org/10.1016/j.tifs.2015.04.008

Defraeye, T., Cronjé, P., Verboven, P., Opara, U. L., & Nicolai, B. (2015b). Exploring

ambient loading of citrus fruit into reefer containers for cooling during marine transport using computational fluid dynamics. *Postharvest Biology and Technology*, *108*, 91–101. https://doi.org/10.1016/j.postharvbio.2015.06.004

Defraeye, T., Lambrecht, R., Delele, M. A., Tsige, A. A., Opara, U. L., Cronjé, P., … Nicolai, B. (2014a). Forced-convective cooling of citrus fruit: Cooling conditions and energy consumption in relation to package design. *Journal of Food Engineering*, *121*(1), 118–127. https://doi.org/10.1016/j.jfoodeng.2013.08.021

Defraeye, T., Lambrecht, R., Delele, M. A., Tsige, A. A., Opara, U. L., Cronjé, P., … Nicolai, B. (2014b). Forced-convective cooling of citrus fruit: Cooling conditions and energy consumption in relation to package design. *Journal of Food Engineering*. https://doi.org/10.1016/j.jfoodeng.2013.08.021

Defraeye, T., Lambrecht, R., Tsige, A. A., Delele, M. A., Opara, U. L., Cronjé, P., … Nicolai, B. (2013). Forced-convective cooling of citrus fruit: Package design. *Journal of Food Engineering*, *118*(1), 8–18. https://doi.org/10.1016/j.jfoodeng.2013.03.026

Defraeye, T., Nicolai, B., Kirkman, W., Moore, S., Niekerk, S. Van, Verboven, P., & Cronjé, P. (2016). Postharvest Biology and Technology Integral performance evaluation of the fresh-produce cold chain : A case study for ambient loading of citrus in refrigerated containers. *Postharvest Biology and Technology*, *112*, 1–13. https://doi.org/10.1016/j.postharvbio.2015.09.033

Defraeye, T., Verboven, P., & Nicolai, B. (2013). CFD modelling of flow and scalar exchange of spherical food products: Turbulence and boundary-layer modelling. *Journal of Food Engineering*, *114*(4), 495–504. https://doi.org/10.1016/j.jfoodeng.2012.09.003

Defraeye, T., Verboven, P., Opara, U. L., Nicolai, B., & Cronjé, P. (2015). Feasibility of ambient loading of citrus fruit into refrigerated containers for cooling during marine transport. *Biosystems Engineering*, *134*(0), 20–30. https://doi.org/10.1016/j.biosystemseng.2015.03.012

Dehghannya, J., Ngadi, M., & Vigneault, C. (2008). Simultaneous aerodynamic and thermal analysis during cooling of stacked spheres inside ventilated packages. *Chemical Engineering and Technology*, *31*(11), 1651–1659. https://doi.org/10.1002/ceat.200800290

Dehghannya, J., Ngadi, M., & Vigneault, C. (2010). Mathematical Modeling Procedures for Airflow, Heat and Mass Transfer During Forced Convection Cooling of Produce: A Review. *Food Engineering Reviews*, *2*(4), 227–243. https://doi.org/10.1007/s12393-010-9027-z

Delele, M. A., Ngcobo, M. E. K., Getahun, S. T., Chen, L., Mellmann, J., & Opara, U. L. (2013). Studying airflow and heat transfer characteristics of a horticultural produce packaging system using a 3-D CFD model. Part I: Model development and validation. *Postharvest Biology and Technology*, *86*, 536–545. https://doi.org/10.1016/j.postharvbio.2013.08.014

Delele, M. A., Schenk, A., Tijskens, E., Ramon, H., Nicolaï, B. M., & Verboven, P. (2009). Optimization of the humidification of cold stores by pressurized water atomizers based on a multiscale CFD model. *Journal of Food Engineering*, *91*(2), 228–239. https://doi.org/10.1016/j.jfoodeng.2008.08.027

Delele, M. A., Tijskens, E., Atalay, Y. T., Ho, Q. T., Ramon, H., Nicolaï, B. M., & Verboven,

P. (2008). Combined discrete element and CFD modelling of airflow through random stacking of horticultural products in vented boxes. *Journal of Food Engineering*, *89*(1), 33–41. https://doi.org/10.1016/j.jfoodeng.2008.03.026

Delgado, A. E., & Sun, D.-W. (2001). Heat and mass transfer models for predicting freezing processes – a review. *Journal of Food Engineering*, *47*(3), 157–174. https://doi.org/10.1016/S0260-8774(00)00112-6

Department of Agriculture, F. and F. (DAFF). (2017). *Fresh Food Trade SA: The South African fresh food trade and supply chain directory 2017*. Pretoria. Retrieved from https://www.nda.agric.za/doaDev/sideMenu/internationalTrade/docs/tradeFacilitation/ftsa-latestjj.pdf

Elia, V., & Gnoni, M. G. (2015). Designing an effective closed loop system for pallet management. *International Journal of Production Economics*, *170*, 730–740. https://doi.org/10.1016/j.ijpe.2015.05.030

Evans, J. A., Foster, A. M., Huet, J. M., Reinholdt, L., Fikiin, K., Zilio, C., … Van Sambeeck, T. W. M. (2014). Specific energy consumption values for various refrigerated food cold stores. *Energy and Buildings*, *74*(2014), 141–151. https://doi.org/10.1016/j.enbuild.2013.11.075

Eyring, V., Köhler, H. W., Van Aardenne, J., & Lauer, A. (2005). Emissions from international shipping: 1. The last 50 years. *Journal of Geophysical Research D: Atmospheres*, *110*(17), 171–182. https://doi.org/10.1029/2004JD005619

Fadiji, T., Ambaw, A., Coetzee, J., Berry, T. M., & Linus, U. (2018). ScienceDirect Application of finite element analysis to predict the mechanical strength of ventilated corrugated paperboard packaging for handling fresh produce, *4*. https://doi.org/10.1016/j.biosystemseng.2018.07.014

Fadiji, T., Coetzee, C., Chen, L., Chukwu, O., & Linus, U. (2016). Susceptibility of apples to bruising inside ventilated corrugated paperboard packages during simulated transport damage. *Postharvest Biology and Technology*, *118*, 111–119. https://doi.org/10.1016/j.postharvbio.2016.04.001

Fadiji, T., Coetzee, J., Berry, T. M., Ambaw, A., & Opara, U. L. (2018). The efficacy of finite element analysis (FEA) as a design tool for food packaging : A review, Biosystems Engineering, *174*, 20-40. https://doi.org/10.1016/j.biosystemseng.2018.06.015

Fadiji, T. S. (2015). Mechanical Design and Performance Evaluation of Ventilated Packages, MEng thesis, Stellenbosch University (March)

Fawole, O. A., & Opara, U. L. (2013). Effects of storage temperature and duration on physiological responses of pomegranate fruit. *Industrial Crops and Products*, *47*, 300–309. https://doi.org/10.1016/j.indcrop.2013.03.028

Getahun, S. (2016). Investigating Cooling Performance and Energy Utilization of Refrigerated Shipping Container Packed with Fresh Fruit using Computational Fluid Dynamics Modelling, PhD thesis, Stellenbosch University.

Getahun, S., Ambaw, A., Delele, M., Meyer, C. J., & Opara, U. L. (2017a). Analysis of airflow and heat transfer inside fruit packed refrigerated shipping container: Part I – Model development and validation. *Journal of Food Engineering*, *203*, 58–68. https://doi.org/10.1016/j.jfoodeng.2017.02.010

Getahun, S., Ambaw, A., Delele, M., Meyer, C. J., & Opara, U. L. (2017b). Analysis of airflow and heat transfer inside fruit packed refrigerated shipping container: Part II – Evaluation of apple packaging design and vertical flow resistance. *Journal of Food Engineering*, *203*, 83–94. http://dx.doi.org/10.1016/j.jfoodeng.2017.02.011

Getahun, S., Ambaw, A., Delele, M., Meyer, C. J., & Opara, U. L. (2018). Experimental and Numerical Investigation of Airflow Inside Refrigerated Shipping Containers. *Food and Bioprocess Technology*, *11*(6), 1164–1176. https://doi.org/10.1007/s11947-018-2086-5

Goedhals-Gerber, L. L., Stander, C., & Dyk, F. E. Van. (2017). Maintaining cold chain integrity : Temperature breaks within fruit reefer containers in the Cape Town Container Terminal. *Southern African Business Review*, *21*, 362–384.

Gruyters, W., Verboven, P., Delele, M., Gwanpua, S. G., Schenk, A., & Nicolaï, B. (2018). A numerical evaluation of adaptive on-off cooling strategies for energy savings during long-term storage of apples. *International Journal of Refrigeration*, *85*, 431–440. https://doi.org/10.1016/j.ijrefrig.2017.10.018

Gruyters, Willem. (2019). *Advanced Computational Fluid Dynamics modelling for a more sustainable and energy efficient postharvest cold chain of pome fruit (Doctoral Disseration)*. KU Leuven.

Han, J. W., BadÍa-melis, R., Yang, X. T., Ruiz-garcia, L., Qian, J. P., & Zhao, C. J. (2017). CFD Simulation of Airflow and Heat Transfer During Forced-Air Precooling of Apples. *Journal of Food Process Engineering*, *40*(2), 1–11. https://doi.org/10.1111/jfpe.12390

Han, J. W., Zhao, C. J., Yang, X. T., Qian, J. P., & Fan, B. L. (2015). Computational modeling of airflow and heat transfer in a vented box during cooling: Optimal package design. *Applied Thermal Engineering*, *91*, 883–893. https://doi.org/10.1016/j.applthermaleng.2015.08.060

Hoang, H. M., Duret, S., Flick, D., & Laguerre, O. (2015). Preliminary study of airflow and heat transfer in a cold room filled with apple pallets: Comparison between two modelling approaches and experimental results. *Applied Thermal Engineering*, *76*, 367–381. https://doi.org/10.1016/j.applthermaleng.2014.11.012

Hoang, M. L., Verboven, P., De Baerdemaeker, J., & Nicolaï, B. M. (2000). Analysis of the air flow in a cold store by means of computational fluid dynamics. *International Journal of Refrigeration*, *23*(2), 127–140. https://doi.org/10.1016/S0140-7007(99)00043-2

Hortgro. (2018). *KEY DECIDOUS FRUIT STATISTICS*. Retrieved from https://www.hortgro.co.za/wp-content/uploads/docs/2019/08/2018-stats-booklet_key-deciduous_web-pdf-revised.pdf

Hossain, M. A., & Bala, B. K. (2007). Drying of hot chilli using solar tunnel drier. *Solar Energy*, *81*(1), 85–92. https://doi.org/10.1016/j.solener.2006.06.008

Hu, Z., & Sun, D. W. (2001). Predicting local surface heat transfer coefficients by different turbulent k-ε models to simulate heat and moisture transfer during air-blast chilling. *International Journal of Refrigeration*, *24*(7), 702–717. https://doi.org/10.1016/S0140-7007(00)00081-5

IIR. (1995). *Guide to refrigerated transport*. International Institution of Refrigeration,Paris, France.

James, S. J., James, C., & Evans, J. A. (2006). Modelling of food transportation systems - a

review. *International Journal of Refrigeration*, *29*(6), 947–957. https://doi.org/10.1016/j.ijrefrig.2006.03.017

Jiménez-Ariza, T., Correa, E. C., Diezma, B., Silveira, A. C., Zócalo, P., Arranz, F. J., … Ruiz-Altisent, M. (2014). The Phase Space as a New Representation of the Dynamical Behaviour of Temperature and Enthalpy in a Reefer monitored with a Multidistributed Sensors Network. *Food and Bioprocess Technology*, *7*(6), 1793–1806. https://doi.org/10.1007/s11947-013-1191-8

Kader, A. A. (2002). *Postharvest technology of horticultural crops* (3311th ed.). University of California: Agriculture and Natural Resources, Publication.

Kaviany, M. (2012). *Principles of heat transfer in porous media*. Springer Science & Business Media.

Keller, M. (2006). *Optimization of Containers for Seaway Logistics of Chilled and Frozen Fishery Products*. University of Iceland.

Khatchatourian, O. A., Toniazzo, N. A., & Gortyshov, Y. F. (2009). Simulation of airflow in grain bulks under anisotropic conditions. *Biosystems Engineering*, *104*(2), 205–215. https://doi.org/10.1016/j.biosystemseng.2009.06.023

Khoo, T. S., Ratnam, M. M., & Abdul Khalil, H. P. S. (2008). Wood Filler(WF)-recycled polypropylene (RPP) composite pallet: Study of static deformation using FEA and shadow moire. *Journal of Reinforced Plastics and Composites*, *27*(16–17), 1733–1744. https://doi.org/10.1177/0731684407081398

Kondjoyan, A. (2006). A review on surface heat and mass transfer coefficients during air chilling and storage of food products. *International Journal of Refrigeration*, *29*(6), 863–875. https://doi.org/10.1016/j.ijrefrig.2006.02.005

Ladanyia, M., & Ladaniya, M. (2010). *Citrus fruit: biology, technology and evaluation*. Academic press.

Laguerre, O., Ben Amara, S., Alvarez, G., & Flick, D. (2008). Transient heat transfer by free convection in a packed bed of spheres: Comparison between two modelling approaches and experimental results. *Applied Thermal Engineering*, *28*(1), 14–24. https://doi.org/10.1016/j.applthermaleng.2007.03.014

Laguerre, O., Duret, S., Hoang, H. M., & Flick, D. (2014). Using simplified models of cold chain equipment to assess the influence of operating conditions and equipment design on cold chain performance. *International Journal of Refrigeration*, *47*, 120–133. https://doi.org/10.1016/j.ijrefrig.2014.07.023

Laguerre, O., Hoang, H. M., & Flick, D. (2013). Experimental investigation and modelling in the food cold chain: Thermal and quality evolution. *Trends in Food Science and Technology*, *29*(2), 87–97. https://doi.org/10.1016/j.tifs.2012.08.001

Laguerre, O., Remy, D., & Flick, D. (2009). Airflow, heat and moisture transfers by natural convection in a refrigerating cavity. *Journal of Food Engineering*, *91*(2), 197–210. https://doi.org/10.1016/j.jfoodeng.2008.08.029

Launder, B., & Spalding, D. (1974). *The numerical computation of turbulent flows*. Comput. Method Appl. M.

Lawrence, J., & Maier, D. E. (2011). Three-dimensional airflow distribution in a maize silo with peaked, levelled and cored grain mass configurations. *Biosystems Engineering*,

110(3), 321–329. https://doi.org/10.1016/j.biosystemseng.2011.09.005

Lisowa, H., Wujec, M., & Lis, T. (2001). Influence of temperature and variety on the thermal properties of apples. *International Agrophysics*, *16*(1), 43–52.

Liu, E., Hu, X., & Liu, S. (2014). Theoretical Simulation and Experimental Study on Effect of Vacuum Pre-Cooling for Postharvest Leaf Lettuce, *2*(8), 443–449. https://doi.org/10.12691/jfnr-2-8-3

Lohan, J., Eveloy, V., & Rodgers, P. (2002). Visualization of forced air flows over a populated printed circuit board and their impact on convective heat transfer. *InterSociety Conference on Thermal and Thermomechanical Phenomena in Electronic Systems, ITHERM*, *2002-Janua*, 501–511. https://doi.org/10.1109/ITHERM.2002.1012498

Louw, L., & Nel, S. (2019). Analysis of the Use of Space and Module-Configured Packaging To Improve Fruit Export Mass in a Refrigerated Container. *South African Journal of Industrial Engineering*, *30*(1), 94–109. https://doi.org/10.7166/30-1-1879

McCoy, M. (2003). Pallets that Make the Extra Trip. *Modern Materials Handling, Reed Business Information, New York*.

Menter, F. R. (1992). Influence of freestream values on κ-ω turbulence model predictions. *AIAA*, *30(6)*, 1657–1659.

Menter, F. R. (1993). Zonal two equation κ-ω turbulence models for aerodynamic flows. In *23rd fluid dynamics, plasmadynamics, and lasers conference* (p. 2906).

Mirade, P. S., & Daudin, J. D. (1998). A New Experimental Method for Measuring and Visualising Air Flow in Large Food Plants. *Journal of Food Engineering*, *36*(1–4), 31–49. https://doi.org/10.1016/S0260-8774(98)00047-8

Mukama, M., Ambaw, A., Berry, T. M., & Opara, U. L. (2017). Energy usage of forced air precooling of pomegranate fruit inside ventilated cartons. *Journal of Food Engineering*, *215*, 126–133. https://doi.org/10.1016/j.jfoodeng.2017.07.024

Myburgh, T. (2016). *An analysis of the optimal packaging sizes for selected fruit types and the impact on the 12m hi-cube refrigerated container*. Stellenbosch University.

Nagle, M., González Azcárraga, J. C., Mahayothee, B., Haewsungcharern, M., Janjai, S., & Müller, J. (2010). Improved quality and energy performance of a fixed-bed longan dryer by thermodynamic modifications. *Journal of Food Engineering*, *99*(3), 392–399. https://doi.org/10.1016/j.jfoodeng.2010.03.006

Nahor, H. B., Hoang, M. L., Verboven, P., Baelmans, M., & Nicolaï, B. M. (2005). CFD model of the airflow, heat and mass transfer in cool stores. *International Journal of Refrigeration*, *28*(3), 368–380. https://doi.org/10.1016/j.ijrefrig.2004.08.014

Nakayama, A., & Kuwahara, F. (2005). Algebraic model for thermal dispersion heat flux within porous media. *AIChE Journal*, *51*(10), 2859–2864. https://doi.org/10.1002/aic.10503

Ngcobo, Mduduzi E K, Delele, M. A., Opara, U. L., Zietsman, C. J., & Meyer, C. J. (2012). Resistance to airflow and cooling patterns through multi-scale packaging of table grapes. *International Journal of Refrigeration*, *35*(2), 445–452. https://doi.org/10.1016/j.ijrefrig.2011.11.008

Ngcobo, Mduduzi Elijah Khulekani. (2013). Resistance to Airflow and Moisture Loss of

Table Grapes Inside Multi- scale Packaging, PhD thesis. Stellenbosch University.

Nield, D. A., & Bejan, A. (2017). *Convection in porous media*. *Convection in Porous Media*. https://doi.org/10.1007/978-3-319-49562-0

Norton, T., & Sun, D. W. (2006). Computational fluid dynamics (CFD) - an effective and efficient design and analysis tool for the food industry: A review. *Trends in Food Science and Technology*, *17*(11), 600–620. https://doi.org/10.1016/j.tifs.2006.05.004

Notteboom, T., & Rodrigue, J. P. (2007). Re-assessing port-hinterland relationships in the context of global commodity chains. *Inserting Port-Cities in Global Supply Chains. London: Ashgate*. https://doi.org/10.1007/BF00419710

O'Sullivan, J., Ferrua, M., Love, R., Verboven, P., Nicolaï, B., & East, A. (2014). Airflow measurement techniques for the improvement of forced-air cooling, refrigeration and drying operations. *Journal of Food Engineering*, *143*, 90–101. https://doi.org/10.1016/j.jfoodeng.2014.06.041

Oberkampf, W. L., & Trucano, T. G. (2002). *Verification and validation in computational fluid dynamics*. *Progress in Aerospace Sciences* (Vol. 38). https://doi.org/10.1016/S0376-0421(02)00005-2

Opara, U.L., Zou, Q. (2006). Novel computational fluid dynamics simulation software for thermal design and evaluation of horticultural packaging. *Int. J. Postharvest Technol. Innov*, *1*, 155–169.

Opara, U. L. (2010). Editorial : High incidence of postharvest food losses is worsening global food and nutrition security. *International Journal of Postharvest Technology and Innovation*, *2*(1), 1–3.

Opara, U. L. (2011). From hand holes to vent holes: What's next in innovative horticultural packaging? *Inaugural Lecture*, Stellenbosch University.

Opara, U.L. (2009). Quality Management: An industrial approach to produce handling. In and S. E. P. W.J. Florkowski, R.L. Shewfelt, B. Brueckner (Ed.), *In Postharvest Handling* (pp. 153–204). San Diego: Academic Press.

Pathare, P. B., Opara, U. L., Vigneault, C., Delele, M. A., & Al-Said, F. A. J. (2012). Design of Packaging Vents for Cooling Fresh Horticultural Produce. *Food and Bioprocess Technology*, *5*(6), 2031–2045. https://doi.org/10.1007/s11947-012-0883-9

Quintard, M., Kaviany, M., & Whitaker, S. (1997). Two-medium treatment of heat transfer in porous media: numerical results for effective properties. *Advances in Water Resources*, *20*(2–3), 77–94. https://doi.org/10.1016/S0309-1708(96)00024-3

Ravindra, M. R., & Goswami, T. K. (2008). Modelling the respiration rate of green mature mango under aerobic conditions. *Biosystems Engineering*, *99*(2), 239–248. https://doi.org/10.1016/j.biosystemseng.2007.10.005

Ristić, S., Isaković, J., Ilić, B., & Ocokoljić, G. (2004). Review of methods for flow velocity measurement in wind tunnels. *Scientific-Technical Review*, *LIV*(3), 60–71. https://doi.org/10.1007/978-1-4419-9834-7

Roache, P. (1998). *Verification and Validation of Computational Fluid Dynamics Simulations*. Hermosa, Albuquerque, NM.

Robertson, G. L. (2016). *Food Packaging: Principles and Practice*. CRC Press.

Rodríguez-Bermejo, J., Barreiro, P., Robla, J. I., & Ruiz-García, L. (2007). Thermal study of a transport container. *Journal of Food Engineering*, *80*(2), 517–527. https://doi.org/10.1016/j.jfoodeng.2006.06.010

Ruegg, T., Stangier, R., Stoeckli, B., Tanner, C., Dorer, V., & Lommel, A. (1994). *3D airflow velocity vector sensor*. Krakow, Poland: Proc. of Roomvent '94.

Schobeiri, M. T. (2010). *Fluid mechanics for engineers: a graduate textbook*. Springer Science & Business Media.

Senguttuvan, S., Youn, J., Park, J., Lee, J., & Kim, S. (2020). Enhanced airflow in a refrigerated container by improving the refrigeration unit design. *International Journal of Refrigeration*. https://doi.org/10.1016/j.ijrefrig.2020.08.019

Sinclair, J. T. (1989). *Refrigerated Containers*. World Bank, Policy Planning and Research Staff, Infrastructure and Urban Development Department.

Sittipod, S., Swasdee, D., Singh, S. P., & Singh, J. (2009). Effect of Truck Vibration during Shipments in Thailand. *Ndustrial Technology*, *3*(1), 6.

Smale, N. J. (2004). *Mathematical modelling of airflow in shipping systems: model development and testing*. *Thesis*. Massey University, Palmerston North, New Zealand.

Smale, N. J., Moureh, J., & Cortella, G. (2006). A review of numerical models of airflow in refrigerated food applications. *International Journal of Refrigeration*, *29*(6), 911–930. https://doi.org/10.1016/j.ijrefrig.2006.03.019

Sun, D. W. (2007). *Computational fluid dynamics in food processing*. CRC Press.

Tanner, D. J., & Amos, N. D. (2003). Temperature variability during shipment of fresh produce. *Acta Horticulturae*, *599*, 193–203. https://doi.org/10.17660/ActaHortic.2003.599.22

Thermo King. (2007). *Maintenance manual, Magnum TK 51122-4-MM. Thermo King Corp*. Minneapolis, USA.

Thompson, J. F., Mejia, D. C., & Singh, R. P. (2010). Energy use of commercial forced-air coolers for fruit. *Applied Engineering in Agriculture*, *26*(5), 919–924.

Van Der Sman, R. G. M. (2002). Prediction of airflow through a vented box by the Darcy – Forchheimer equation. *Journal of Food Engineering*, *55*, 49–57.

Verboven, P., Hoang, M. L., Baelmans, M., & Nicolaï, B. M. (2004). Airflow through beds of apples and chicory roots. *Biosystems Engineering*, *88*(1), 117–125. https://doi.org/10.1016/j.biosystemseng.2004.02.002

Verboven, Pieter, Flick, D., Nicolaï, B. M., & Alvarez, G. (2006). Modelling transport phenomena in refrigerated food bulks, packages and stacks: basics and advances. *International Journal of Refrigeration*, *29*(6), 985–997. https://doi.org/10.1016/j.ijrefrig.2005.12.010

Verboven, Pieter, Tijskens, E., Ramon, H., & Nicolaï, B. M. (2005). Virtual filling and airflow simulation of boxes with horticultural products. *Acta Horticulturae*, *687*, 47–54. https://doi.org/10.17660/ActaHortic.2005.687.4

Versteeg, H. K., & Malalasekera, W. (2007). An Introduction to Computational Fluid Dynamics - The Finite Volume Method. *Pearson Education*.

Vigneault, C., De Castro, L. R., & Cortez, L. A. B. (2004). Effect of peripheral openings on cooling efficiency of horticultural produce. *ASAE Annual International Meeting 2004*, *0300*(04), 6937–6947. https://doi.org/10.13031/2013.16970

Vigneault, Clément, Thompson, J., Wu, S., Hui, K. P. C., & Leblanc, D. I. (2009). Transportation of fresh horticultural produce. *Research Signpost*, *37661*(2), 1–24.

Wakao, N., & Kagei, S. (1982). *Heat and mass transfer in packed beds* (Vol.1). Taylor & Francis.

Wang, L., & Sun, D. W. (2003). Recent developments in numerical modelling of heating and cooling processes in the food industry - A review. *Trends in Food Science and Technology*, *14*(10), 408–423. https://doi.org/10.1016/S0924-2244(03)00151-1

Wild, Y. (2009). Refrigerated containers and CA technology. In *Container Handbook*. GDV, Die Deutschen Versicherer. Berlin. Retrieved from http://www.containerhandbuch.de/

Wu, W., & Defraeye, T. (2018). Identifying heterogeneities in cooling and quality evolution for a pallet of packed fresh fruit by using virtual cold chains. *Applied Thermal Engineering*, *133*, 407–417. https://doi.org/10.1016/j.applthermaleng.2017.11.049

Xia, B., & Sun, D. W. (2002). Applications of computational fluid dynamics (CFD) in the food industry: A review. *Computers and Electronics in Agriculture*, *34*(1–3), 5–24. https://doi.org/10.1016/S0168-1699(01)00177-6

Zhai, Z. J., Zhang, W., Zhang, Z., & Chen, Q. Y. (2007). Evaluation of various turbulence models in predicting airflow and turbulence in enclosed environments by CFD: part 1 - Summary of prevalent turbulence models. *Hvac&R Research*, *13*(6), 853–870. https://doi.org/10.1080/10789669.2007.10391459

Zhao, C. J., Han, J. W., Yang, X. T., Qian, J. P., & Fan, B. L. (2016). A review of computational fluid dynamics for forced-air cooling process. *Applied Energy*, *168*(December 2017), 314–331. https://doi.org/10.1016/j.apenergy.2016.01.101

Zou, Q., Opara, L. U., & McKibbin, R. (2006). A CFD modeling system for airflow and heat transfer in ventilated packaging for fresh foods: I. Initial analysis and development of mathematical models. *Journal of Food Engineering*, *77*(4), 1037–1047. https://doi.org/10.1016/j.jfoodeng.2005.08.042